การศึกษาการลดแรงเสียดทานการไหลในท่อขดโดยสารเติมแต่งพอลิเมอร์

นายอาสาฬห์ชัย สุขเกื้อ

วิทยานิพนธ์นี้เป็นส่วนหนึ่งของการศึกษาตามหลักสูตรปริญญาวิศวกรรมศาสตรมหาบัณฑิต

สาขาวิชาวิศวกรรมเครื่องกล ภาควิชาวิศวกรรมเครื่องกล

คณะวิศวกรรมศาสตร์ จุฬาลงกรณ์มหาวิทยาลัย

ปีการศึกษา 2552

STUDY OF DRAG REDUCTION IN COILED TUBE FLOW BY POLYMER ADDITIVES

MR. ARSANCHAI SUKKUEA

A Thesis Submitted in Partial Fulfillment of the Requirements
for the Degree of Master of Engineering Program in Mechanical Engineering

Department of Mechanical Engineering
Faculty of Engineering
Chulalongkorn University

Academic Year 2009

Thesis Title	STUDY OF DRAG REDUCTION IN COILED TUBE FLOW BY POLYMER ADDITIVES
By	Mr. Arsanchai Sukkuea
Field of Study	Mechanical Engineering
Thesis Advisor	Assistant Professor Sompong Putivisutisak, Ph.D.
Thesis Co-Advisor	Associate Professor Kuntinee Maneeratana, Ph.D.

Accepted by the Faculty of Engineering, Chulalongkorn University in Partial Fulfillment of the Requirements for the Master's Degree

.... Dean of the Faculty of Engineering

(Associate Professor Boonsom Lerdhirunwong, Dr.Ing)

THESIS COMMITTEE

.... Chairman

(Assistant Professor Tul Manewattana, Ph.D.)

.... Thesis Advisor

(Assistant Professor Sompong Putivisutisak, Ph.D.)

.... Thesis Co-Advisor

(Associate Professor Kuntinee Maneeratana, Ph.D.)

.... External Examiner

(Associate Professor Varangrat Juntasaro, Ph.D.)

นายอาสาฬห์ชัย สุขเกื้อ : การศึกษาการลดแรงเสียดทานการไหลในท่อขดโดยสารเติมแต่งพอลิเมอร์. (STUDY OF DRAG REDUCTION IN COILED TUBE FLOW BY POLYMER ADDITIVES) อ.ที่ปรึกษาวิทยานิพนธ์หลัก : ผู้ช่วยศาสตราจารย์ ดร.สมพงษ์ พุทธิวิสุทธิศักดิ์, อ.ที่ปรึกษาวิทยานิพนธ์ร่วม : รองศาสตราจารย์ ดร.กุณฑินี มณีรัตน์ 124 หน้า.

วิทยานิพนธ์นี้นำเสนอการทดลองการลดแรงเสียดทานการไหลในท่อขด โดยการเปลี่ยนปริมาณความเข้มข้นของสารเติมแต่งพอลิเมอร์และอัตราส่วนความโค้ง โดยศึกษาอัตราส่วนความโค้งที่แตกต่างกัน 3 ชนิด คือ อัตราส่วนความโค้ง 0.012, 0.018 และ 0.024 ส่วนชนิดของสารเติมแต่งพอลิเมอร์ที่ศึกษา คือ พอลิอะคริลาไมด์ (Polyacrylamide), พอลิไวนิลแอลกอฮอล์ (Polyvinyl Alcohol), แอนไอออนิก พอลิอะคริลาไมด์ (Anionic Polyacrylamide), และ แคทไอออนิก พอลิอะคริลาไมด์ (Cationic Polyacrylamide) การศึกษากระทำโดยการเปลี่ยนปริมาณความเข้มข้นของสารเติมแต่งพอลิเมอร์ทั้งหมด 6 ความเข้มข้น คือ ความเข้มข้น 0.01, 0.03, 0.05, 0.07, 0.10, และ 0.15% โดยปริมาตร โดยใช้ปัจจัยเรื่องการลดความเสียดทานสูงสุดเพื่อหาค่าความเข้มข้นที่ดีที่สุด นอกจากนี้ยังทำการจำลองแบบการคำนวณโดยใช้โปรแกรมเชิงพานิชย์ (FLUENT) เพื่อตรวจสอบพฤติกรรมการลดแรงเสียดทาน โดยเปรียบเทียบผลที่ได้กับผลการทดลอง

ผลการทดลองแสดงให้เห็นว่าการเติมปริมาณสารเติมแต่งเพียงเล็กน้อย จะสามารถลดความเสียดทานการไหลลงได้ค่อนข้างมาก ค่าการลดความเสียดทานสูงสุดคือ 60% ที่ปริมาณความเข้มข้น 0.07% โดยปริมาตร ของสารเติมแต่ง แอนไอออนิก พอลิอะคริลาไมด์ (Anionic Polyacrylamide) สมการความสัมพันธ์ที่ได้จากการทดลองแสดงผลแนวโน้มการทำนายที่ค่อนข้างแม่นยำเมื่อเทียบกับผลการทดลอง สำหรับผลการจำลองแบบโดยโปรแกรมเชิงพานิชย์แสดงแนวโน้มสอดคล้องกับผลการทดลอง อย่างไรก็ตาม การจำลองเชิงตัวเลขและการคำนวณโดยใช้แบบจำลองยกกำลัง (Power Fluid Model) แสดงการลดแรงเสียดทานเพียงแค่ 2-7% เนื่องจากแบบจำลองความปั่นป่วน (Turbulence Model) และ แบบจำลองนอน-นิวโตเนียน (Non-Newtonian Model) ในโปรแกรมเชิงพานิชย์ที่ใช้อาจมีความไม่เหมาะสมในการศึกษาการลดแรงเสียดทานการไหลในท่อขด

ภาควิชา วิศวกรรมเครื่องกล ลายมือชื่อนิสิต

สาขาวิชา วิศวกรรมเครื่องกล ลายมือชื่ออ.ที่ปรึกษาวิทยานิพนธ์หลัก

ปีการศึกษา 2552 ลายมือชื่ออ.ที่ปรึกษาวิทยานิพนธ์ร่วม

4970706921 : MAJOR MECHANICAL ENGINEERING

KEYWORDS : DRAG REDUCTION / POLYMER ADDITIVE / COILED TUBE / CFD

ARSANCHAI SUKKUEA : STUDY OF DRAG REDUCTION IN COILED TUBE FLOW BY POLYMER ADDITIVES. THESIS ADVISOR: ASST. PROF. SOMPONG PUTIVISUTISAK,Ph.D., THESIS CO-ADVISOR : ASSOC. PROF. KUNTINEE MANEERATANA,PH.D., 124 pp.

This thesis presents a laboratory experiment of drag reduction in coiled tubes with various concentrations of polymer additives and curvature ratios. Three different curvature ratios i.e. 0.012, 0.018, and 0.024, are studied. The employed polymer additives are Polyacrylamide, Polyvinyl Alcohol, Anionic Polyacrylamide, and Cationic Polyacrylamide. For each additive, six concentrations of polymer solution of 0.01, 0.03, 0.05, 0.07, 0.10, and 0.15% by volume are studied. The best concentration is determined from the drag reduction exhibited by the fluid. In addition, computational simulation by a commercial software (FLUENT), is used to investigate the drag reduction behavior. Of these techniques, the emphasis is on the laboratory experiment while the simulation is used to verify and compare the experimental results.

The results showed that, in the laboratory experiment, small amounts of polymer additive could reduce the solvent friction pressure substantially. Highest friction pressure decrease is 60% at the concentration of 0.07% by volume with Anionic Polyacrylamide additive. The empirical correlations indicate excellent agreement between the experimental data and existing predicting trends. For the numerical simulation, the results showed simulation trends which conformed to the experimental measurements. However, the numerical simulation and the simulation with power fluid model illustrated only 2-7% drag reduction which indicated that the turbulence and non-Newtonian fluid model in the commercial software were not suitable for studying the drag reduction in coiled tubes.

Department : Mechanical Engineering Student's Signature Arsanchai Sukkuea

Field of Study Mechanical Engineering Advisor's Signature

Academic Year : 2009 Co-Advisor's Signature

Acknowledgements

I would like to express my gratitude to all those who gave me the possibility to complete this thesis. At first, I would like to thank my advisor, Assistant Professor Dr. Sompong Putivisutisak, and my especially co-advisor, Associate Professor Dr. Kuntinee Maneeratana, very mush for their supervision throughout the period of this thesis work. I would also like to thank the thesis committee- Assistant Professor Dr. Tul Manewattana, and Associate Professor Dr. Varangrat Juntasaro.

In addition, I would like to thank IAESTE, the International Association for the Exchange of Students for Technical Experience, for giving me opportunity to make an internship at Department of Chemical Engineering, Manipal Institute of Technology, Manipal University, Karnataka, India.

I am deeply indebted to my supervisor Professor Dr. Javadeva Bhat and all the technician staffs whose help, stimulating suggestions, and encouragement helped me in all the time of my research. I have furthermore to thank my coworker from Oman, Majed Said who together worked in the beginning of this research.

Moreover, I also would like to thank all friends in the Computational Modeling and Optimization Laboratory who always help me when I had a problem either my thesis work or daily life.

Finally, I would like to thank my parents, my sister and my brother whose have helped me during this thesis work, with out their help it would have been difficult.

Contents

Page

Page

List of Tables

List of Tables (continued)

List of Tables (continued)

List of Figures

List of Figures (continued)

List of Figures (continued)

Figure Page

List of Abbreviations

Abbreviations used in this thesis work are as follows:

CCl_4	Carbon tetra chloride
Hg	Mercury
PAM	Polyacrylamide
PVA	Polyvinyl alcohol
2D	Two Dimensions
3D	Three Dimensions
FVM	Finite Volume Method
r/R	curvature ratio
f	Fanning friction factor
d	Coiled tube diameter
l	Length of coiled tube
ΔH	Head loss
g	Acceleration gravity
v	Bulk mean velocity
Re	Reynolds number
ρ	Density
μ	Viscosity
DR	Drag Reduction
f_p	Fanning friction factor of polymeric fluid
f_s	Fanning friction factor of solvent
τ_{xy}	Shear stress exerted by the fluid
n	Flow behavior index
τ_y	Minimum yield stress
μ_p	Fluid viscosity - a constant of proportionality
t	Time
h	Height of the column
R_m	Difference in height of manometric fluid

List of Abbreviations (continued)

ρ_m	Density of manometric fluid
ρ_f	Density of flowing fluid
K	Consistency index

Chapter I

Introduction

1.1 Motivation

One of the energy saving techniques in pumping application, such as oil transposition, is to add small amount of polymers to the transported fluid in order to reduce friction between the turbulent fluid and the inside surface of the pipeline. Due to the ability to extend their length, suppress, absorb the turbulent fluctuation and, hence, streamline the turbulence, polymer additives can reduce friction and drag. Thus, this technique lowers the pressure drop and increases the flow rate of the fluid.

The first pioneer of drag reduction with polymer solution was generally attributed to Toms [1] who discovered it by chance in the summer of 1949 when he investigated the mechanical degradation of polymer solution and found that the solution had less resistance to flow under constant pressure than the solvent itself. After Toms' paper was published, the drag reduction topic has been extensively studied to decrease pressure drop and increase the flow rate of fluids with different additives such as polymer, surfactants, and fiber. Generally, polymer is the best drag reducing additive as it is possible to reduce drag up to 80% in the straight pipe with only few parts per million of added polymer.

The fluid flow in a straight pipe has been investigated by many researchers but there are few researches about fluid flow in a coiled tube. The phenomenon of fluid flow with additives in a coiled tube had not been clearly investigated until Srinivasan et al. [2] which described important factors affecting the phenomenon of fluid flow in a coiled tube. For the drag reduction, Shah and Zhou [3] continued the study of drag reduction by polymer solutions with the same experiment set up as those in Sinivasan et al. [2]. It was found that the tube diameter, curvature ratio, and polymer concentration were the important parameters. Thus, the study of drag reduction in a coiled tube with various types of additive could be systematically studied.

In this thesis, selected parameters that may facilitate the drag reduction in coiled tube by polymer additive are studied. Two different techniques, the laboratory experiment and computational simulation by commercial software, are used to investigate the drag reduction behavior. Of these techniques, the emphasis is on the laboratory experiment while the simulation is used to verify and compare the results with the experimental measurement.

1.2 Research Objectives

The objectives of this thesis are as follows.

1. To conduct laboratory experiments that systematically investigate the drag reduction of flows in coiled tubes.
2. To obtain the correlations that predict the value of fanning friction factor for flows in coiled tubes with polymer additives.
3. To simulate the coiled tube flow by commercial software and compare the results with the experimental measurements.

1.3 Research Scopes

The scopes of this thesis are as follows.

1. The laboratory experiments are tested on coiled tubes with three different curvature ratio (r/R) of 0.012, 0.018, and 0.024.
2. The laboratory experiments study water flows with 4 different polymer additive fluids – polyacrylamide, polyvinyl alcohol, anionic polyacrylamide (A-110), and cationic polyacrylamide (C-492) solutions.
3. The computational simulation uses the FLUENT commercial software to simulate the fluid flows in 2D straight tubes and 3D coiled tubes.

1.4 Research Benefits

The benefits from this thesis are as follows.

1. The friction factor correlations from the laboratory experiment can be used in the study of the drag reduction by polymer additives.

2. The computational simulation can be used to design the experimental set up for the study of the drag reduction by polymer additives.

3. The friction factor can be used in the design and operation of pipeline.

1.5 Research Methodologies

The research proceeds by following these steps.

1. To study previous researches of fluid flow and drag reduction in straight and coiled tubes with Newtonain and Non-newtonain fluids.

2. To conduct experiments on all specified solutions to measure viscosity, pressure drop, and flow rate.

3. To compare the results of laboratory experiments with previous researches.

4. To study the finite volume method and commercial software, FLUENT.

5. To simulate the fluid flow in coiled tubes by commercial software, FLUENT.

6. To compare the results from the experiment and the computational simulation.

7. To analyze and conclude the results.

Chapter II

Literature Review

2.1 Drag Reduction Background

The drag reduction by additive solutions has been investigated extensively for over 50 years. Many experiments have been set up to study the drag reduction problems. The experiment on a practical problem was started during the World War II by Agoston et al. [4] which investigated the flow of gasoline thickened with napalm surfactant additive, the main fuel used by the United States in flame throwers and, in the last stages of World Was II, fire bombs.

Because of wartime conditions, the experiment was all rather hurried and could lay no claim to high precision, but it was believed that the main results were significant. The experiment was set up to compare the pressure drop at the same flow rates between pure gasolines and dilute napalm additive in the same pipe. The flow rate was measured by weighing the discharge over a timed interval in order to avoid any uncertainty inherent in volumetric measurement. The pipe was 1/8 inch in diameter. The gages were attached to sleeves silver-soldered over a 1/16 inch clean hole drilled in the pipe wall. The consistency of the napalm surfactant additive was estimated at 20 gram Gardner.

The obtained results are shown in Figure 2.1, along with the calculated line according to Fanning's correlation. The pressure drop for gasoline was found to be higher than the expected value. Indeed, both the experimental and the calculated values for pure gasoline were definitely higher. In addition, the experimental measurements from pure gasoline were as much as 70% higher that those from gasoline thickened with napalm surfactant additive. The explained reason for this behavior by Agonston et al. is that a less turbulent, more streamlined flow of napalm surfactant additive could reduce the pressure drop even while the viscosity was much higher.

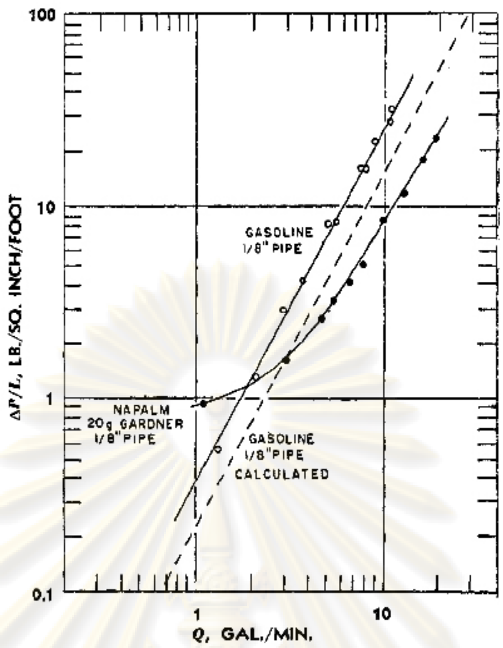

Figure 2.1 Experimental Results of Agonston et al. [4]

After the experiment of Agonston et al. was published, many researchers have been studied to explain the drag reduction phenomenon by experimentation with different methods. Those studies can be classified into three main topics which are the range of flow, types of pipes (straight pipe and coiled tube), and types of additives.

2.2 Range of Flow

The Reynolds number is an important parameter that classifies the flow into laminar or turbulent. The drag reduction researches have been studied in both flow ranges which there were a few researches in the laminar flow range due to the low potential of drag reduction. For the drag reduction in turbulent flow range, it was possible to reduce the drag up to 80% by adding small polymer.

2.2.1. Laminar Flow

Laminar or streamline flow with generally the Reynolds number of less than 2000, occurs when a fluid flows in parallel layers with no disruption between these layers.

For the drag reduction, there are few researches in the laminar flow range due to the reason that the fluid slip at the wall made the free surface energy of the solid was very low and small decreased the energy when adding the additives, thus, less interest in the experiments. However, in 2001, the drag reduction in laminar and turbulent flow was investigated by Watanabe and Udagawa [5], who clarified the influence of the physical characteristics of the wall surface on laminar drag reduction.

The phenomena was tested on straight circular pipes with 0.006 m and 0.43 m in length. The test fluid was PEO15 aqueous solutions in a concentration range of 30-1000 ppm. The pressure drop in the tested section was measured by estimation a pressure transducer and a U-tube manometer. The report value is the best estimate of the result, and with 95% confidence limit.

Figure 2.2 shows the relationship between the viscosity and the laminar drag reduction ratio. The drag reduction ratio increased gradually with the increase in viscosity before plateaus. This result suggested that there was a limit to the drag reduction ratio in laminar flows in a pipe with a highly water repellent wall. In addition, the obtained results agreed with the previous researches that drag reduction in laminar range were small with only 10-15% drag reduction.

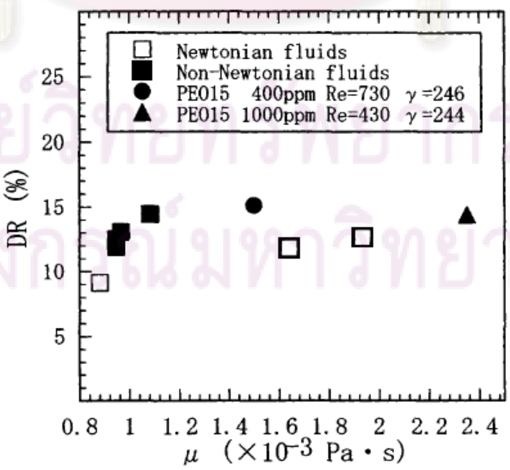

Figure 2.2 Viscosity and Laminar Drag Reduction Ratio [5]

2.2.2. Turbulent Flow

Turbulent flow regime is characterized by disorder and property changes which include low momentum diffusion, high momentum convection, and rapid variation of pressure and velocity. Flows with high Reynolds numbers, usually Reynolds number above 4000, become turbulent.

Because of the good drag reduction results in the turbulent range, which was first observed in a straight pipe by Toms [1], many studies related to this effect have been reported. Dan Toonder el al. [6] continually studied in drag reduction by polymer additive in turbulent and transition to turbulent flow range. This research investigated the influence of polymer additives in the turbulent regime theoretically as well as experimentally. The aim of this research was to study the influences of the preparation of the solution, the hydration of the molecules and the effect of different pumps on the time behavior of the turbulent pipe flow of polymeric fluids, using three different commercial polymers known for their large effectiveness in reducing drag in a turbulent pipe flow.

The experimental setup consisted of a pipe of length 4.25 m with an inner diameter of 16.3 mm. A membrane differential pressure meter was used to measure the pressure drop, while the flow rate was used an electro magnetic velocity meter. Flow at three different flow rates were studied, 9.5 liter/min, 12.1 liter/min, and 15 liter/min, the range of Reynolds number were 12400, 15600, and 19500 respectively.

The research of Dan Toonder el al. [5] explained that the drag-reduction in turbulent flow range was influenced by many parameters which were the concentration, the type of solvent, the type of polymer (flexibility, molecular weight, chemical composition), and the diameter of the pipe. Particularly, linear, high molecular weight polymers were the most effective drag reducers. Also it has been experimentally found that there exists a so-called maximum drag reduction asymptote when the friction data fall on this asymptote, then increasing the concentration does not result in higher drag reduction.

2.3 Type of Pipes

The types of pipes in drag reduction researches are usually straight pipes or coiled tubes. The drag reduction in straight pipes has been investigated since Toms' discovery and it is generally know that small polymer additive could be reduced up to 80%. For the drag reduction by additives in coiled tubes, it could be reduced the drag by 10 to 30% compared to the straight pipe.

2.3.1. Straight Pipe

The mechanism of flow in straight pipe without additives was first explained by Drew el al. [7] who investigated the relationship between the friction factor and the correlation of water flow in a straight pipe. The Drew's correlation has been used to compare the experiments of water flow in straight pipes until the presents.

The researches in the drag reduction with additives in straight pipes have been investigated since Toms' discovery [1]. It is commonly known that with only small parts per million polymers adding to the straight pipeline fluid, the drag could be reduced up to 80%. This phenomenon is usually explained by the fact that the fluid flow in straight pipe can be differenhated into three layers, which are laminar sub layer, buffer layer, and turbulent core [8]. Small parts per million polymers suppress the formation of turbulent bursts in the buffer layer and, thus, suppress the formation and propagation of turbulent eddies as shown in figure 2.4.

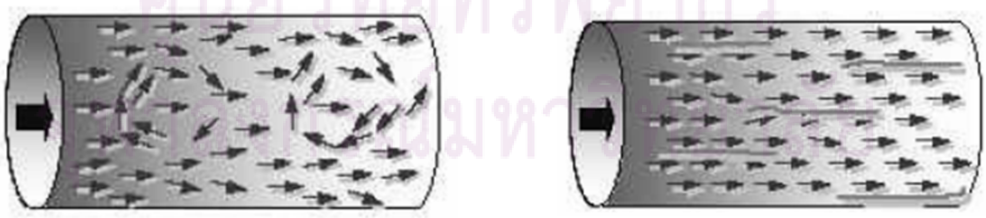

without additive with additive

Figure 2.3 Small Parts per Million Polymers Suppression [8]

A typical example of drag reduction in straight pipe research was published by Shah et al. [9]. The research presented an experimental study of drag reduction by a high-molecular-weight polymer in a 10 ft straight pipe. The pressure transducers with the range between 0-100 Psi, was used to measure the frictional pressure losses in the pipe. A micro sensor with the range between 0 and 30 gal/min, was used to measure the flow rate. Five different concentrations of polymer were tested to find the optimum concentration which maximized drag reduction in the pipe.

The obtained results in figure 2.4 showed that the drag reduction increased as the flow rate or Reynolds number increased. The drag could be reduced up to 75% for the investigated Reynolds number range with the concentration of the 0.07% of polymer.

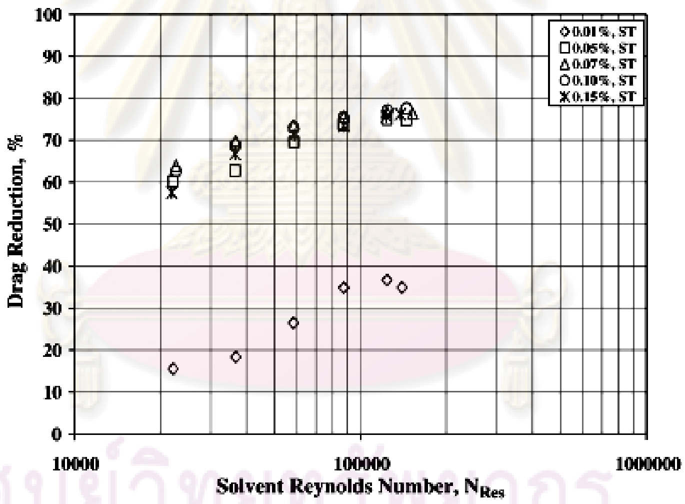

Figure 2.4 Percent Drag Reduction in Straight Pipe [9]

2.3.2. Coiled tube

The mechanism of flow in coiled tube without additives was first investigated by Eustice [10] who investigated and studied the effect of curvature change in water flow. In this early research on fluid flows in coiled tubes, the experiment set up (figure 2.5) used the water tank to generate a static head instead of a pump in recent researches. The pressure drop was measured by a manometer, the flow of water was regulated by the supply valve, and the flow rate was measured by collected water.

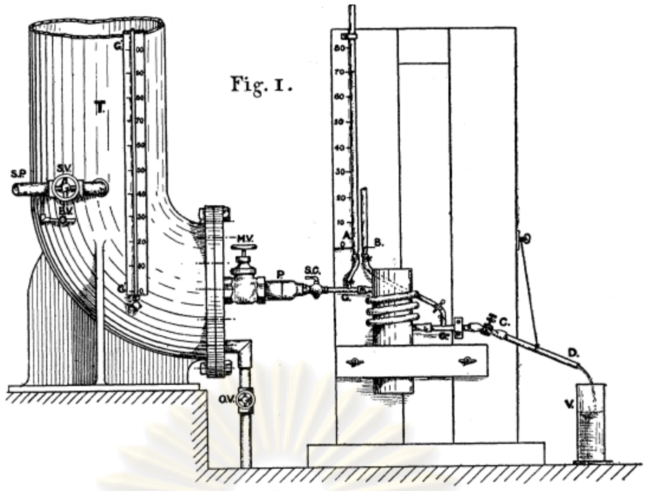

Figure 2.5 Experimental Set Up for Testing Flow in Coiled Tube [10]

The results of Eustice's experiment showed that the curvature ratio and number of coiled tube were the factors that increased friction in coiled tube. For comparison, flows in straight tubes were tested and compared with the friction loss in the coiled tubes. The results showed that the friction loss in coiled tube was five times as much when compared with the straight tube with the same length.

After Eustice's research was published, many researchers have been studied this topic to find the parameters and correlations. For example, Dean [11], through his theoretical analysis of the flow of incompressible Newtonian fluids in torus, confirmed the observation by Eustice. Various experimental as well as theoretical studies have also been attempted to obtain correlations for pressure drop in one-turn circular tubes and in regular coiled tubes. Srinivasan et al. [2] and Ramana Rao and Sadasivudu [12] described the correlation to predict the friction factor as a function of curvature ratio and Reynolds number for Newtonian fluids coiled tubes. Azouz et al. [13] experimentally investigated the tubular frictional pressure loss in coiled tubing and straight sections of seamed and seamless tubing and suggested that tubing curvature exerted more significant effect on the frictional pressure losses than the tubing seam.

For the drag reduction by additives in coiled tubes, Shah and Zhou [3] studied the drag reduction of polymer solutions in coiled tubing. Results showed that the tubing diameter, curvature ratio, and polymer concentration were important factors affecting the drag reduction in coiled-tubing. Zhou et al. [14] experimented the effects of coiled-tubing curvature on the drag-reduction behavior of polymeric fluids in turbulent flow and found that the coiled-tubing curvature could reduce the drag reduction by 10 to 30% comparing to the straight tubing, depending on the flow conditions.

2.4 Additives

There are many types of additives for drag reduction fluids that can be used to decrease pressure drop and increase the flow rate. The additives can be classified into three different types depending on the structure of each additive, namely polymers, surfactants, and fibers.

2.4.1. Polymers

Dissolving a small amount of polymer in water can reduce the friction of turbulent flow. This phenomenon was first discovered by Toms [1] and has since received a lot of attention. Though the polymers are active on the smallest length scales, they are able to influence the macroscopic scales of the flow. At first, Elperin et al. [15] suggested that it was the wall effect of adsorbed layer of polymer molecules at the pipe wall which lower the viscosity, create a slip, damp turbulence and prevent any initiation of vortices at the wall. However, from later experiments, it has become clear that the adsorption of the additives on surfaces could in fact be an experimental artificiality and it cannot be the reason for the drag-reducing effect.

A few years later, Lumley [16] outlined the physical phenomena of drag reduction and mentioned that the most effective drag reducing polymers were essentially linear in structure with maximum extension for a given molecular weight with polyethyleneoxide, polyisobutylene and polyacrylamide as typical examples of liner polymers.

Virk experiments [17] showed drag reduction was limited by an asymptotic, Vick's asymptote. Figure 2.6 shows the limiting asymptote for drag reduction by polymer additives which located between laminar and water turbulent line.

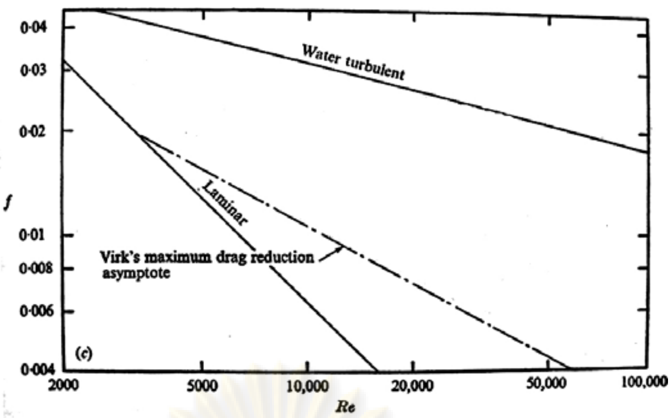

Figure 2.6 Phenomena of Drag Reduction by Polymer Additive [17]

Later studies put more emphases on the interaction between the polymer and the turbulence. Arianne [18] studied drag reduction by polymer additives in a turbulent pipe flow by laboratory experiments and numerical simulations. He stated that there were three models for explaining polymeric drag reduction. The first one was the extensional viscosity model in which the separated polymer molecules extend in long turbulent flow fields increased the thickness of the laminar sub layer. The second one was anisotropy model in which polymer aggregates might form large hydrodynamic domains which could stop small scale turbulence by resisting changes in alignment. The last one was elasticity model in which the long threads of the polymer solution interacted with the larger turbulent disturbances at the center of the pipe.

2.4.2. Surfactants

Surfactants are surface active agents that are the main component in soaps and detergents. Based on the molecular structure, concentration and type of solvent, three types of surfactants can be distinguished by shape: spheres, rods, and discs. The drag reduction ability of a surfactant solution depends strongly on the shape of these surfactants.

Although the effect of surfactant solutions on drag reduction was conducted by Mysels [19] as early as 1949, the research was not been as exhaustive and has received less attention than polymer solutions. It was not until a decade later that the interest in drag reduction by surfactants was revived by Dodge and Metzner

[20]. Surfactant solutions have become a favorite drag reducer owing to their chemical and mechanical stability that is an important requirement for practical applications. Development of surfactant systems that exhibited drag reduction at concentrations similar to dilute polymer solutions of less than 100 ppm have been disclosed in a number of recent patents.

When the flows of surfactant solutions were compared with those of polymer solutions, it was obvious that the drag reduction behaviors in these two cases were different. Shenoy [21] mentioned that surfactant solutions exhibited drag reduction with low wall shear stress values. The polymer solutions showed relatively small drag reduction at low Reynolds numbers and increasingly large reduction at high Reynolds numbers. These two behaviors were obviously a consequence of the structural difference between surfactant and polymeric structures. Therefore, the flexible polymer molecule needed to be extended by a large velocity gradient before its full drag reducing ability could be developed. The surfactant particles were much more easily directed at lower velocity gradients, but the surfactants broke at high shear stresses associated with large velocity gradients. In terms of equivalent molecular weight, surfactants were known to be larger than polymers and, therefore, they would shift the onset of drag reduction to a lower shear stress value.

2.4.3. Fibers

In the case of fiber additive in drag reduction, Inaba et al. [22] reported the drag reduction and heat transfer characteristics of the water suspension flow mixed with fine fibers in a circular straight pipe. Measurements of velocity and temperature profiles in a circular pipe were made in order to examine the flow drag and heat transfer characteristics of the laminar and turbulent flows. The results showed that for drag reduction, the fiber additives could reduce the friction loss by only 15-20%.

The fiber was also selected as a type of flow drag reduction additive instead of the polymer or surfactant. The microscope video picture of the fibers dispersing in water is shown in Figure 2.7. The video pictures of fibers showed the fiber diameter is in the range between 6.45 μm and 29.0 μm.

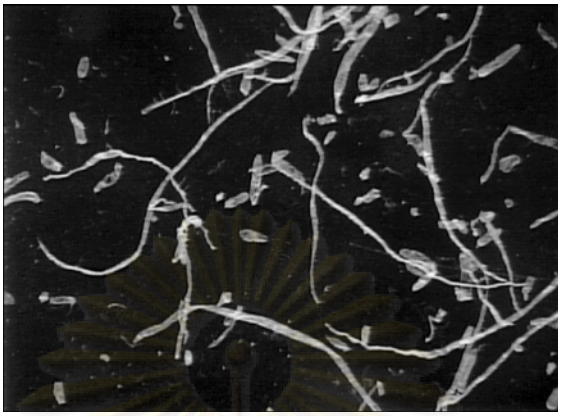

Figure 2.7 Photograph of Fiber Suspension in Water [22]

Fiber length could be divided into two groups. One was the long fiber group in which fiber length was about 50 times longer than the pulp fiber diameter. The other was the short pulp fiber group with a length of about 1–2 times the pulp fiber diameter. The fiber could be easily resolved since the pulp fiber consisted of the vegetable fiber used in paper manufacturing. Therefore, the fiber did not have a harmful effect on the environment, and it was promising material as a flow drag reduction additive. The main ingredient of the fiber was the cellulose which was a kind of polysaccharide. Moreover, it was difficult to dissolve in water and, therefore, the fibers containing in the liquid in dispersion phase was treated as suspension.

2.5 Literature Review Conclusions

After many previous studies of drag reduction problems have been considered, this problem can be classified in three main parts which depend upon methods or types of previous researches as shown in Table 2.1. All in all, most of researches in drag reduction were studied in turbulent flow range, tested in the straight tube, and used polymers as the additive.

Table 2.1 Summary of Literature Reviews on Drag Reduction Problem.

Year	Researcher	Flow		Tubes		Additives			
		Laminar	Turbulent	Straight	Coiled	Polymers	Surfactants	Fibers	without additives
1910	Eustice [10]		o		o				o
1927	Dean [11]		o		o				o
1932	Drew et al. [7]		o	o					o
1945	Agoston et al. [4]		o	o			o		
1949	Toms [1]		o	o		o			
1949	Mysels [19]		o	o			o		
1959	Dodge and Metzner [20]		o	o			o		
1967	Elperin [15]		o	o		o			
1969	Lumley [16]		o	o		o			
1970	Srinivasan et al. [2]		o		o				
1974	Ramana Rao and Sadasivudu [12]	o	o		o				
1975	Virk [17]		o	o		o			
1984	Shenoy [21]		o	o			o		
1995	Dan Toonder et al. [6]		o	o		o			
1996	Arianne [18]	o	o	o		o			
1998	Azouz et al. [13]		o	o	o	o			
1999	Warholic et al. [7]		o	o		o	o		
2000	Inaba et al. [22]	o	o	o				o	
2001	Watanabe and Udagawa [5]	o	o	o		o			
2003	Shah and Zhou [3]		o		o	o			
2004	Zhou et al. [14]		o		o	o			
2006	Shah et al. [9]		o	o	o	o			
2006	Omatayo [8]		o	o		o			

Chapter III

Coiled Tube Experiments

3.1 Experimental Set Up

The laboratory experiments were conducted in the re-circulatory coiled tubes flow facility of the Laboratory for Hydrodynamics, Department of Chemical Engineering, Manipal Institute of Technology, India between 1 June 2007 to 28 December 2007 under the guidance of Prof. Javadeva Bhat. The experimental set up as shown in Figure 3.1 consists of a tank, a pump, manometers, one by-pass and recycles valve, and circular tubes.

Figure 3.1 Coiled Tube Experimental Set up

The schematic diagram is shown in Figure 3.2. First, the tank is filled up with the experimental liquid. At the start of each experiment, the appropriate recycled valve is open to allow the pumped fluid to flow through the coiled tube under investigation. The flow rate is controlled by opening the recycled valve to the maximum, and then closing the by-pass valve. After the steady state is reached, the flow rate is kept constant before starting measuring data. The flow rate is obtained by measuring the time duration for the pre-weighted bucket to fill up with the fluid. The pressure drop across the coiled tubes is measured by a manometer.

In order to measure the two different ranges of pressure, two manometers are used, i.e. CCl_4 manometer for the laminar flows and mercury manometer for finding out at the turbulent range.

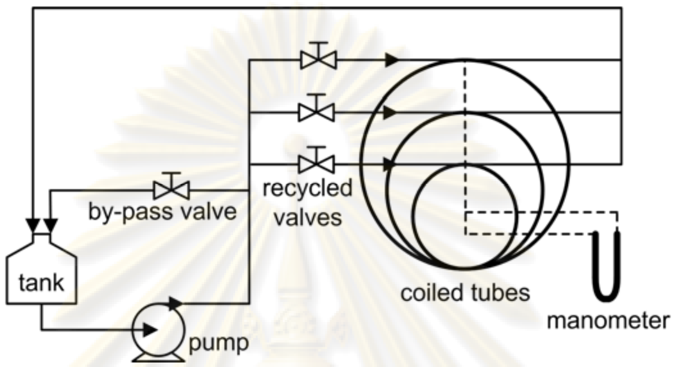

Figure 3.2 Details of Experimental Set up

3.2 Test Procedure

1. Switch on the pump.
2. Remove air bubbles in the manometers and check for leakage.
3. Open the valve of the desired coiled tube and wait until the steady state is reached
4. Keep the flow rate constant and collect the water in a pre-weighted bucket for specified amount of time.
5. Note down the manometer readings.
6. Then, increase the flow rate for the next reading and repeat the steps 3 to 5.
7. Increase the flow rate by opening the coil valve to the maximum, and then the close the bypass valve in order to further increase the flow rate. About seven readings each for laminar and turbulent range.
8. For drag reduction studies, the same procedure is adopted for required solutions.

However, some precautions are needed to be taken in order to ascertain good results.

1. To wait for steady state before readings.

2. To check if there are any air bubbles presented in the manometer as this can lead to erroneous reading.

3. The water should be collected for a considerable amount of time for accurate flow rate calculates.

3.3 Parametric Studies

The parameters that are varied in the experiments are the curvature ratios *r*/*R* between the tube/core radius and the additive concentrations.

3.3.1. Curvature Ratios

The specifications of the three coiled tubes are summarized in Table 3.1. The tubes, with outer diameter OD and inner diameter ID, are coiled into different core diameter CD. Due to the difference in core diameters, different numbers of coiled turns ensure an equal flow distance of 3.77 m.

Table 3.1 Specifications of Coiled Tubes

OD (m)	ID (m)	CD (m)	Ratio (*r*/*R*)	No. of turns
0.0076	0.00714	0.6	0.012	2
0.0076	0.00714	0.4	0.018	3
0.0076	0.00714	0.3	0.024	4

3.3.2. Additive Concentrations

Viscosity is an important factor in this experiment because the viscosity of a fluid changes when the additive concentration increases. The viscosity is defined as the force in Newton per square meter required to maintain a difference of velocity of meter per second, between two parallel layers of the held at a distance of meter from each other.

The viscosity, μ of a liquid is given by Hagen-Poiseuille's equation,

$$\mu = \pi r^4 t \rho g h / 8Vl \, , \tag{3.1}$$

Where r is radius, t is time, ρ is the density of liquid, g is the acceleration due to gravity, h is height of the column, V is volume of liquid, and l is length.

In this experiment, it can be assumed that the viscosity ratio between fluid 1 and 2 , μ_1 , μ_2 , is a linear relationship with the time t_1, t_2 .

$$\mu_1 / \mu_2 = t_1 / t_2 \tag{3.2}$$

In this thesis, five different types of fluids are studied, namely water and water-based Polyacraylamide (PAM), Polyvinyl alcohol (PVA), Anionic Polyacrylamide (Anionic PAM), and Cationic Polyacrylamide (Cationic PAM) solutions at various concentrations. The viscosity μ is measured by a capillarity viscometer and values are summarized in Table 3.2, as compared to the water viscosity of 0.0010000 Ns/m^2. It is found that the viscosity increases when the concentration of polymer additives increases. At the same concentration, the viscosity of the fluid with Anionic PAM is the highest viscosity of all test fluids. The viscosity of the fluid with PAM additive is less than the Anionic PAM additive fluid. Then, the viscosity of Cationic PAM is less than Anionic PAM and PAM additive solution. The viscosity of the fluid with PVA is the lowest viscosity of all fluids.

Table 3.2 Viscosity of Studied Fluids

Additive concentration	Viscosity μ (Ns/m^2)			
	PAM	PVA	Anionic PAM	Cationic PAM
0.01%	0.0010757	0.0010313	0.0011802	0.0010574
0.03%	0.0013107	0.0010444	0.0015927	0.0011514
0.05%	0.0014569	0.0010574	0.0023498	0.0012324
0.07%	0.0015065	0.0010862	0.0031749	0.0012536
0.10%	0.0021436	0.0010940	0.0042297	0.0016240
0.15%	0.0022506	0.0012689	-	-

3.4 Calculation

The dimensionless Fanning friction factor f is calculated by using basic equations of fluid mechanics.

Mass flow rate $\dot{m}$ is calculated from

$$\dot{m} = w / t \, , \tag{3.3}$$

where w is weight of collected water, and t is the time duration.

Velocity v is calculated from

$$v = \dot{m} / \rho A \, , \tag{3.4}$$

where $\dot{m}$ is mass flow rate, ρ is density of fluid, and A is cross sectional area of coiled tube.

The dimensionless Fanning friction factor f, which relates the head loss or pressure loss due to friction along a given length of pipe to the average velocity of the flow, is calculated from

$$f = dg\Delta H / 2lv^2 \, , \tag{3.5}$$

where d is tube diameter, g is gravity, l is length of manometric fluid, v is velocity and ΔH is the head loss, of which

$$\Delta H = R_m(\rho_m / \rho_t - 1) \, , \tag{3.6}$$

where R_m is difference in height of monomeric fluid, ρ_m is density of monomeric fluid and ρ_t is density of the tested fluid.

The Reynolds number Re is calculated by

$$\mathrm{Re} = \rho_t v d / \mu \, , \tag{3.7}$$

where Re is Reynolds number, ρ_t is density of the tested fluid, v is the velocity of fluid flow , d is inner tube diameter, and μ is fluid viscosity.

3.5 Experimental Results

Table 3.3-3.8 show the measurements and calculations for water test with different curvature ratios (*r/R*). The experimental data are measured by using different manometers which are CCl_4 and mercury monometer.

Table 3.3 Measurements and Calculations for Water Test with *r/R*: 0.012 (CCl_4)

R (cm)		Weight, w (kg)	Time, t (s)	Mass flow rate, $\dot{m}$ (kg/s)	Velocity, v (m/s)	Head loss, ΔH (m of water)	Reynolds Number, Re	Friction factor, f
57.2	48.2	0.08	10	0.008	0.200	0.052	1426	0.012246
65.5	40.0	0.16	10	0.016	0.400	0.149	2853	0.008674
70.7	34.8	0.19	10	0.019	0.475	0.210	3388	0.008660
83.5	22.0	0.26	10	0.026	0.650	0.360	4636	0.007922
93.0	12.4	0.30	10	0.030	0.750	0.473	5349	0.007799

Table 3.4 Measurements and Calculations Water Test with *r/R*: 0.012 (Hg)

R (cm)		Weight, w (kg)	Time, t (s)	Mass flow rate, $\dot{m}$ (kg/s)	Velocity, v (m/s)	Head loss, ΔH (m of water)	Reynolds Number, Re	Friction factor, f
49.2	42.8	0.40	10	0.040	1.000	0.803	7132	0.007451
53.2	38.8	0.63	10	0.063	1.576	1.807	11234	0.006758
56.2	35.8	0.76	10	0.076	1.901	2.560	13552	0.006579
60.9	31.1	0.94	10	0.094	2.351	3.740	16762	0.006282
65.4	26.6	1.10	10	0.110	2.752	4.870	19615	0.005973

Table 3.5 Measurements and Calculations for Water Test with *r/R*: 0.018 (CCl_4)

R (cm)		Weight, w (kg)	Time, t (s)	Mass flow rate, $\dot{m}$ (kg/s)	Velocity, v (m/s)	Head loss, ΔH (m of water)	Reynolds Number, Re	Friction factor, f
57.0	48.5	0.07	10	0.007	0.175	0.049	1248	0.015106
63.0	42.5	0.12	10	0.012	0.300	0.120	2139	0.012397
70.5	35.0	0.18	10	0.018	0.450	0.208	3209	0.009541
80.9	24.6	0.24	10	0.024	0.587	0.330	4190	0.008878
88.5	17.0	0.27	10	0.027	0.675	0.419	4814	0.008541

Table 3.6 Measurements and Calculations for Water Test with *r/R*: 0.018 (Hg)

R (cm)		Weight, *w* (kg)	Time, *t* (s)	Mass flow rate, $\dot{m}$ (kg/s)	Velocity, *v* (m/s)	Head loss, ΔH (m of water)	Reynolds Number, Re	Friction factor, f
49.8	42.2	0.42	10	0.042	1.050	0.954	7489	0.008025
53.8	38.2	0.64	10	0.064	1.601	1.958	11412	0.007094
59.4	32.6	0.86	10	0.086	2.151	3.364	15335	0.006750
63.4	28.6	1.00	10	0.100	2.502	4.368	17832	0.006482
67.2	24.8	1.11	10	0.111	2.777	5.322	19793	0.006410
72.5	19.5	1.26	10	0.126	3.152	6.653	22468	0.006218

Table 3.7 Measurements and Calculations for Water Test with *r/R*: 0.024 (CCl_4)

R (cm)		Weight, *w* (kg)	Time, *t* (s)	Mass flow rate, $\dot{m}$ (kg/s)	Velocity, *v* (m/s)	Head loss, ΔH (m of water)	Reynolds Number, Re	Friction factor, f
59.0	46.0	0.08	10	0.008	0.200	0.076	1426	0.017689
67.2	37.7	0.16	10	0.016	0.400	0.171	2853	0.010035
73.3	31.9	0.19	10	0.019	0.475	0.242	3388	0.009987
83.2	21.7	0.24	10	0.024	0.600	0.360	4279	0.009298
91.0	14.0	0.27	10	0.027	0.675	0.451	4814	0.009198
100.5	4.5	0.31	10	0.031	0.775	0.563	5527	0.008699

Table 3.8 Measurements and Calculations for Water Test with *r/R*: 0.024 (Hg)

R (cm)		Weight, *w* (kg)	Time, *t* (s)	Mass flow rate, $\dot{m}$ (kg/s)	Velocity, *v* (m/s)	Head loss, ΔH (m of water)	Reynolds Number, Re	Friction factor, f
49.3	42.7	0.38	10	0.038	0.950	0.828	6776	0.008514
52.6	39.2	0.56	10	0.056	1.401	1.682	9986	0.007959
56.7	35.3	0.73	10	0.073	1.826	2.686	13017	0.007480
60.5	31.5	0.87	10	0.087	2.176	3.640	15513	0.007137
66.2	25.8	1.04	10	0.104	2.602	5.071	18545	0.006958
71.8	20.2	1.19	10	0.119	2.977	6.477	21220	0.006787

3.6 Conclusions

In this chapter, the varied parameters in the experiments are the curvature ratios *r*/*R* between the tube/core radius and the additive concentrations. For the curvature ratio parameter, three differences in core diameters were studied. For the additive with different concentrations, the viscosity is an important factor because the viscosity of a fluid increases when the additive concentration increases. Comparing at the same concentration, the viscosity of the fluid with Anionic PAM is the highest viscosity of all test fluids. The viscosity of the fluid with PAM additive is less than the Anionic PAM additive fluid. The viscosity of Cationic PAM is less than Anionic PAM and PAM additive solution. The viscosity of the fluid with PVA is the lowest viscosity of all fluids.

Chapter IV

Experimental Results and Discussion

In this chapter, comparison between the experimental measurements and the previous researches is made. After that, the effect of polymer concentration and curvature ration will be analyzed. Then, the onset of drag reduction will be plotted on the Prandtl-Karman coordinates to investigate the drag reduction behavior of fluid. Finally, the empirical correlations will be developed and compared with the data points.

4.1 Water Test

The experimental measurements from water test are first compared with Srinivasan [2] and Ramana Rao [12] correlations which relate the Reynolds number with Fanning friction factor for turbulent flows of Newtonian fluids in coiled tubes. The water test results are compared with both Srinivasan and Ramana Rao correlations because the ranges of Reynolds number and the curvature ratio are applicable to this study.

Srinivasan correlation [2] is used when Re > 3,000 and curvature ratio $0.0097 \le r/R \le 0.1350$.

$$f = 0.084(r/R)^{0.1}\,\mathrm{Re}^{-0.2} \tag{4.1}$$

Ramana Rao correlation [12] is used when $3{,}000 \le \mathrm{Re} \le 27{,}000$ and curvature ratio $0.0159 \le r/R \le 0.0556$.

$$f = 0.0382e^{11.17r/R}\,\mathrm{Re}^{-0.2} \tag{4.2}$$

Figure 4.1 shows the plot of Fanning friction factor f and Reynolds number Re for water from Srinivasan and Ramana Rao correlations as well as experimental measurements. In all plots, the Fanning friction factor decreases when the Reynolds number increases and increases with the increase of the curvature ratio r/R.

The experimental results are in a closer agreement with the Ramana Rao correlation. This is due to the fact that the Srinivasan correlation is commonly used in very high Reynolds number range while the Ramana Rao correlation is applicable only in a low Reynolds number range (3,000 ≤ Re ≤ 27,000).

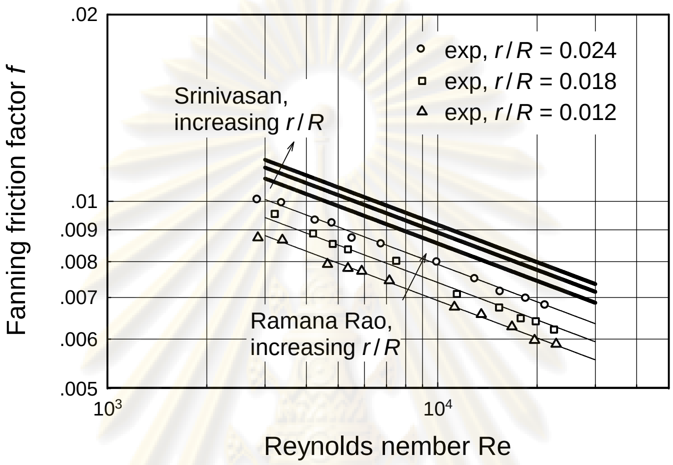

Figure 4.1 Fanning Friction Factor and Reynolds Number for Water

4.2 Effect of Additive Concentration on Drag Reduction

The drag reduction DR, exhibited when the additive is added into the solvent, is defined as the reduction of friction between the wall and fluid at the same Reynolds number,

$$DR = 1 - (f_p / f_s), \tag{4.3}$$

where f_p is the Fanning friction factor of polymer fluid and f_s is the Fanning friction factor of the solvent.

Figure 4.2 presents percentage drag reduction from various concentrations of polyacrylamide (PAM) additives at all three curvature ratios. As more PAM is added, the percentage drag reduction increases until the drag reduction reaches the maximum value at 0.10% by volume of polyacraylamide additive. The maximum drag reduction is 42% at the curvature ratio of 0.012 and Reynolds number of 20,000.

Figure 4.3 shows the effect of polyvinyl alcohol (PVA) additive concentration on the drag reduction. The best drag reduction is achieved at the PVA concentration of 0.03% by volume. The maximum drag reduction is 24% on the coiled tube with curvature ratio of 0.012 and Reynolds number of 20,000.

Figure 4.4 shows the effect of Anionic PAM additive concentration on the drag reduction. The maximum drag reduction of 60% is achieved at the Anionic PAM concentration of 0.07% by volume on the coiled tube with curvature ratio of 0.012 and Reynolds number of 20,000.

Figure 4.5 shows the effect of Cationic PAM additive concentration on the drag reduction. The maximum drag reduction of 57% is achieved at the Cationic PAM concentration of 0.05% by volume on the coiled tube with curvature ratio of 0.012 and Reynolds number of 20,000.

Comparing the percentage drag reductions for all test additives solutions, it is clear that the Anionic PAM is the most effective drag reducing additive because the longer molecule structure of Anionic PAM better facilitates absorption of the turbulent fluctuation at the center of the pipe and reduction of the friction between wall and fluid.

The study of the additive concentration effects on drag reduction has shown that when the concentration of polymer additives is higher than the best concentration, the percentage of drag reduction decreases. This is probably because the turbulent intensity is suppressed by the more viscous fluid from the higher additive concentration.

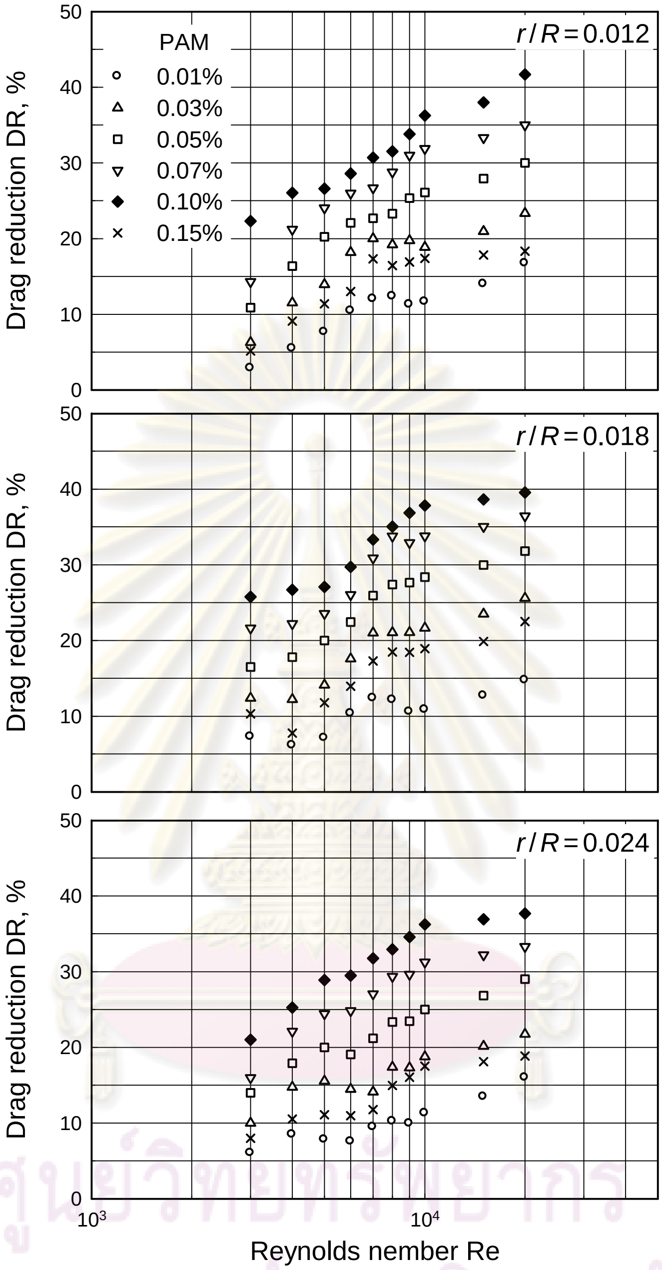

Figure 4.2 Effect of PAM Concentration on Drag Reduction

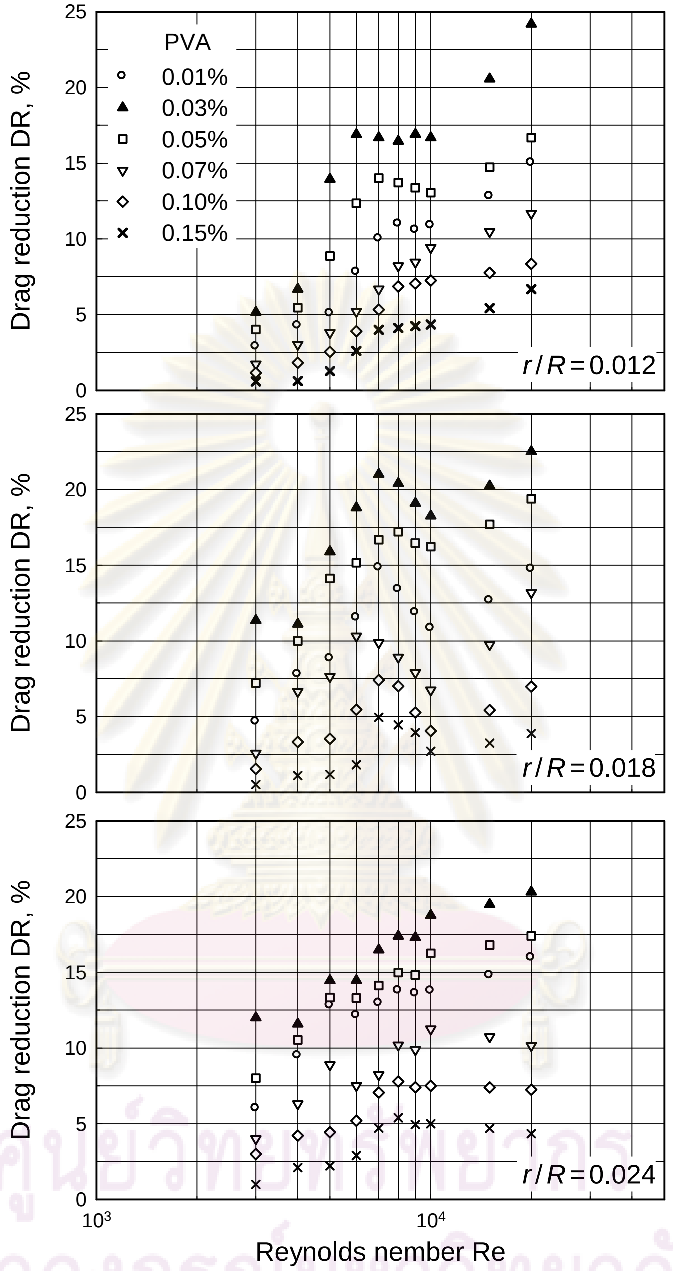

Figure 4.3 Effect of PVA Concentration on Drag Reduction

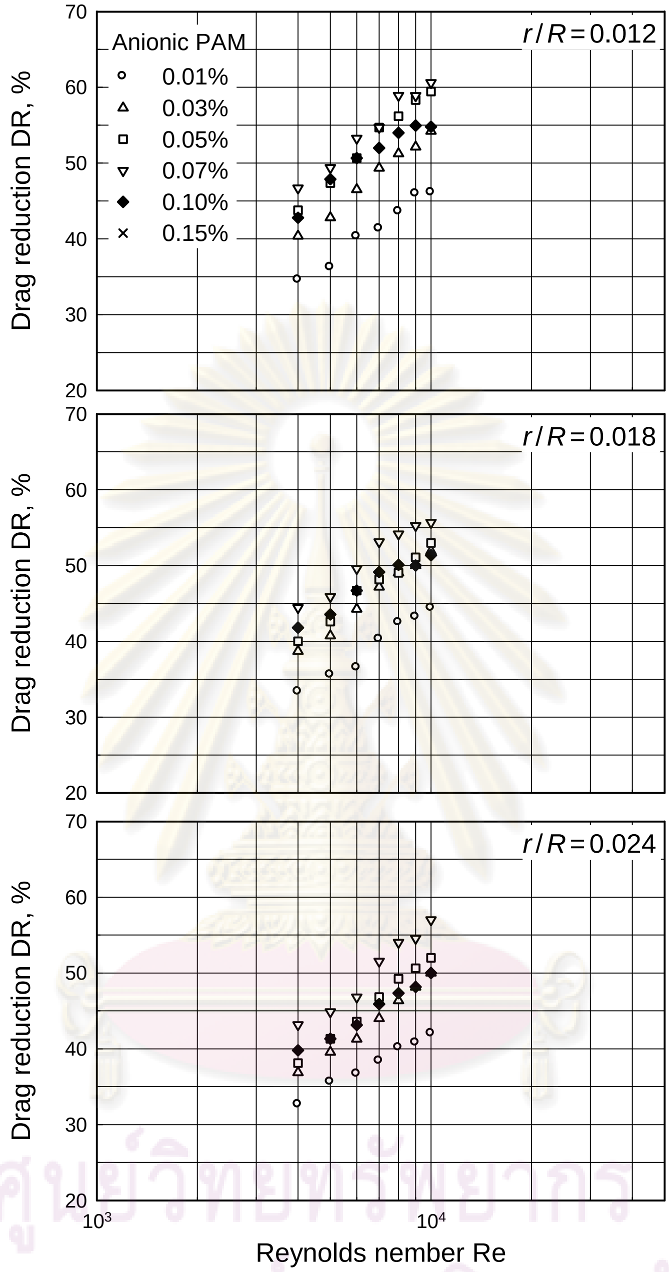

Figure 4.4 Effect of Anionic PAM Concentration on Drag Reduction

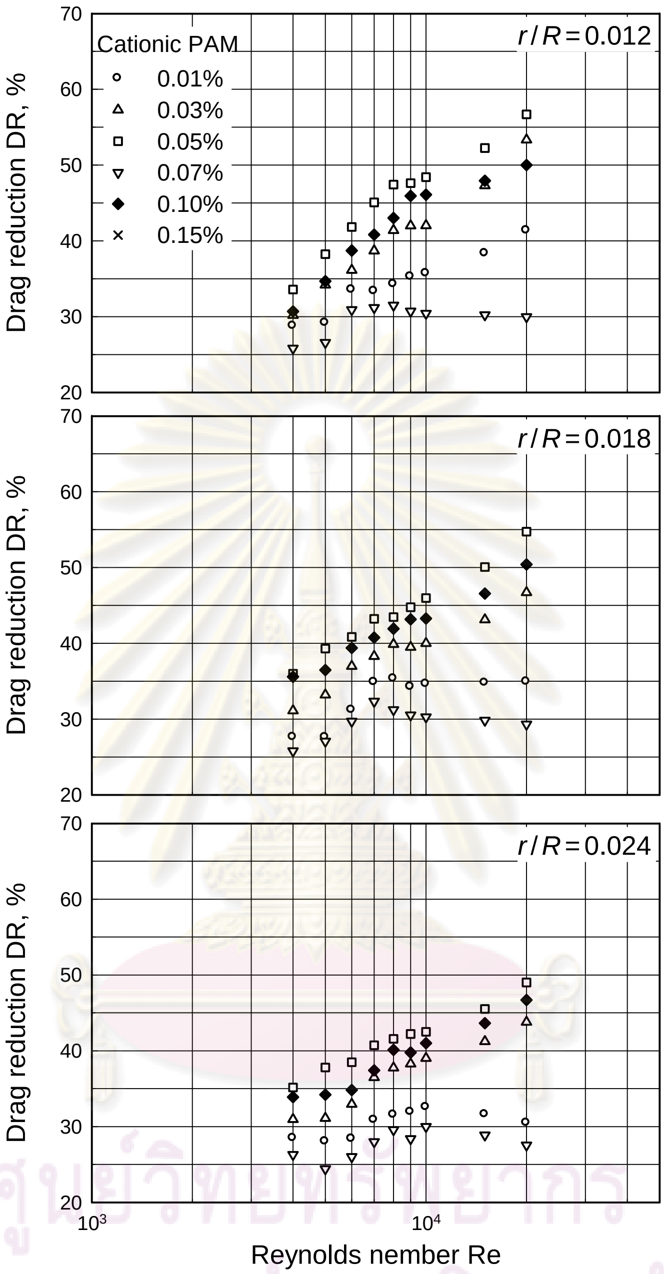

Figure 4.5 Effect of Cationic PAM Concentration on Drag Reduction

4.3 Effect of Curvature Ratio on Drag Reduction

In coiled tubes, the fluid in the tube center is forced outwards due to the centrifugal force. The slower part along the wall is forced inwards, causing secondary flow perpendicular to the main flow. This secondary flow effects increase as the curvature increases, resulting in a higher Fanning friction factors f than those of straight pipes. In short, curvature ratio is an important parameter as the friction loss between the wall and fluid in coiled tube is dependent on the core diameter of coiled tube.

The maximum possible drag reduction in laminar range for straight tubes is represented by

$$f = 16/\mathrm{Re} \tag{4.4}$$

The maximum drag reduction for turbulent flows of polymer solutions in straight tubes is limited by Virk's asymptote [17] as

$$1/\sqrt{f} = 19.0\log_{10}\mathrm{Re}\sqrt{f} - 32.4 \tag{4.5}$$

On another limit, the Srinivasan correlation [2] for coiled tubes is described in Equation (4.1). Even though the Ramana Rao correlation fits the water test results better, the Srinivasan correlation is used as it provides a more conservative limit.

Figure 4.6-4.9 show the relationship between the fanning factor f and Reynolds number Re at the three different curvature ratios for the 0.10% of PAM solution, 0.03% of PVA, 0.07% of Anionic PAM, and 0.05% of Cationic PAM solutions, respectively. For comparison, the limiting values in the laminar range, the Virk's asymptote and the Srinivasan correlation are given.

All figures show that the experimental data locate between the limiting values of the Virk's asymptote and Srinivasan correlation. As the curvature ratio increases, the friction loss and the associated Fanning fraction increase. This phenomenon is due to the centrifugal force in the circular coiled tubes as previously described.

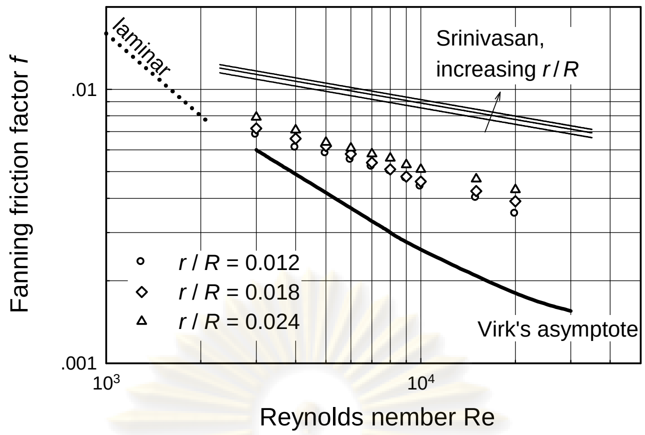

Figure 4.6 Effect of Curvature Ratio on 0.10% PAM Solution

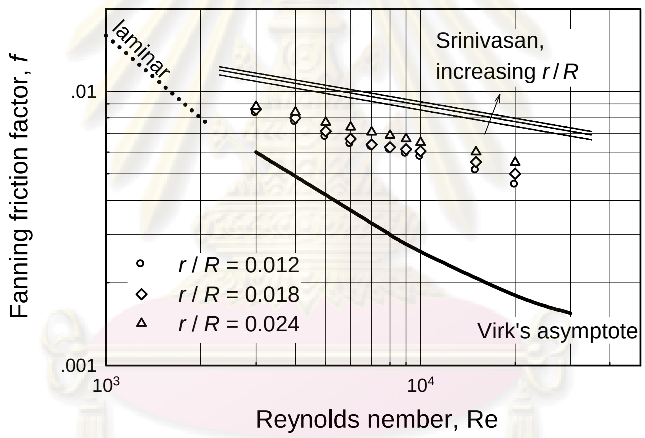

Figure 4.7 Effect of Curvature Ratio on 0.03% PVA Solution

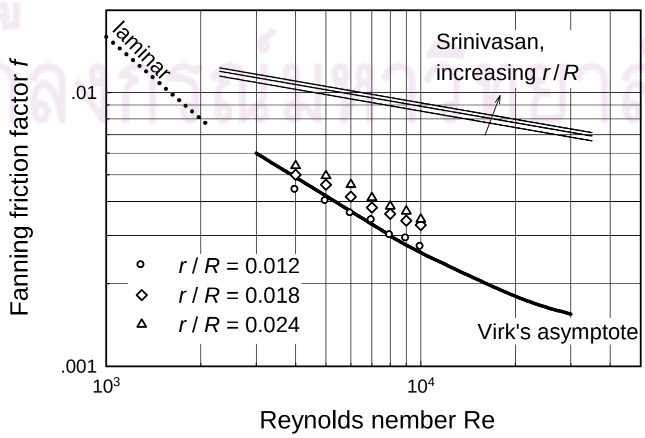

Figure 4.8 Effect of curvature ratio on 0.07% Anionic PAM solution

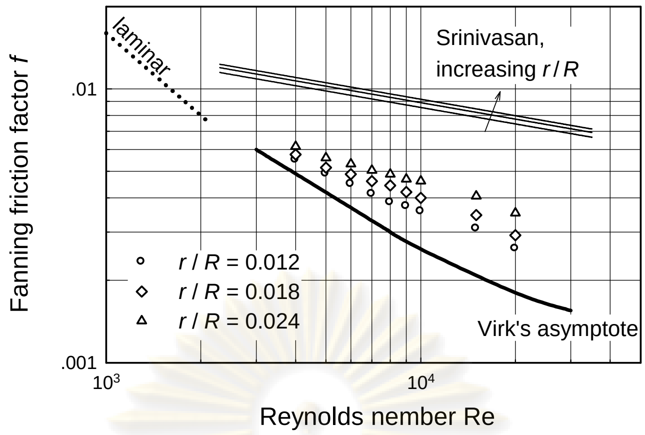

Figure 4.9 Effect of curvature ratio on 0.05% Cationic PAM solution

4.4 Onset of Drag Reduction

The drag reduction behavior of fluid can be better understood when the Fanning friction factors and Reynolds number data are plotted on the Prandtl-Karman coordinates along with the modified drag reduction envelope.

According to Shah et al. [9], the Virk's drag reduction envelope for a straight tube may be modified by replacing the zero drag reduction for straight tube based on Pandtl-Karman law in Equation (4.5) by Srinivasan correlation in Equation (4.1) for turbulent flows of Newtonian fluids in coiled tubes.

$$1/\sqrt{f} = 4.0\log_{10} \mathrm{Re}\sqrt{f} - 0.4 \qquad (4.6)$$

The Pandtl-Karman coordinates linearly relate drag reduction phenomena to flow and other polymer related variables. The axes of the plot are $1/\sqrt{f}$ as the ordinate and $\mathrm{Re}\sqrt{f}$ as the abscissa which is simply related to fluid property.

Figure 4.10 compares the drag reduction effects of 0.10% and 0.15% PAM additives on the Prandtl-Karman coordinates. It can be seen that the data sets exhibit linear relationships. As the polymer concentration is increased from 0.10% to 0.15%, the onset of drag reduction moves further to the right, indicating an onset delay of drag reduction.

Figures 4.11-13 shows a similar relationships for solutions with 0.03% and 0.05% by volume of PVA additives, 0.07% and 0.10% by volume of Anionic PAM additives, and 0.05% and 0.07% by volume of Cationic PAM additive. All graphs exhibit similar characteristics on both features. In addition, for all polymer concentrations used in this study, all measured data are above the base line.

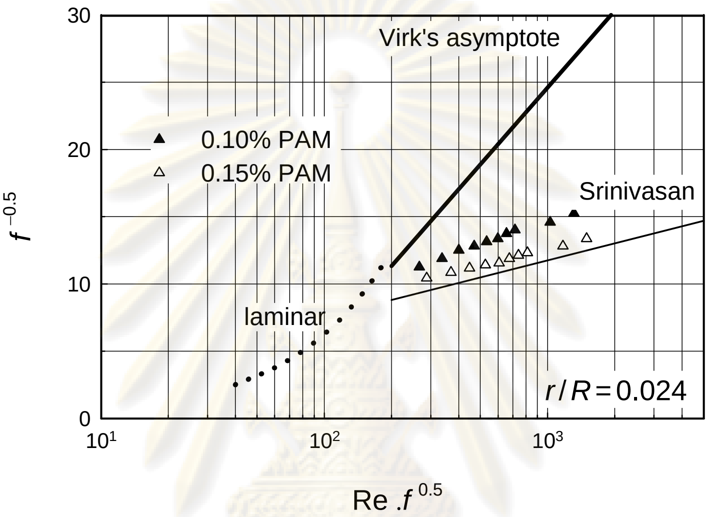

Figure 4.10 PAM Effect on Prandtl-Karman Coordinates

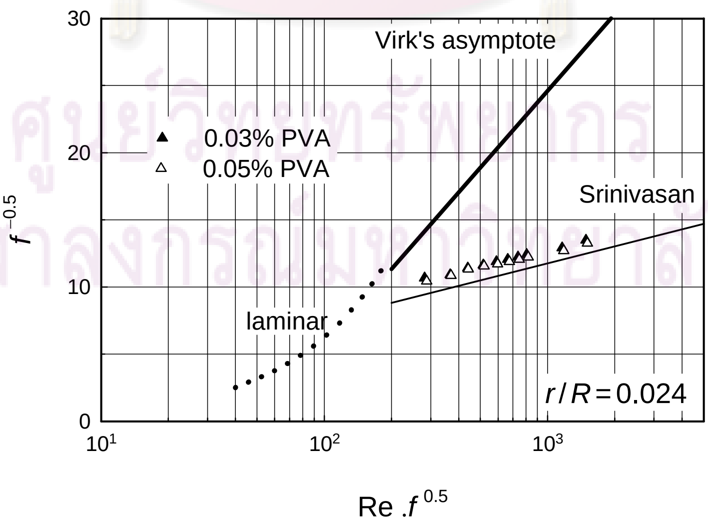

Figure 4.11 PVA Effect on Prandtl-Karman Coordinates

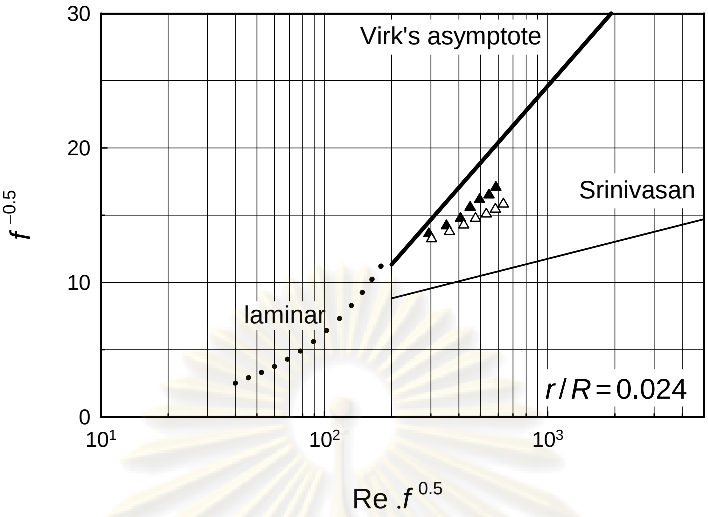

Figure 4.12 Anionic PAM Effect on Prandtl-Karman Coordinates

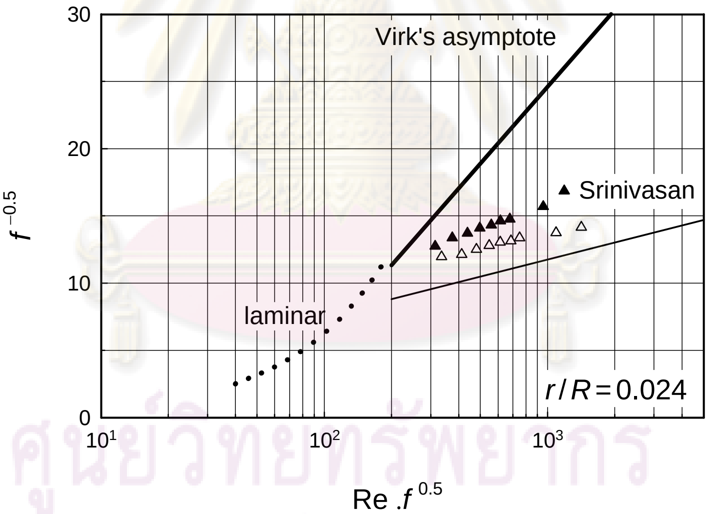

Figure 4.13 Cationic PAM Effect on Prandtl-Karman Coordinates

4.5 Correlation

The empirical correlations for the Fanning friction factor prediction as a function of Reynolds number and curvature ratio are developed from the data points at the best concentration with different curvatures. From Srinivasan et al. [2], the correlation for coiled tubes assumes by the following definition

$$f = A(r / R)^{B} \mathrm{Re}^{C}, \tag{4.7}$$

where the values of correlation coefficients - A , B , and C - depending on the type of polymer additives, curvature ratio, and range of Reynolds number. By fitting experimental results with least square regression with Equation (4.5), correlation coefficients can be obtained with satisfactory fitting as shown in Table 4.1.

Table 4.1 Predicted Correlation for Ranges 3,000 ≤ Re ≤ 20,000 and 0.012 ≤ *r*/*R* ≤ 0.024

Additive	Correlation	Fitting R^2
0.10% PAM	$f = 0.2284(r/R)^{0.1923}\,\mathrm{Re}^{-0.3336}$	0.9846
0.03% PVA	$f = 0.1590(r/R)^{0.1780}\,\mathrm{Re}^{-0.2763}$	0.9750
0.07% Anionic PAM	$f = 0.1238(r/R)^{0.3265}\,\mathrm{Re}^{-0.5046}$	0.9908
0.05% Cationic PAM	$f = 0.5149(r/R)^{0.3060}\,\mathrm{Re}^{-0.3925}$	0.9788

Figures 4.14 -17 compare the experimental data points and the predicted correlations. The R^2 values of obtained correlation coefficients are close to unity, indicating excellent agreements between the experimental data and predicting correlation equation.

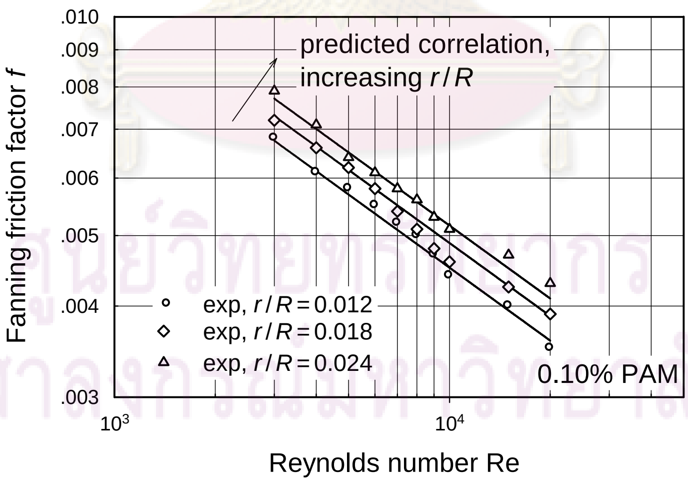

Figure 4.14 Predicted Correlation for 0.10% PAM Solution

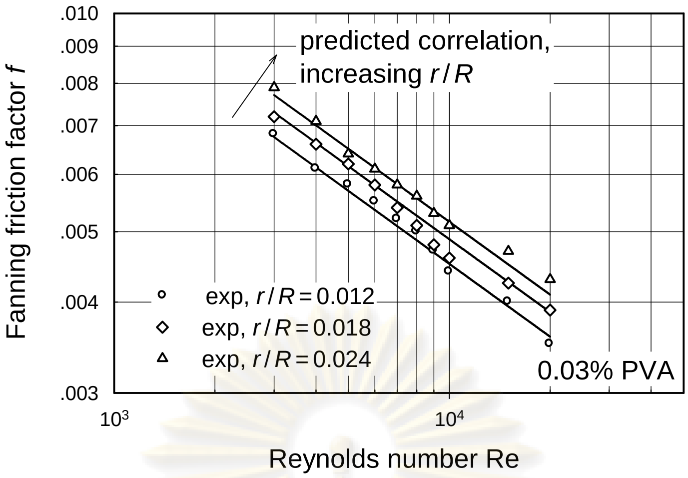

Figure 4.15 Predicted Correlation for 0.03% PVA Solution

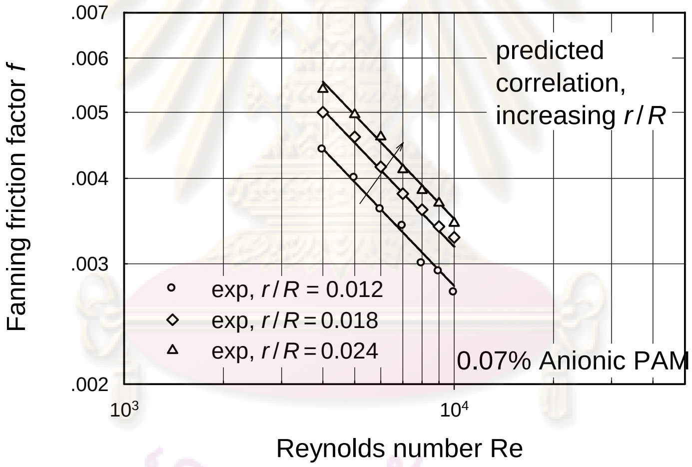

Figure 4.16 Predicted Correlation for 0.07% Anionic PAM Solution

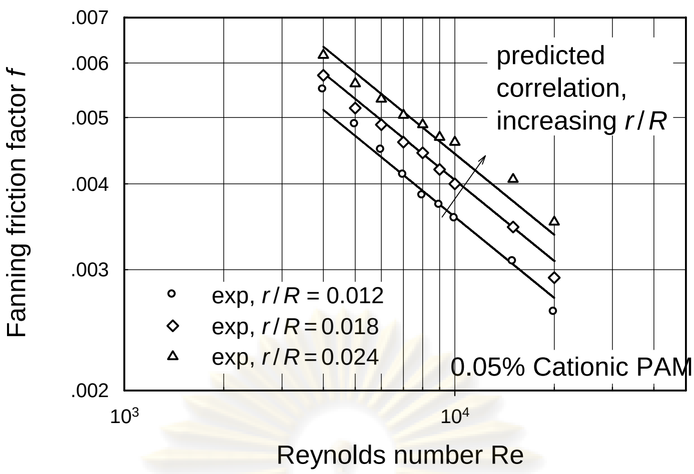

Figure 4.17 Predicted Correlation for 0.05% Cationic PAM Solution

4.6 Conclusions

The experimental measurements from water test are first compared with Srinivasan [2] and Ramana Rao [12] correlations which relate the Reynolds number with Fanning friction factor for turbulent flows of Newtonian fluids in coiled tubes. The experimental results are in a closer agreement with the Ramana Rao correlation. This is due to the fact that the Srinivasan correlation is commonly used in very high Reynolds number range while the Ramana Rao correlation is applicable only in a low Reynolds number range (3,000 ≤ Re ≤ 27,000).

The study of the additive concentration effects on drag reduction have been shown that when the concentration of polymer additives is higher than the best concentration, the percentage drag reductions decrease. This is probably because the turbulent intensity is suppressed by the more viscous fluid from the higher additive concentration. In addition, the study of the curvature ration has been shown when the curvature ratio increases, the friction loss and the associated Fanning fraction increase. This phenomenon is due to the centrifugal force in the circular coiled tubes as previously described.

The empirical correlations for the Fanning friction factor prediction as a function of Reynolds number and curvature ratio are developed from the data points at the best concentration with different curvatures. When comparing the experimental data points with the predicted correlations, the R^2 values of obtained correlation coefficients are close to unity, indicating excellent agreements between the experimental data and predicting correlation equation.

Chapter V

Computational Fluid Dynamics

5.1 Introduction to CFD Analysis

Computational Fluid Dynamics, CFD [23] is the science of predicting fluid flow, heat and mass transfer, chemical reactions, and related phenomena by solving numerically the set of governing mathematical equations

The conservation of mass equation is

$$\frac{\partial \rho}{\partial t} + div(\rho U) = 0 \qquad (5.1)$$

The conservation of momentum is

$$\rho \frac{\partial U}{\partial t} + \rho(U.\nabla)U = -\nabla p + \rho \vec{g} + \nabla.\tau_{ij} \qquad (5.2)$$

5.2 Procedure of CFD

CFD procedure is to replace the continuous problem domain with a discrete domain using a grid system. In the continuous domain, each flow variable is defined at every point in the domain. For instance, the pressure p in the continuous 1D domain shown in the figure below would be given as

$$p=p(x),\ 0 \leq x \leq 1$$

In the discrete domain, each flow variable is defined only at the grid points. Thus, in the discrete domain shown below, the pressure would be defined only at the N grid points.

$$p_i = p(x_i),\ i = 1,2,....,N$$

Continuous domain | Discrete domain

$0 \leq x \leq 1$ | $x = x_1, x_2, x_3, ..., x_N$

Coupled PDEs + Boundary conditions in continuous variables | Coupled algebraic equations. In discrete variables

Figure 5.1 The Strategy of CFD

In a computational fluid dynamics solution, one would directly solve for the relevant flow variables only at the grid points. The values at other locations are determined by interpolating the values at the grid points.

The governing partial differential equations and boundary conditions are defined in terms of the continuous variables p, $\vec{V}$ etc. One can approximate these in the discrete domain in terms of the discrete variables p_i, $\vec{V}_i$ etc. The discrete system is a large set of coupled, algebraic equations in the discrete variables. Setting up the discrete system and solving it (which is a matrix inversion problem) involves a very large number of repetitive calculations and is done by the digital computer.

5.3 Finite-Volume Method

The finite-volume method is commonly referred to as a cell and a grid point as a node. In 2D, one could also have triangular cells. In 3D, cells are usually hexahedrals, tetrahedrals, or prisms. In the finite-volume approach, the integral form of the conservation equations are applied to the control volume defined by a cell to get the discrete equations for the cell. The integral form of the continuity equation for steady, incompressible flow is

$$\int_{s} U \cdot \hat{n} dS = 0 \tag{5.3}$$

The integration is over the surface S of the control volume and $\hat{n}$ is the outward normal at the surface. Physically, this equation means that the net volume flow into the control volume is zero.

The methodology used in deriving discredited equations in the one-dimensional case can be extended to two-dimensional problems. The portion of the two-dimensional grid used for the discrimination is shown in Figure 5.2. The two-dimension rectangular cell consists of four faces and the cell center. The velocity at face i is taken to be $U_i = u_i\hat{i} + v_i\hat{j}$.

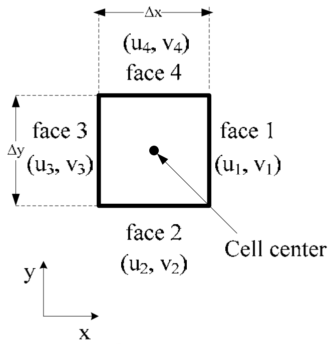

Figure 5.2 Two Dimension Rectangular Cell

Applying the mass conservation Equation (5.3) to the control volume defined by the cell gives

$$-u_1\Delta y - v_2\Delta x + u_3\Delta y + v_4\Delta x = 0 \tag{5.4}$$

This is the discrete form of the continuity equation for the cell. It is equivalent to summing up the net mass flow into the control volume and setting it to zero. Thus it ensures that the net mass flow into the cell is zero i.e. that mass is conserved for the cell. Usually, the values at the cell centers are stored. The face values u_1, v_2, etc. are obtained by suitably interpolating the cell-center values at adjacent cells. Similarly, one can obtain discrete equations for the conservation of momentum and energy for the cell. One can readily extend these ideas to any general cell shape in 2D or 3D and any conservation equation.

5.4 Commercial Software Validations

The numerical simulation first considers the accuracy of the commercial software, FLUENT [24], to make sure that the commercial software is accurately reliable by testing with the basic fluid flow problems. FLUENT is a computational fluid dynamics (CFD) software package to stimulate fluid flow problems. It uses the finite volume method to solve the governing equations for a fluid. The software provides the capability to use different physical models such as incompressible or compressible, inviscid or viscous, laminar or turbulent etc.

In the beginning of computational simulation, the FLUENT software version 6.3.26 [24] will be tested on the laminar pipe flow and turbulent pipe flow problems. Figure 5.3 shows the simulation model of circular pipe of constant cross-section with pipe diameter D=0.00714 m and length L=0.2142 m.

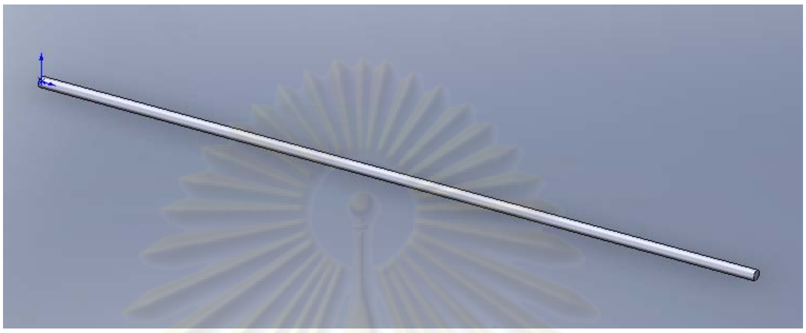

Figure 5.3 Circular Pipe

5.4.1. Laminar Pipe Flow Problem Validations

The laminar pipe flow problem is a basic fluid flow problem. This well known problem is used to introduce the basic concepts of CFD including, the finite-volume mesh, the discrete nature of the numerical solution, and the dependence of the result on the mesh refinement. The Numerical results are presented for a sequence of finer meshes, and the dependency of the truncation error on mesh size is verified experimentally. The comparison test results validate the analysis.

A procedure can be obtained by following these six steps;

1. Problem Specification

2. Define Boundary Conditions

3. Define the Solution

4. Refine Mesh

5. Analyze the Results

6. Compare the Results with Theoretical Solution

- Problem Specification

The pipe is represented in 2D by a rectangle. The pipe geometry is displayed in Figure 5.4. The geometry consists of a wall, a centerline, and periodic inlet and outlet boundaries. The radius and the length of the pipe can be specified.

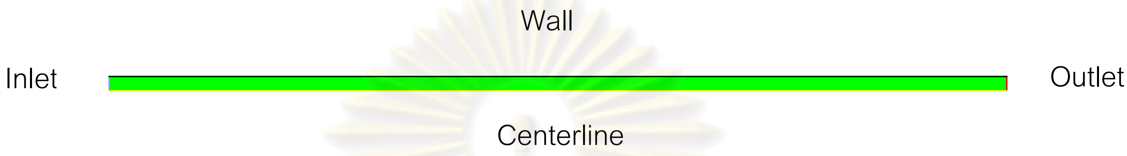

Figure 5.4 Boundary Conditions for Circular Pipe

For the laminar, the inlet velocity is defined as V_{in}=0.01403 m/s. Consider the velocity to be constant over the inlet cross-section. Take density ρ =998.2 kg/ m^3 and coefficient of viscosity μ = 0.00103 kg/ms. The Reynolds number Re based on the pipe diameter

$$\mathrm{Re} = \frac{\rho V_{in} D}{\mu} = 100$$

- Define Boundary Conditions

The mass flow rate or the fluid can be specified. The assigned boundary conditions in FLUENT are shown in Table 5.1

Table 5.1 Boundary Conditions

Edge Position	Name	Type
Left	inlet	VELOCITY_INLET
Right	outlet	OUTFLOW
Top	wall	WALL
Bottom	centerline	AXIS

- Define the Solution

The mesh is exported to FLUENT along with the physical properties and the initial conditions specified. The material properties and the initial conditions are read through the case file. Instructions for the solvers are provided through a journal file. When the solution is converged or the specified number of iterations is met, FLUENT exports data.

- Refine Mesh

After the solution is converged, it is important to assess the dependence of results on the mesh used by repeating the same calculation on different meshes and comparing the results. Figure 5.5 shows six different meshes of 100x5, 100x20, 100x40, 200x40, 400x40, and 800x40.

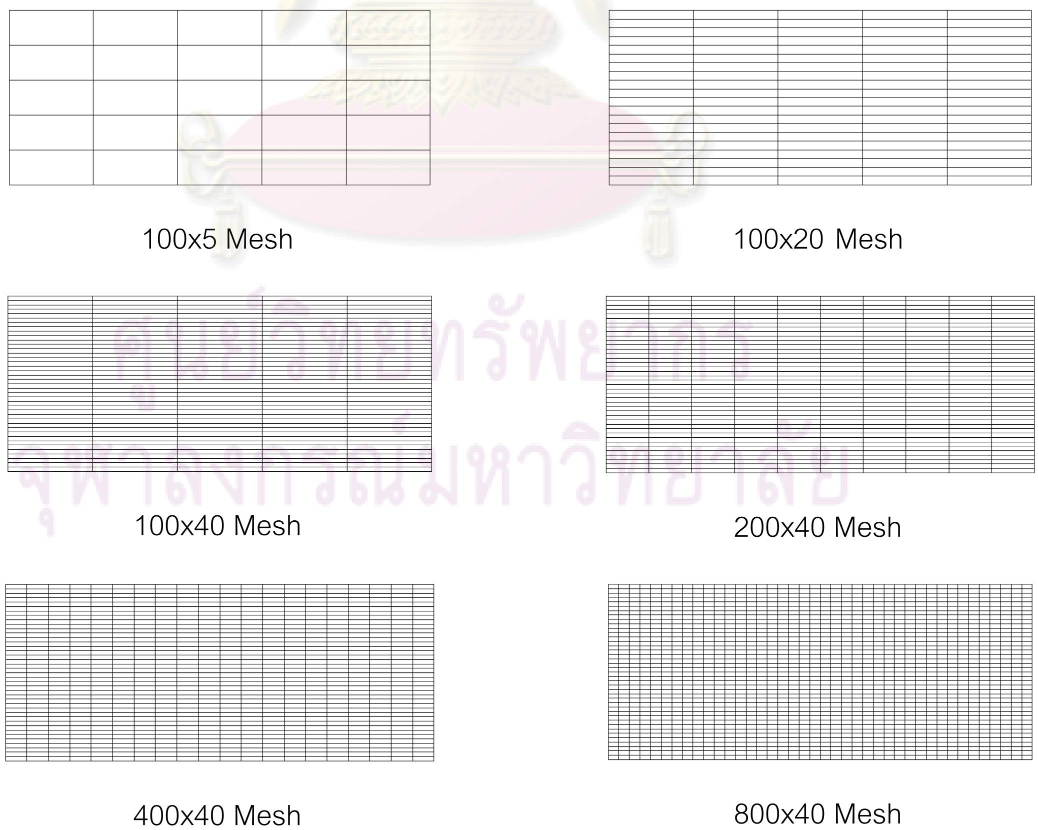

Figure 5.5 Refine Mesh for Laminar Problem

- Analyze the Results

Firstly, this brings up a plot of the axial velocity as a function of the distance along the centerline of the pipe. Figure 5.6 shows the axial velocity that the velocity reaches a constant value beyond a certain distance from the inlet. This is the fully-developed flow region. Figure 5.7 shows the velocity plot at the outlet as a function of the distance from the center of the pipe.

Additionally, the same calculation on different meshes and comparing the results show that the axial velocity and velocity profile plots are not changed when the mesh of geometry is 400x40, thus, the 400x40 mesh give the mesh independent results.

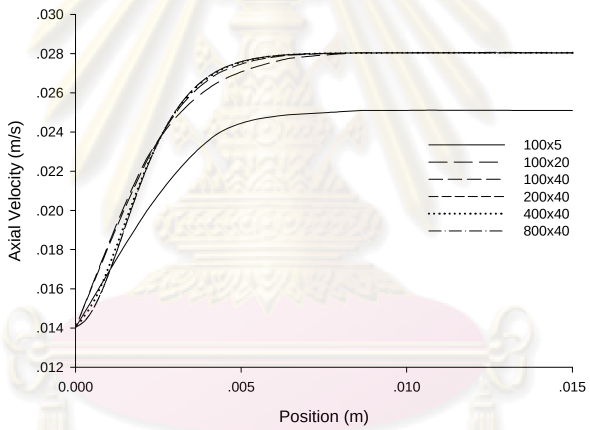

Figure 5.6 Axial Velocity Plot for Laminar Flow

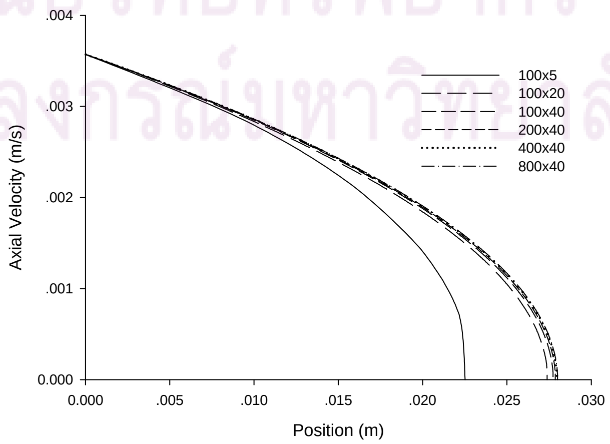

Figure 5.7 Velocity Profile Plot for Laminar Flow

- Compare the Results with Theoretical Solution

To compare the results with theoretical solution for incompressible laminar flow, equation (5.5) describes the variation of local fluid *u* across the pipe which can be seen from the equation that the velocity profile is parabolic.

$$u/u_{max} = 1 - r^2/R^2 \qquad (5.5)$$

The maximum velocity occurs on the pipe centerline (*r* = 0), hence,

$$u_{max} = 2V \qquad (5.6)$$

The flow is internal flow which is constrained by boundary walls. The viscous effect will grow and permeate the entire length of flow. In the pipe through the entrance region a nearly inviscid upstream flow converges and enters the tube. The viscous boundary layer growing downstream retards the axial flow velocity *u(r,x)* at the wall and thereby accelerates the center-core flow to maintain the incompressible continuity requirement. Figure 5.8 shows the comparison of the results with the theoretical solution. The simulation result is quite close to the theoretical solution.

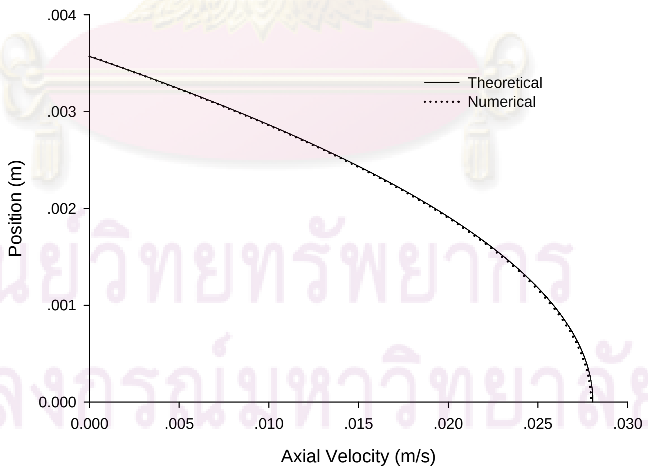

Figure 5.8 Axial Velocity Distribution Comparing with the Theoretical Solution

5.4.2. Turbulent Pipe Flow Problem Validations

The turbulent pipe flow problem is also a basic fluid flow problem which is used to introduce the basic concepts of CFD. Turbulence is selected in the Physics form of the operation menu, the appropriate turbulence model and wall treatment is applied based upon the Reynolds number. The physical models are recommended as shown in Table 5.2

Table 5.2 Turbulence Models Based on Pipe Reynolds Number [24]

Reynolds Number	Models
Re<2000	Laminar Flow
2000 = Re<10000	k- omega Model
10000 = Re<15000	k- epsilon with Enhanced Wall Treatment
Re = 15000	k- epsilon Model

A procedure can be obtained by following these six steps;

1. Problem Specification

2. Define Boundary Conditions

3. Define the Solution

4. Refine Mesh.

5. Analyze the Results

6. Compare the Results with Theoretical Solution

- Problem Specification

The pipe is represented in 2D by a rectangle grid. The pipe geometry is displayed in figure 5.3. The geometry consists of a wall, a centerline, and inlet and outlet boundaries. For the turbulent, the inlet velocity is defined as V_{in}=1.445 m/s. which the Reynolds number is 10,000.

- Define Boundary Conditions

The following boundary conditions are assigned in FLUENT; Boundary also assigned as in table 5.1

- Define the Solution

The mesh is exported to FLUENT along with the physical properties and the initial conditions specified. When the solution is converged or the specified number of iterations is met, FLUENT exports data.

- Refine Mesh

It is very important to assess the dependence of results on the mesh used by repeating the same calculation on different meshes. Figure 5.9 shows the mesh of four difference meshes, i.e., 100x40, 200x40, 400x40, and 800x40.

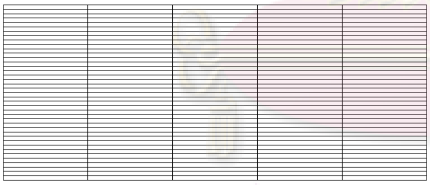

Grid 100x40

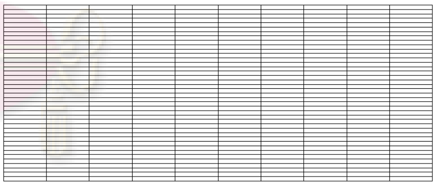

Grid 200x40

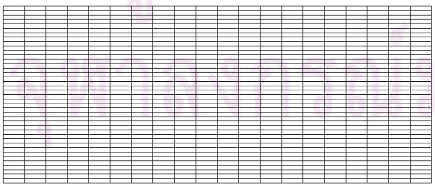

Grid 400x40

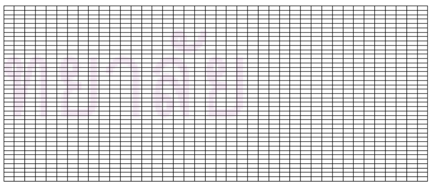

Grid 800x40

Figure 5.9 Refine Mesh for Turbulent Problem

- Analyze the Results

Turbulent flows are significantly affected by the presence of walls. The *k*-ε turbulence model is primarily valid away from walls and special treatment is required to make it valid near walls. The near-wall model is sensitive to the grid resolution which is assessed in the wall unit y^+ which is defined in section 10.9.1 of the FLUENT user manual. [24] Based on the grid considerations for turbulent flow simulations, the following physical models are recommended as presented in Table 5.3.

Table 5.3 Grid Considerations for Turbulent Flow Simulations [24]

Reynolds Number	Models
2000<Re<15000	Enhanced Wall Treatment Y plus<5.0
Re >15000	Standard Wall Functions Y plus>30

Figure 5.10 shows plot of y^+ values for wall-adjacent cells to check how it compares with the recommendation mentioned above. For the 400x40 mesh, the wall y^+ value is between 3.95 and 4.10 in fully developed flow. Since this is less than 5, the near-wall grid resolution is acceptable.

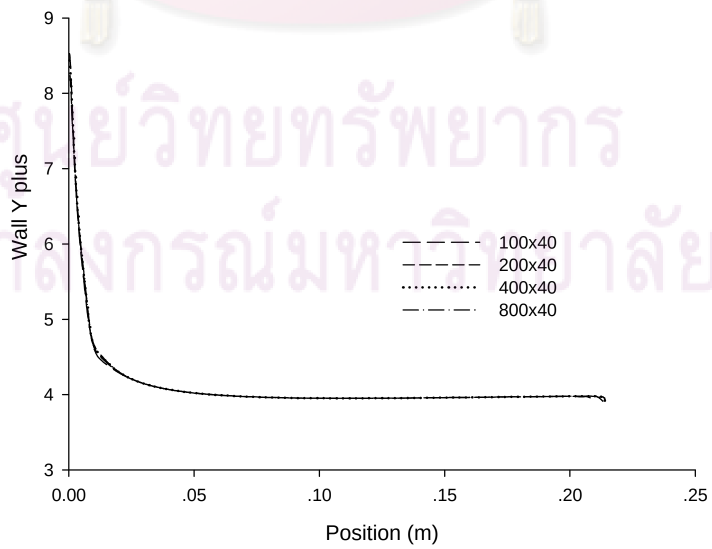

Figure 5.10 Wall Y plus Plot

Figure 5.11 shows a plot of the axial velocity as a function of the distance along the centerline of the pipe. The velocity reaches a constant value beyond a certain distance from the inlet. This is the fully-developed flow region. The fully developed region starts around x=0.15m with the centerline velocity becoming constant at a value of 1.80 m/s.

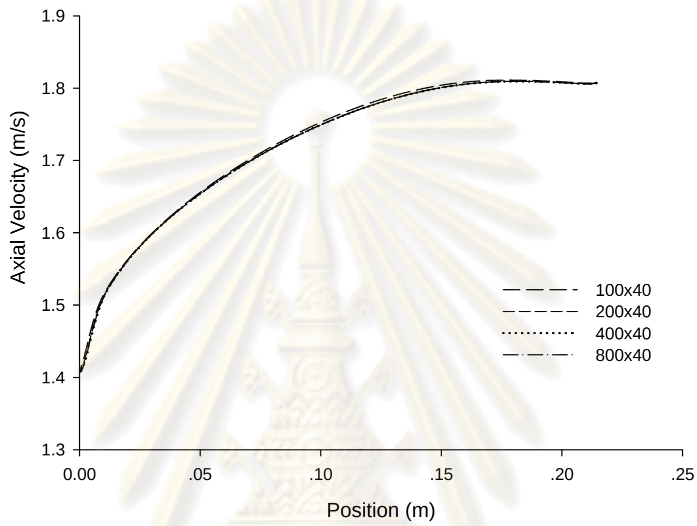

Figure 5.11 Axial Velocity Plot for Turbulent Flow

Figure 5.12 illustrates the velocity plot at the outlet as a function of the distance from the center of the pipe. The axial velocity is maximum at the centerline.

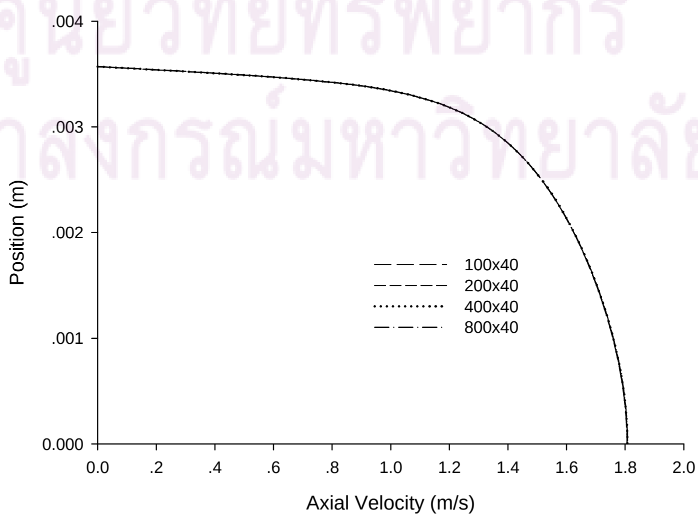

Figure 5.12 Velocity Profile Plot for Turbulent Flow

All in all, the results show that the y^+ is less than 5 and velocity profile plot is not changed when the mesh of geometry is finer than 400x40, thus, using the 400x40 mesh is fine enough to give the mesh-independent results.

- Compare the Results with Theoretical Solution

From the recommendations in Table 5.2 and 5.3, the first simulation is studied on the turbulent pipe flow with Reynolds number 10,000 by using different model the k-ε model [25] with enhanced wall treatment and k-ω model [26] to find the approximation model for the further study. Figure 5.13 displays the results of two different model comparisons with the theoretical solution, 1/7 law. The plot shows that the k-ε with enhanced wall treatment model and k-ω model are not closed to the theoretical solution because the numerical models in commercial software are not suitable to predict the flow of fluid in transition range.

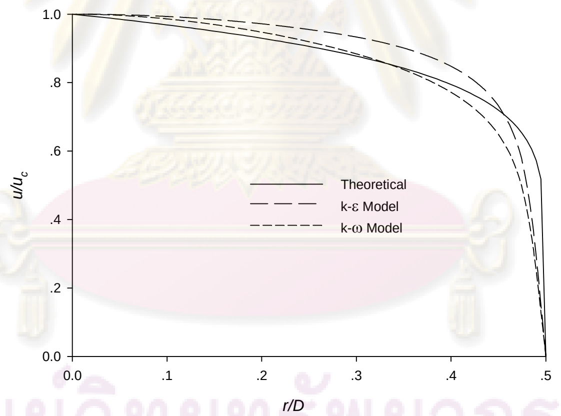

Figure 5.13 Result Comparison with Theoretical Solution, Re=10,000

To find to suitable range of Reynolds number for the simulation by commercial software, the simulations with different Reynolds number are studied. Figure 5.14 shows the simulation with two different models at the Reynolds number range between 3,000-100,000. The results commonly show that in the Reynolds number range below 50,000, the k-ε with enhanced wall treatment model and k-ω model are not closed to the theoretical solution but, for the Reynolds number range more than 50,000, the result is well closed to the theoretical solution. In addition, Re=100,000, the simulation with two different models are closer to the solution. This is because the simulation over the transition range, the algorithms in turbulent model is suitable at high Reynolds number.

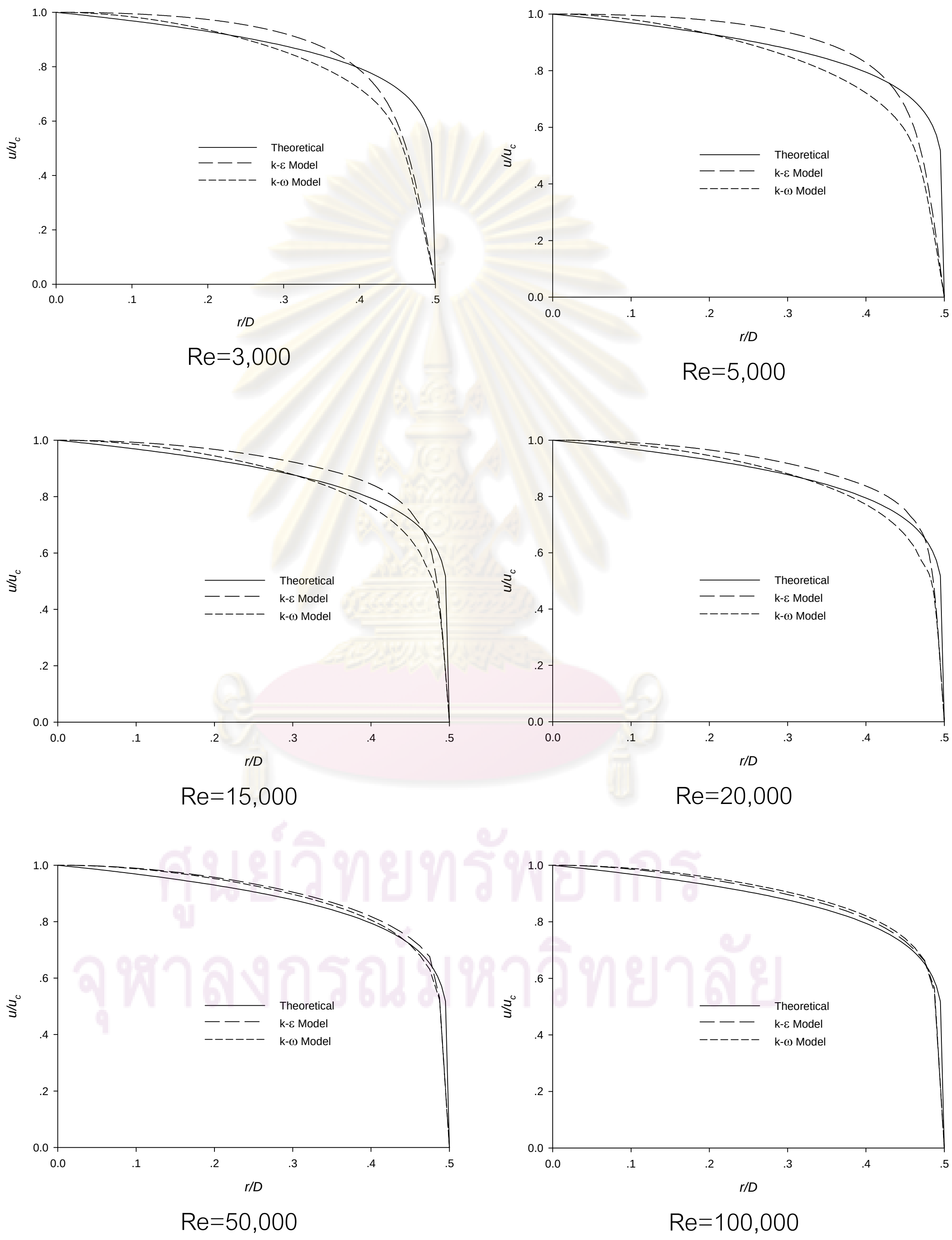

Figure 5.14 Result Comparisons with Different Reynolds Number

Chapter VI

Coiled Tube Simulations

In this chapter, fluid flow in coiled tube will be simulated by the commercial software, FLUENT, and compared the results with the experimental measurement. A Solution can be obtained by following these six steps;

1. Create Geometry in SolidWorks

2. Mesh Geometry in Gambit

3. Specify Boundary Types in GAMBIT

4. Set Up the Problem in FLUENT

5. Solve the Problem in FLUENT

6. Analyze the results

6.1 Create Geometry in SolidWorks

The coiled tube geometry is created by the SolidWorks software which is shown in Figure 6.1. The coiled tubes are created by measuring the size and dimension of all three different experiment coiled tubes. From the left hand side to right hand side in Figure 6.1 show the coiled tubes with curvature ration 0.012, 0.018, and 0.024.

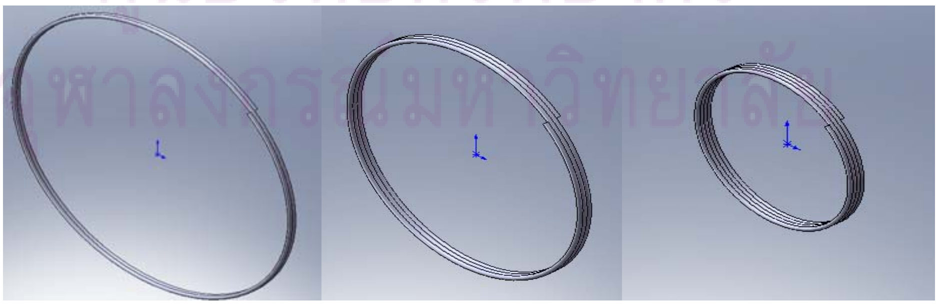

r/R=0.012 *r/R*=0.018 *r/R*=0.024

Figure 6.1 Geometry of Coiled Tubes

6.2 Mesh Geometry in GAMBIT

Figure 6.2 shows the geometry of coiled tube which is imported in STEP file to the GAMBIT software and then the volume of coiled tube is meshed by GAMBIT software which define the element as HEX/WEDGE, Copper type and 10 interval counts of Spacing.

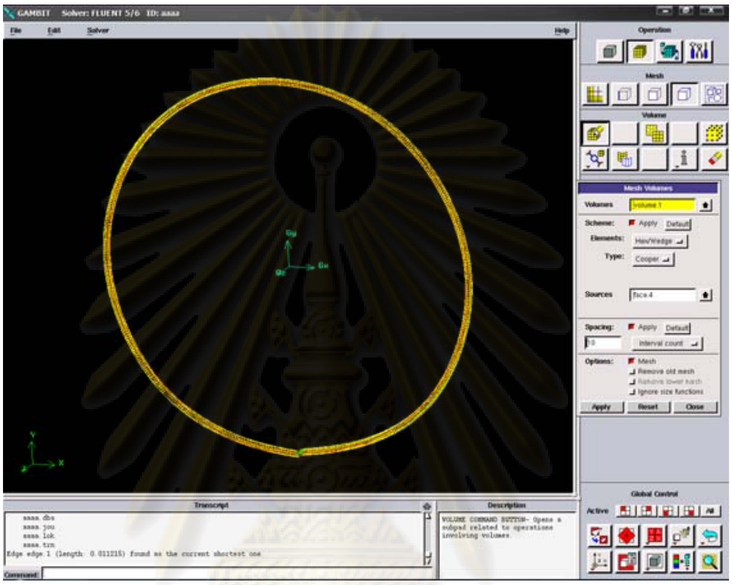

Figure 6.2 Import the Geometry to the GAMBIT Software

6.3 Specify Boundary Types in GAMBIT

The boundary types are shown in the Table 6.1. The Face4 is the inlet which is defined as velocity inlet. The Face1 is the outlet and defined as outflow. The Face2 and 3 are defined as wall type. After Specify Boundary Types, the Mesh is saved and exported as the mesh type.

Table 6.1 Boundary Conditions for Coiled Tube

Face	Name	Type
Face1	outlet	OUTFLOW
Face2	wall	WALL
Face3	wall	WALL
Face4	inlet	VELOCITY_INLET

6.4 Set Up the Problem in FLUENT

The mesh is exported to FLUENT along with the physical properties and the initial conditions specified. The material properties and the initial conditions are read through the case file. Instructions for the solvers are provided through a journal file when the solution is converged or the specified number of iterations is met exports data.

Firstly, the mesh from GAMBIT is imported to the FLUENT software which is shown in Figure 6.3; the mesh is checked to make sure that there are no errors. Any errors in the mesh would be reported at this time.

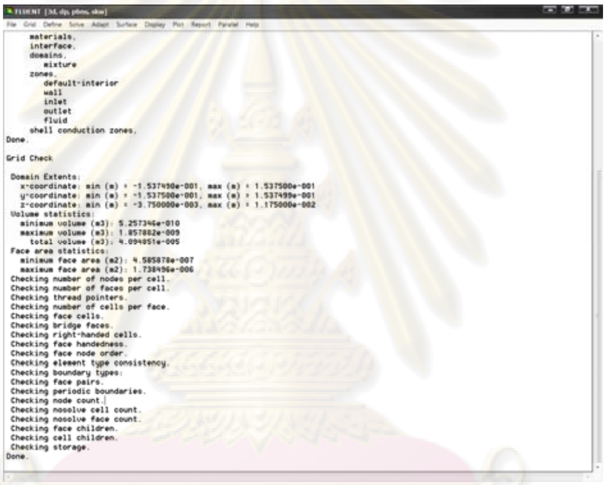

Figure 6.3 Check the Errors in the Mesh

Then, the solver properties are defined as shown in Figure 6.4. Pressure based solver, implicit formulation, 3D space, steady flow and absolute velocity formulation are defined.

Figure 6.4 Define Solver Properties

Then, the material properties are defined as shows in Figure 6.5. water-liquid (h2o<l>) [24] is selected from the FLUENT data base as the flow fluid.

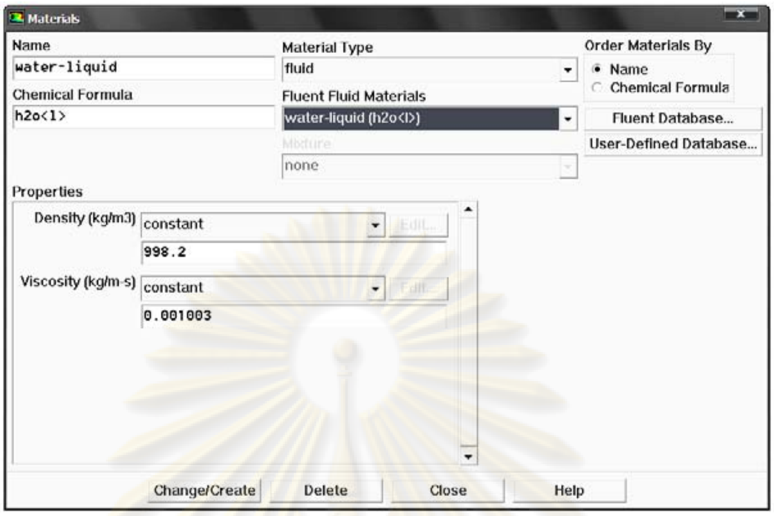

Figure 6.5 Define Material Properties

Then, four types of boundaries are specified as zones. Figure 6.6 display the inlet zone is defined. This defines the velocity of the fluid entering at inlet boundary and sets the magnitude velocity is normal to boundary. For the turbulence properties, the turbulent kinetic energy is 1 m^2/s^2 and specific dissipation is 1 s^{-1}.

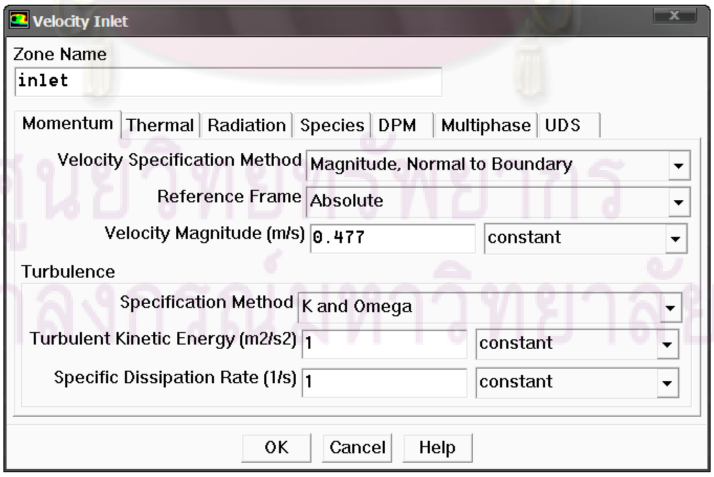

Figure 6.6 Define Inlet Boundary Condition

Then, the wall zone is defined which shows in Figure 6.7. The wall zone is specified as the stationary wall, no slip condition, and $4.5x10^{-5}$ of wall roughness.

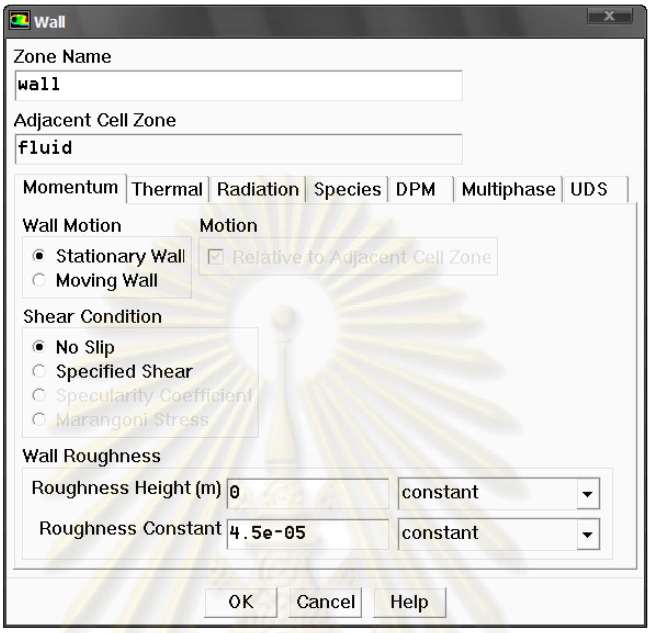

Figure 6.7 Define Wall Boundary Condition

6.5 Solve the Problem in FLUENT

The solution controls are defined which shows in Figure 6.8. The SIMPLE, Semi-Implicit Method for Pressure-Linked Equations, is used. The algorithm was originally put forward by Patankar and Spalding [27].

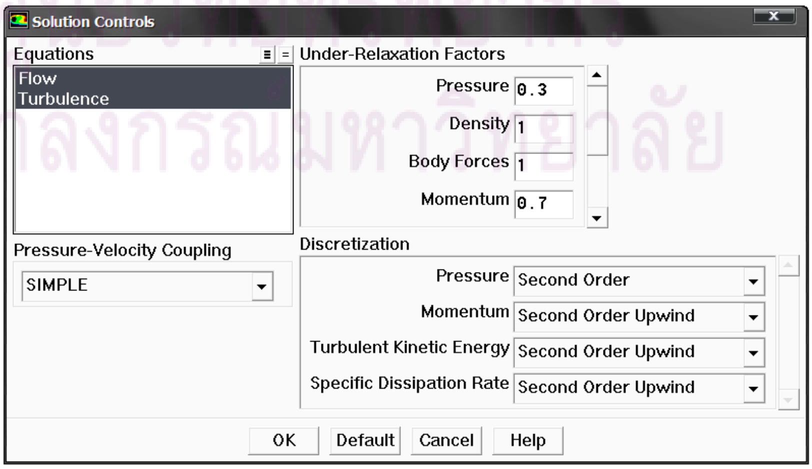

Figure 6.8 Define Solution Controls

Then, the convergence criteria are set. FLUENT reports a residual for each governing equation. The residual is a measure of how well the current solution satisfies the discrete form of each governing equation. Figure 6.9 shows the solution is iterated until the residual for each equation falls below $1e^{-6}$. This completes the problem specification.

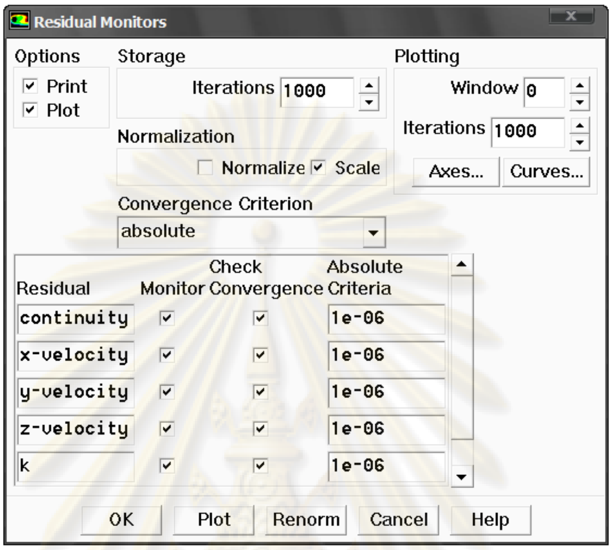

Figure 6.9 Residual Monitors

6.6 Results Analysis

6.6.1. Water Test

For the numerical simulation by commercial software, the results are first compared with experimental results of water test which are simulated at the same curvature ratio and Reynolds number ranges. Figure 6.10 shows a comparison plot of Fanning friction factor f and Reynolds number Re for experimental measurements as well as from numerical simulations. In all plots, the results conform to the experimental measurements that the Fanning friction factor decreases when the Reynolds numbers increases and increases with the increasing curvature ratio *r/R*.

The numerical simulation results are not close to the experimental measurements. This is due to the fact that numerical simulations are in the transition range of fluid flow. However, at Re=20,000 (the experimental limit), the results are closer to the experimental measurements.

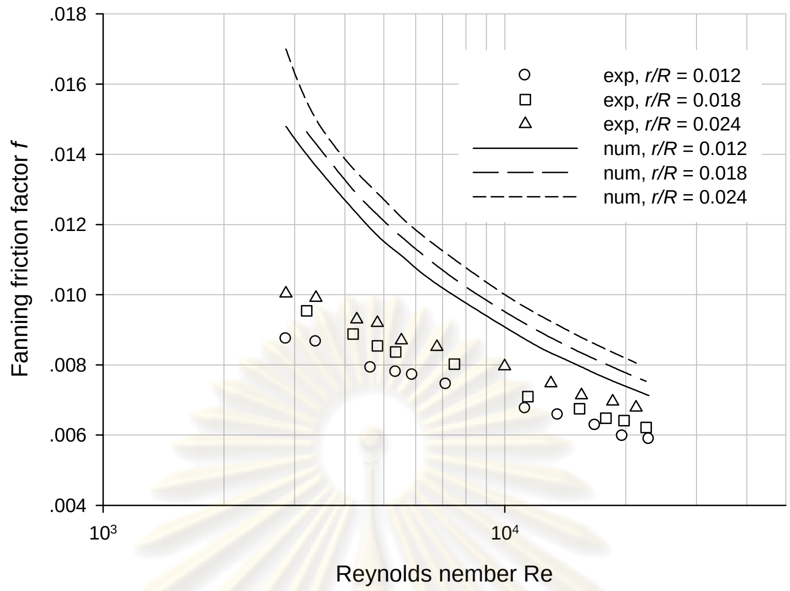

Figure 6.10 Compare Experimental and Numerical Results

As the fluid moves through the coiled tube, the friction between the fluid and the wall of coiled tube within the fluid itself creates pressure. Thus, the pressure contours in coiled tubes with different curvature ratio for 0.012, 0.018, and 0.024 are shown in Figures 6.11, 6.12, and 6.13. For all figures, the maximum pressure is at the inlet of coiled tube. After that, the pressure decrease, then, the minimum pressure is at the out let of coiled tube. In addition, comparing the pressure drops at the same Reynolds number, pressure drop in coiled tube with curvature ratio for 0.024 is the highest value which is matched with laboratory experiments.

Moreover, the velocity contours in coiled tubes with different curvature ratio for 0.012, 0.018, and 0.024 are shown in Figures 6.14, 6.15, and 6.16. The velocity at the inlet of coiled tube is uniform velocity, then, the velocity is fully developed profile through the coiled tube. At the outlet of coiled tube, the velocity reaches. The velocity profile of the outlet is maximum lower the centerline. This phenomenon come from the centrifugal force in the circular coiled tube as previously described. In addition, at the wall of coiled tube, the velocity is zero to satisfy the no-slip boundary condition for viscous flow.

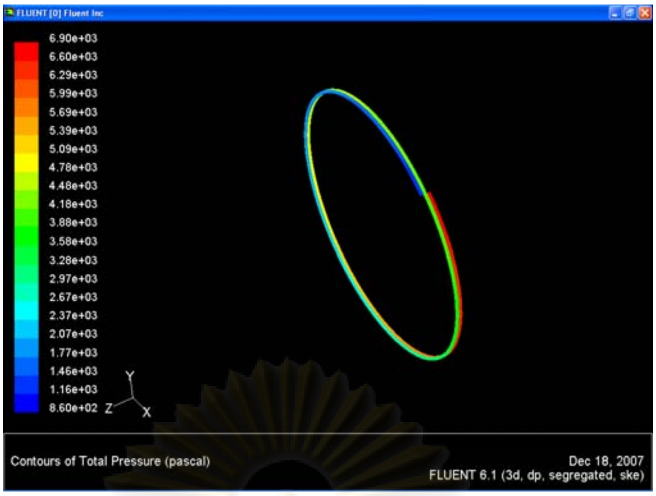

Figure 6.11 Pressure Contour of Water Test for Curvature Ratio 0.012

Figure 6.12 Pressure Contour of Water Test for Curvature Ratio 0.018

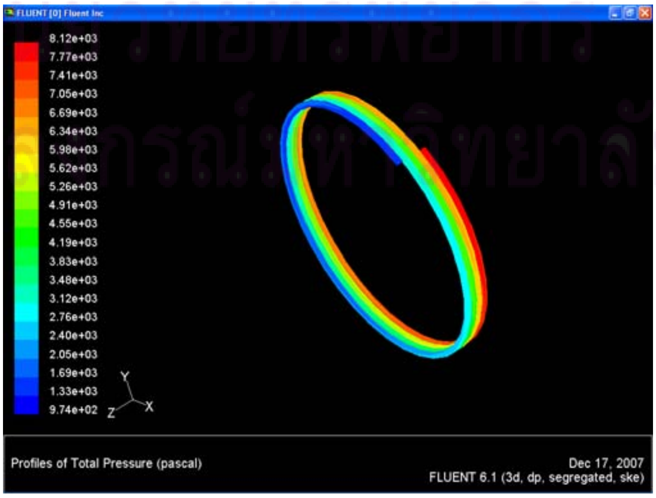

Figure 6.13 Pressure Contour of Water Test for Curvature Ratio 0.024

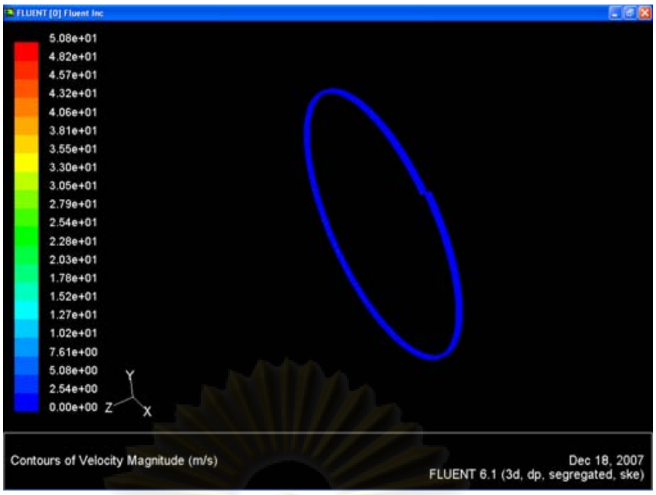

Figure 6.14 Velocity Contour of Water Test for Curvature Ratio 0.012

Figure 6.15 Velocity Contour of Water Test for Curvature Ratio 0.018

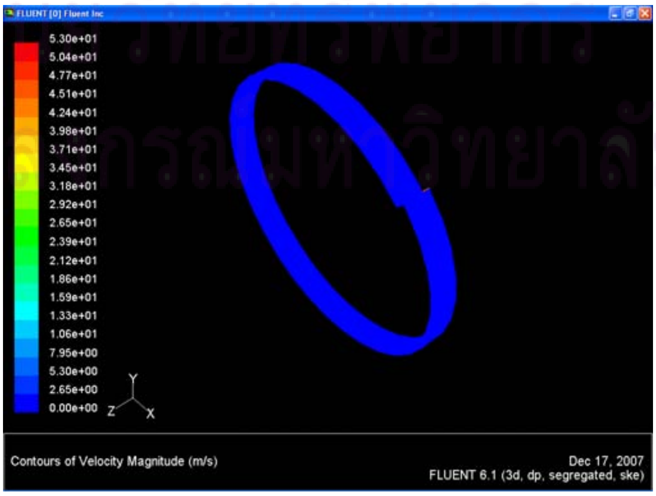

Figure 6.16 Velocity Contour of Water Test for Curvature Ratio 0.024

6.6.2. Polymer Additive Solutions Test

The next analysis is concentrated on the polymer additive solution which simulates by used the constant viscosity and power law fluid model assumption.

- Constant Viscosity Assumption

For this analysis, the simulation will be defined the viscosity of fluid is constant as a Newtonian fluid which is a fluid whose stress versus strain rate curve is linear and passes through the origin. The viscosity values of additives with different concentrations are used from the measurement data which shows in Table 3.2. The viscosity increases when the concentration of polymer additives increases.

Figure 6.17 shows a comparison plot of Fanning friction factor f and Reynolds number Re for experimental measurements as well as from numerical simulations with difference concentrations of polymer additive on curvature ratio of 0.012. In all plots, the Fanning friction factor decrease when the Reynolds numbers increases, however, the simulation with difference concentrations of polymer additive increase, the result with different concentration plots on Fanning friction factor f and Reynolds number Re are not different. This is due to the fact that simulation in the transition range and numerical model is not suitable for analysis the drag reduction by polymer additive.

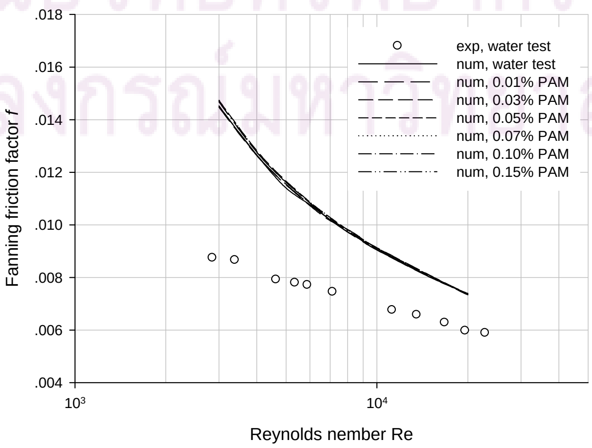

Figure 6.17 Numerical Simulations on Curvature Ratio of 0.012

In addition, the velocity profiles of fluid flow in coiled tube with different concentrations are shown in Figure 6.18. The velocity profile at the outlet reaches the maximum below the centerline. This phenomenon come from the centrifugal force in the circular coiled tube as previously described. The velocity below the center line increases with increasing the concentration of PAM additives.

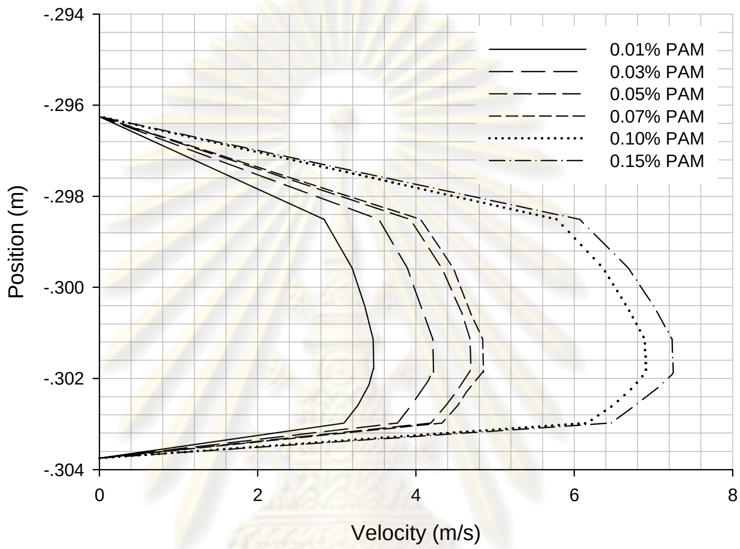

Figure 6.18 Velocity Profiles of Additive Solutions on Curvature Ratio 0.012

Anyway, the behavior of fluid flow in coiled tube will be continually studied in higher Reynolds number. The analysis is concentrated on fluid flow in coiled tube in higher Reynolds number ranges which are between 20,000 and 100,000. Figure 6.19 shows a comparison plot of Fanning friction factor f and Reynolds number Re for numerical simulation of water test and polymer additive with different types and concentrations. In all plots, the Fanning friction factor decreases when the Reynolds number increases which conform to the experimental data. Fanning friction factors of all polymer additives are less than the water test which conforms to the experimental data. This result shows that small polymer additives can reduce the friction in coiled tube.

In addition, the Drag Reduction DR with different types of polymer additives is also analyzed to explain the effect of polymer additives with different concentrations. Figure 6.20 presents percentage drag reduction from various types and concentration of polymer additives. When the Reynolds number increases, the percentage drag reduction decreases. However, the results of all polymer additives show a small drag reduction which the drag reductions are only 2 to 4 percentages.

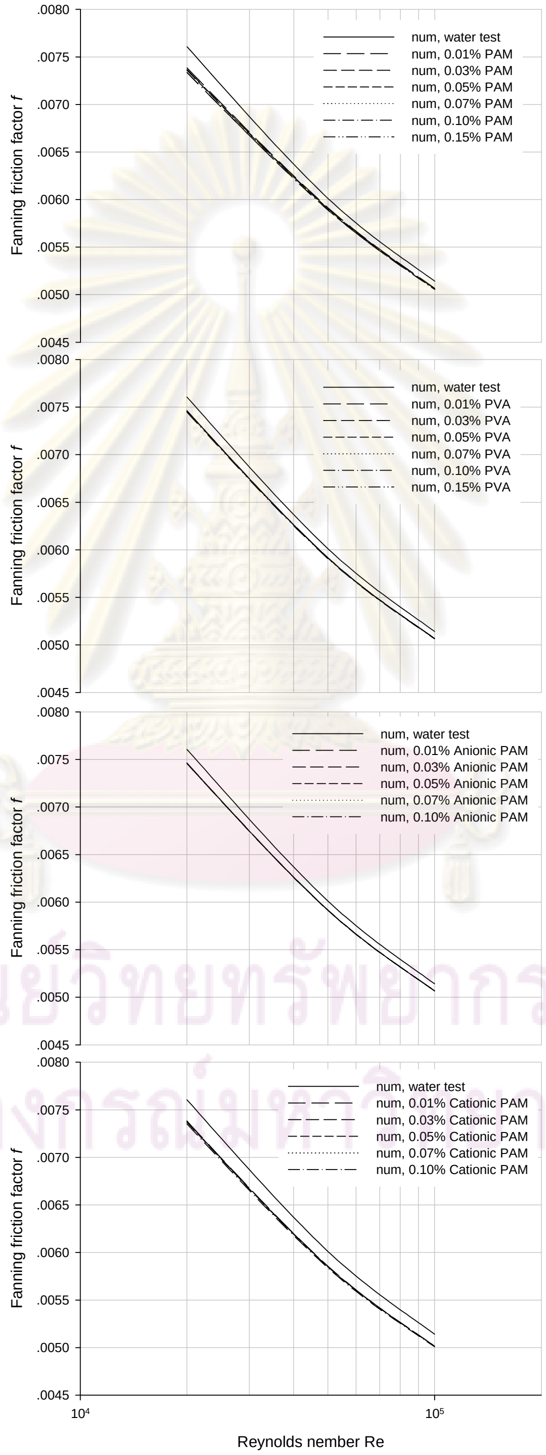

Figure 6.19 Fanning Friction Factor and Reynolds Number for Numerical Simulations

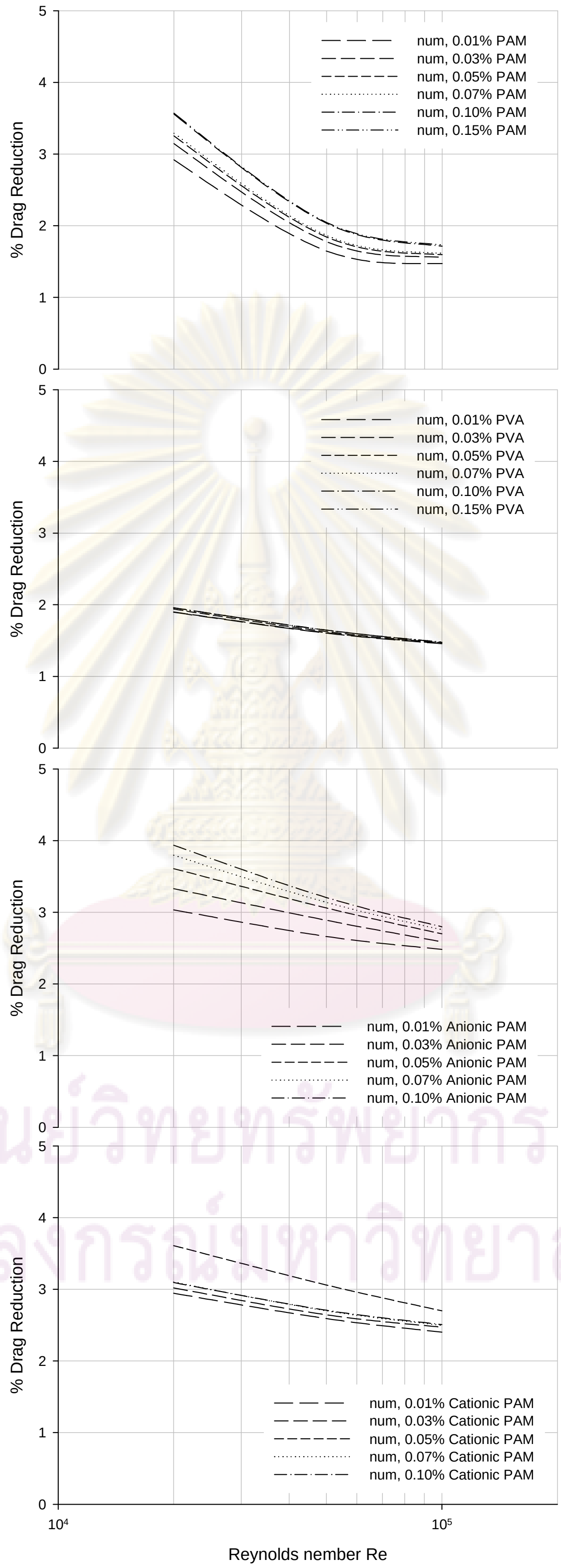

Figure 6.20 Different Types of Polymer Additives on Drag Reduction

- Power Law Fluid Model Assumption

For this analysis, viscosity of fluid is defined as a power law fluid which is a shear stress is not directly proportional to deformation rate. The viscosity is governed by the Power law as

$$\mu = K * \gamma^{(n-1)} \tag{6.1}$$

where μ is fluid viscosity, n is the power law index, K is the consistency index, and γ is the local shear rate.

Normally, for the polymer additive solutions, the value of power law index, *n* is nearly 1 and the consistency index, *K* increases when the concentrations of polymer additive increases. Because of this behavior of additive solution, the simulation will be emphasizing on the effect of the consistency index, *K*.

For the FLUENT software, it is possible to set up the material for non-Newtonian viscosity and switch to turbulence formulation for the same using text user interface (TUI) command which is shown in Figure 6.21.

```
define/models/viscous/turbulence-expert/turb-non-newtonian>

Enable turbulence for non-Newtonian fluids? [no] yes
```

Figure 6.21 Define the Turbulent Non-Newtonian Viscosity

After define the turbulent non-Newtonian viscosity, the effect of the consistency index for the additive solution are tested on additive solutions with four different consistency index (*K*) of 0.0010, 0.0015, 0.0020, 0.0025 and all simulations are firstly tested on the Reynolds number 20,000.

To analyze the effect of the consistency indices, Figure 6.21 show the results of numerical simulations. Firstly, the viscosity contours of fluid in coiled tube with four different consistency indices (*K*) are displayed. The fluid with *K*=0.0010, which is the smallest, show small changing of viscosity contour but for the fluid with K=0.0025, it clearly shows that the viscosity is separated as the contour layers. The viscosity reaches the maximum below the centerline which conforms to the effect of centrifugal force in coiled tube.

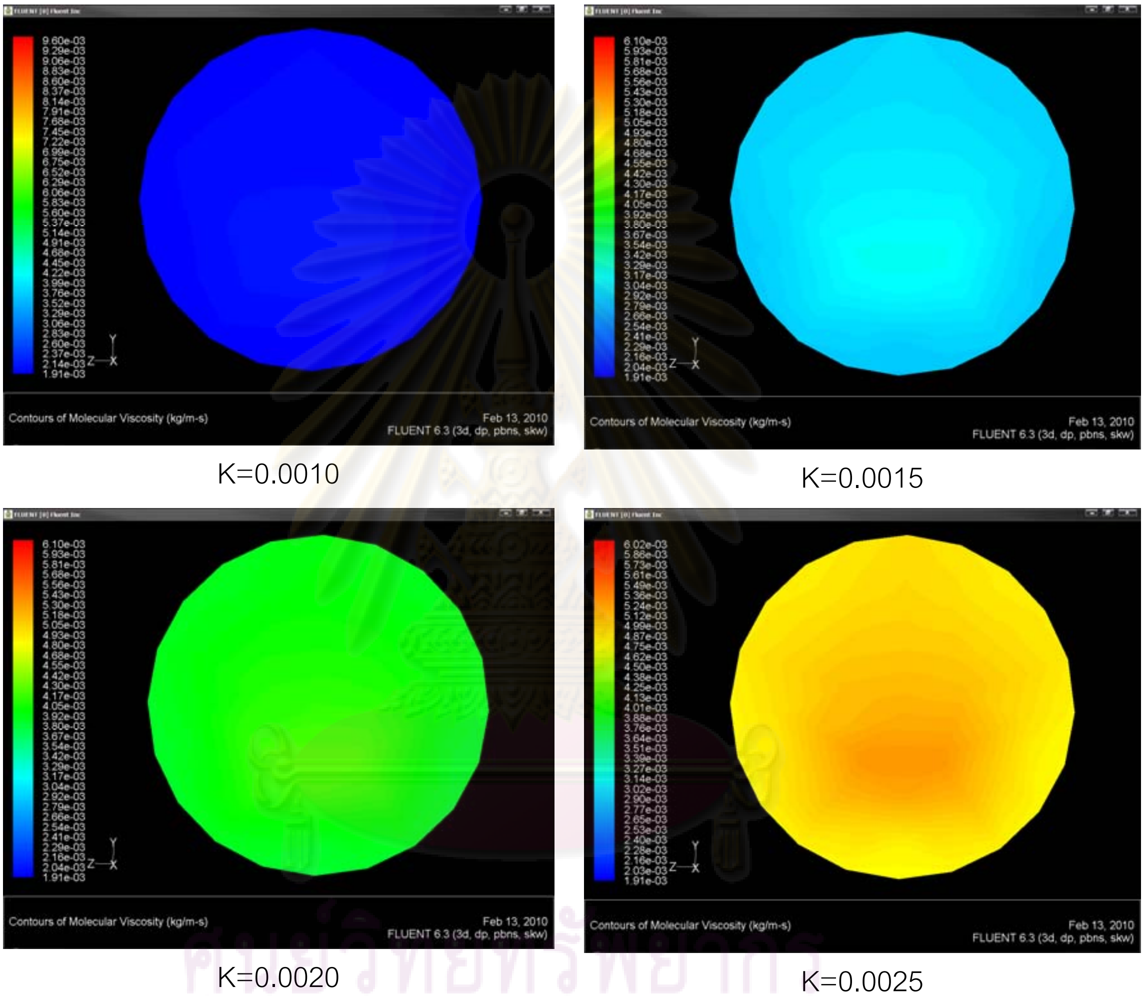

Figure 6.22 Viscosity Contours of Four Different Consistency Index (K)

In addition, the effect of consistency index (K) in higher Reynolds number ranges, which are between 20,000 and 100,000, are studied. Figure 6.23 presents a comparison plot of Fanning friction factor f and Reynolds number Re for water test and the fluid with different consistency indices which are 0.001, 0.002, 0.003, 0.004, and 0.005. The results illustrate that the friction factor of water test is higher than all fluid with various consistency indices, then, when the consistency index increases, the fiction factor decreases but shows small different.

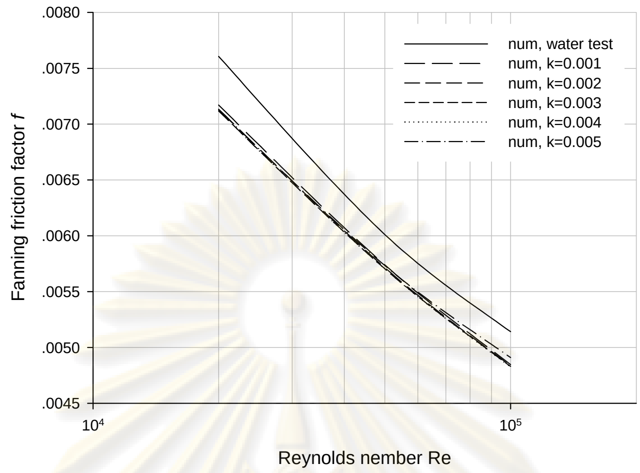

Figure 6.23 Different Consistency Index (*K*) on Fanning Friction Factor and Re Plot

For the drag reduction, Figure 6.24 shows the percentage drag reduction from various consistency indices. As the consistency index increases, the percentage drag reduction increases until the drag reduction reaches the maximum value at consistency index = 0.004. The maximum drag reduction is only 6.5 % at the Reynolds number of 20,000. However, when the Reynolds number increases, the drag reduction decreases which is only 4.6 % at Reynolds number of 100,000.

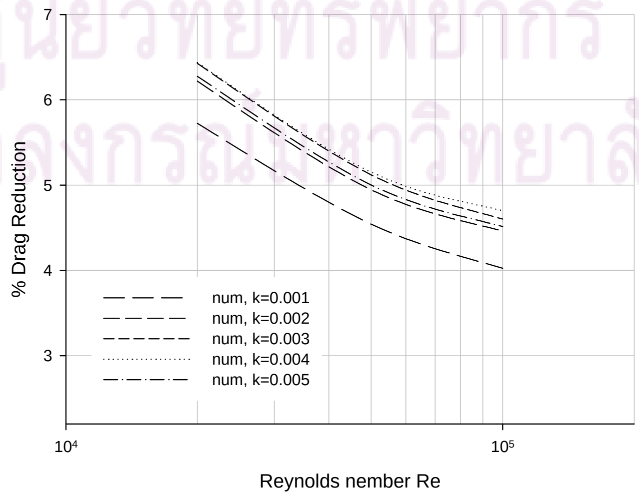

Figure 6.24 Different Consistency Index (*K*) on Drag Reduction

6.7 Conclusions

The numerical simulation by commercial software method showed simulation treads in all plots, the results conformed to the experimental measurements that the Fanning friction factor decreased when the Reynolds numbers increased and increased with the increasing curvature ratio r/R.

The numerical simulation results were not closed to the experimental measurements due to the fact that numerical simulations were in the transition range of fluid flow. However, at Re=20,000 (the experimental limit), the results are closer to the experimental measurements.

For the analysis in higher Reynolds Number, which were between 20,000 and 100,000. The results displayed the Fanning friction factor decreased when the Reynolds number increased. Nevertheless, the results of all polymer additives in higher Reynolds number ranges showed a small drag reduction which the drag reductions are only 2 to 4 percents (those of the experimental measurements are up to 50 %). It might be concluded that the numerical model and some parameters were not suitable for analysis of the drag reduction.

Finally, the simulation with power law fluid model was studied by changing the consistency index. The results showed that the consistency index increases, the percentage drag reduction increased. The drag reduction increased and reached the maximum value at consistency index 0.004. The maximum drag reduction is only 6.5% at the Reynolds number of 20,000 and 4.6% at Reynolds number of 100,000. The numerical simulation results with power law fluid model showed small drag reduction. It might be due to the approximation of viscosity and some parameters were not suitable for analysis of the drag reduction.

Even if the study of drag reduction by numerical simulation showed small drag reduction results, this method could be performed in order to be able to make some decision for the design of the future experiment.

Chapter VII

Conclusions

7.1 Conclusions

7.1.1 Experimental Measurements

The drag reduction study involved an experimental study in coiled tubes of PAM, PVA, Anionic PAM, and Cationic PAM solutions. The tests confirmed that the Fanning friction factor f increased with increasing Reynolds number Re and Curvature ratio r/R. The Fluid friction pressure could be reduced by polymer additives.

The study of the additive concentration effects on drag reduction showed that when the concentration of polymer additives was higher than the best concentration, the percentage drag reductions decreased. It was probably because the turbulent intensity was suppressed by the more viscous fluid from the higher additive concentration. In addition, the study of the curvature ration showed that as the curvature ratio increased, the friction loss and the associated Fanning fraction increased. This phenomenon is due to the centrifugal force in the circular coiled tubes as previously described.

The empirical correlations for the Fanning friction factor prediction as a function of Reynolds number and curvature ratio were developed from the data points at the best concentration with different curvatures. The empirical best concentration for PAM is 0.10% by volume, for PVA is 0.03%, for Anionic PAM is 0.07%, and for Cationic PAM is 0.05%. Thus, the Anionic PAM was the most effective for this application due to the longest molecular chain.

In addition, the predicted correlations for all additive solutions at the best concentration were obtained from empirical data. The results showed that the exiting correlation by Srinivasan was well suited to these dilute polymer solutions. When comparing the experiment data points with the predicted correlations, excellent agreements were obtained.

7.1.2 Numerical Simulations

The computational simulation used the FLUENT commercial software to simulate the fluid flows in 2D straight tubes and 3D coiled tubes.

For 2D straight tubes simulation, the problems were simulated with different Reynolds number between 3,000-100,000 with two different models, k-ε with enhanced wall treatment model and k-ω model. The results showed that in the Reynolds number range below 50,000, results from the k-ε with enhanced wall treatment model and k-ω model were not close to the theoretical solutions. But for the Reynolds number range more than 50,000, the result was quite close to the theoretical solution. In addition, at Re=100,000, the simulation with both different models were closer to the solution because the algorithms in turbulent model was more suitable at high Reynolds number than the transition range.

For 3D coiled tubes simulation, the simulation of water flow were first simulated and compared with the experimental results. The numerical simulation results were not close to the experimental measurements and over estimate due to the fact that numerical simulations were in the transition range and the turbulent models in the commercial software were not suitable to estimate the water flow in transition range. However, at Re=20,000 (the experimental limit), the results were closer to the experimental measurements.

For the drag reduction in coiled tubes, the simulation was tested at the same range Reynolds number of the experiment (Re=3,000-20,000) and higher Reynolds Number (Re=20,000-100,000). The results showed that the Fanning friction factor decreased when the Reynolds number increased. Nevertheless, the results of all polymer additives in higher Reynolds number ranges showed a small drag reduction with the drag reductions of only 2 to 4 percents (those of the experimental measurements were up to 50 %). It might be concluded that the numerical model and some parameters in commercial software were not suitable for analysis of the drag reduction.

Finally, the simulation with power law fluid model was studied by changing the consistency index. The results showed that the consistency index increases, the percentage drag reduction increased. The drag reduction increased and reached the maximum value at consistency index 0.004. The maximum drag reduction is only 6.5% at the Reynolds number of 20,000 and 4.6% at Reynolds number of 100,000. The numerical simulation results with power law fluid model showed small drag reduction. It might be due to the approximation of viscosity and some parameters were not suitable for analysis of the drag reduction.

7.2 Recommendations for Future Works

The recommendations for future works are as follows.

1. Different types of polymer additives could be studied. The higher Molecular Weight of polymer additives, the greater the drag reduction for a given concentration and Reynolds number. The longer polymer chain provides more chance for entanglement and interaction with the flow.

2. The obtained correlations that predict the value of fanning friction factor for flows in coiled tubes with polymer additives could be used to conduct the full-scale test on the laboratory experiments and investigate the drag reduction of flows in coiled tubes.

3. For the numerical experiments, the simulation with complex geometry and using various fluid models for the polymer solution could be further studied.

4. For the further fluid model development, the accurate turbulent and non-Newtonian fluid model to predict the behavior of fluid flow in transition range could be studied.

References

[1] Toms, B.A. 1949. Some observations on the flow of linear polymer solutions through straight tubes at large Reynolds numbers. Proceeding of the First International Congress on Rheology 2 : 135-141.

[2] Srinivasan, P.S., Nandapurkar, S.S., and Holland, F.A. 1970. Friction factors for coils. Transactions of the Institution of Chemical Engineers 48 : 156-161.

[3] Shah, S.N. and Zhou, Y. 2003. An experimental study of drag reduction of polymer solutions in coiled tubing. SPE Production and Facilities : 280-287.

[4] Agoston, G.A., Harte, W.H., Hottel, H.C., Klemm, W.A., Mysels, K.J., Pomeroy, H.H., and Thompson, J.M. 1954. Flow of gasoline thickened by napalm. Industrial and Engineering Chemistry 46(5) : 1017-1019.

[5] Watanabe, K. and Udagawa, H. 2001. Drag reduction of non-Newtonian fluids in a circular pipe with a highly water-repellent wall. American Institute of Chemical Engineers Journal 47(2) : 256-262.

[6] Dan Toonder, J.M.J., Draad, A.A., Kuiken, G.D.C., and Nieuwstadt, F.T.M. 1995. Degradation effects of dilute polymer solutions on turbulent drag reduction in pipe flows. Journal of Applied Sciences Research 55 : 63-82.

[7] Drew, T.B., Koo, E.C., and McAdams, W.H. 1932. The friction factor for clean round pipes. Transactions of the American Institute of Chemical Engineers 28 : 56-72.

[8] Omotayo, M.T. 2006. Shear Degradation of Polymer Oil Drag Reducer in Non-Isothermal Environment. Master's Thesis Department of Petroleum Engineering Faculty of Science and Technology Universitetet i Stavanger Norway.

[9] Shah, S.N., Kamel, A., and Zhou, Y. 2006. Drag reduction characteristics in straight and coiled tubing-an experimental study. Journal of Petroleum Science and Engineering 53 : 179-188.

[10] Eustice, J. 1910. Flow of water in curved pipes. Proceedings of the Royal Society of London 84 : 107-118.

[11] Dean, W.R. 1927. Notes on the motion of fluid in a curved pipe. Philosophical Magazine 4 : 208-233.

[12] Ramana Rao, and M.V., Sadasivudu, D. 1974. Pressure drop studies in helical coils. Indian Journal Technology 12 : 473.

[13] Azouz, I., Shah, S.N., Vinod, P.S., and Lord, D.L. 1998. Experimental investigation of frictional pressure losses in coiled tubing. SPE Production and Facilities 13(2) : 91-96.

[14] Zhou, Y., Shah, S.N., and Gujar, P.V. 2004. Effects of coiled tubing curvature on drag reduction of polymeric fluids. SPE Production & Operations Journal 21 : 134-141.

[15] Elperin, I.T., Smolskii, B.M., and Leventhal, L.I. 1967. Decreasing the hydrodynamic resistance of pipelines. International Chemical Engineering 7 : 276-295.

[16] Lumley, J.L. 1969. Drag reduction by additives. Annual Review of Fluid Mechanics 1 : 367-384.

[17] Virk, P.S. 1975. Drag reduction fundamentals. American Institute of Chemical Engineers Journal 21 : 625-656.

[18] Arianne, A. 1996. Drag Reduction by Polymer Additives in a Turbulent Pipe Flow: Laboratory and Numerical Experiments. Doctoral Dissertation Department of Mechanical Engineering Faculty of Engineering Technische Universiteit Delft Netherland.

[19] Mysels, K.J. 1949. Flow of thickened fluids. United States Patent Office number : 2492173.

[20] Dodge, D.W. and Metzner, A.B. 1959. Turbulent flow of non-Newtonian systems. American Institute of Chemical Engineers Journal 5 : 189-204.

[21] Shenoy, A.V. 1984. A review on drag reduction with special reference to micellar systems. Colloid and Polymer Science 262 : 319–337.

[22] Inaba, H., Haruki, N., and Horibe, A. 2000. Flow drag and heat transfer reduction of flowing water containing fibrous material in a straight pipe. International Journal of Thermal Sciences 39 : 18-29.

[23] Versteeg, H.K., Malalasekera, W. 2007. An Introduction to Computational Fluid Dynamics: The finite volume method. 2nd ed. London: Pearson Education.

[24] Fluent In. 2007. Fluent 6.3.26 User's Guide.

25] Launder, B.E. and Spalding, D.B. 1974. The numerical computation of turbulent flows. Computational Methods for Applied Science and Engineering 3 : 269-289.

[26] Wilcox, D.C. 1988. Reassessment of the scale-determining equation for advanced turbulent models. American Institute of Aeronautics and Astronautics Journal 26 : 1299-1310.

[27] Wilcox, D.C. 1972. A calculation procedure for heat, mass and momentum tranfer in three-dimensional parabolic flows. International Journal of Heat and Mass Transfer 15 : 1787.

Appendices

Appendix A

Newtonian and Non-Newtonian fluids are classified by the relationship between the shear stress and deformation rate. Figure A.1 show the classification fluid types. The fluid in which shear stress is directly proportional to deformation rate is Newtonian fluid. The fluid in which shear stress is not directly proportional to deformation rate is Non-Newtonian fluid.

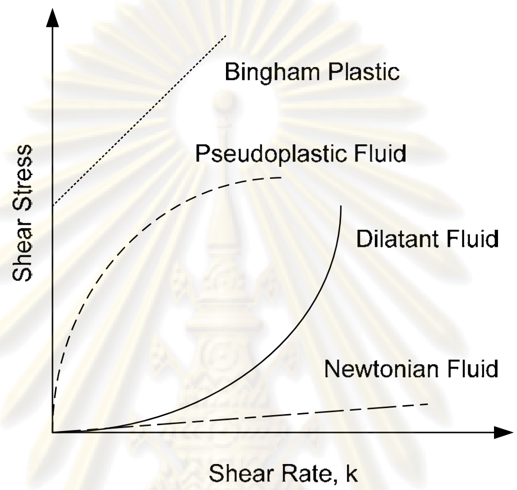

Figure A.1 Classification Fluid Types

A.1 Newtonian Fluid

Most common fluids such as water, air, and gasoline are Newtonian under normal condition. Newtonian fluids will deform at different rates under the action of the same applied shear stress. The constant of proportionality in equation is the absolute viscosity, μ. For one dimensional flow, the viscosity is given by

$$\tau_{xy} = \mu \frac{du}{dy} \qquad \text{(A.1)}$$

where τ_{xy} is the shear stress exerted by the fluid, μ is the fluid viscosity - a constant of proportionality, du/dy is the velocity gradient perpendicular to the direction of shear.

The properties of viscosity depend on the type of fluids. For example, the viscosity of gases increases with temperature, where as the viscosity of liquids decreasing with increasing temperature.

A.2 Non-Newtonian Fluid

Fluids in which shear stress is not directly proportional to deformation rate are non-Newtonian fluids. Many common fluids exhibit non-Newtonian behavior. Non-Newtonian fluids commonly are classified as having time-independent and time-dependent fluids behavior.

Numerous equations have been proposed to model the observed relation between τ_{xy} and du/dy for time-independent fluids. They may be represented for many engineering applications by the power law model, which for one-dimensional flow becomes.

$$\tau_{xy} = K\left(\frac{du}{dy}\right)^{n} \qquad \text{A.2}$$

where n is the flow behavior index and K is the consistency index.

Time-independent non-Newtonian fluids can be classified into three types, depend on properties for each fluid. The first group, the fluids in which the apparent viscosity decreases with increasing deformation rate ($n<1$), is called Pseudoplastic (or shear thinning) fluids. Most non-Newtonian fluids fall in to this group, such as polymer solution, colloidal suspensions, and paper pulp in water. The second group is the dilatants (or shear thinning) fluids of which the apparent viscosity increases with increasing deformation rate ($n>1$).The third group is the fluids that behaves as a solid until a minimum yield stress, τ_y, are exceeded and subsequently exhibit a linear relation between stress and rate of deformation, an ideal or Bingham plastic. Examples of substances exhibiting this behavior are clay suspensions, drilling, and toothpaste. The appropriation of the shear stress model is

$$\tau_{xy} = \tau_y + \mu_p \frac{du}{dy} \qquad \text{A.3}$$

where τ_y is the minimum yield stress and μ_p is the fluid viscosity - a constant of proportionality

Appendix B

Table B.1-B.131 show the observation data for additive solutions test with different types and curvature ratios (*r/R*). The experimental data are measured by using different manometers which are CCl_4 and mercury monometer.

Table B.1 Observation for 0.01% PAM Solution with *r/R*: 0.012 (CCl_4)

R (cm)		Weight, w (kg)	Time, t (s)	Mass flow rate, $\dot{m}$ (kg/s)	Velocity, v (m/s)	Head loss, ΔH (m of water)	Reynolds Number, Re	Friction factor, f
60.0	59.0	0.01	10	0.001	0.025	0.006	166	0.087087
61.6	57.5	0.10	20	0.005	0.125	0.024	829	0.014282
63.7	54.8	0.18	20	0.009	0.225	0.052	1492	0.009569
68.3	50.5	0.12	10	0.012	0.300	0.104	1989	0.010765
70.3	48.3	0.14	10	0.014	0.350	0.129	2321	0.009775

Table B.2 Observation for 0.01% PAM Solution with *r/R*: 0.012 (Hg)

R (cm)		Weight, w (kg)	Time, t (s)	Mass flow rate, $\dot{m}$ (kg/s)	Velocity, v (m/s)	Head loss, ΔH (m of water)	Reynolds Number, Re	Friction factor, f
48.8	43.3	0.39	10	0.039	0.976	0.690	6465	0.006736
52.2	39.6	0.62	10	0.062	1.551	1.582	10278	0.006106
56	35.8	0.82	10	0.082	2.052	2.536	13593	0.005596
59.3	32.7	0.97	10	0.097	2.427	3.339	16080	0.005266
64.8	26.7	1.20	10	0.120	3.002	4.783	19893	0.004929

Table B.3 Observation for 0.01% PAM Solution with *r/R*: 0.018 (CCl_4)

R (cm)		Weight, w (kg)	Time, t (s)	Mass flow rate, $\dot{m}$ (kg/s)	Velocity, v (m/s)	Head loss, ΔH (m of water)	Reynolds Number, Re	Friction factor, f
59.4	58.5	0.04	45	0.001	0.022	0.005	147	0.099197
60.5	57.1	0.06	20	0.003	0.075	0.020	497	0.032899
60.7	57.0	0.08	20	0.004	0.100	0.022	663	0.020139
61.5	56.0	0.10	20	0.005	0.125	0.032	829	0.019159
67.3	50.0	0.22	20	0.011	0.275	0.102	1823	0.012451

Table B.4 Observation for 0.01% PAM Solution with *r/R*: 0.018 (Hg)

R (cm)		Weight, *w* (kg)	Time, *t* (s)	Mass flow rate, $\dot{m}$ (kg/s)	Velocity, *v* (m/s)	Head loss, ΔH (m of water)	Reynolds Number, Re	Friction factor, f
47.8	44.2	0.58	20	0.029	0.726	0.452	4807	0.007974
49.0	43.1	0.78	20	0.039	0.976	0.741	6465	0.007226
52.3	39.8	1.18	20	0.059	1.476	1.569	9781	0.006689
55.5	36.3	1.52	20	0.076	1.902	2.410	12599	0.006192
58.9	33.2	1.78	20	0.089	2.227	3.226	14754	0.006044
64.8	26.7	2.28	20	0.114	2.852	4.783	18898	0.005461
74.6	17.0	2.84	20	0.142	3.553	7.231	23540	0.005321

Table B.5 Observation for 0.01% PAM Solution with *r/R*: 0.024 (CCl_4)

R (cm)		Weight, *w* (kg)	Time, *t* (s)	Mass flow rate, $\dot{m}$ (kg/s)	Velocity, *v* (m/s)	Head loss, ΔH (m of water)	Reynolds Number, Re	Friction factor, f
59.0	57.4	0.04	30	0.001	0.033	0.009	221	0.078378
60.0	56.4	0.12	30	0.004	0.100	0.021	663	0.019594
64.5	51.9	0.28	30	0.009	0.234	0.074	1547	0.012596
71.2	44.7	0.46	30	0.015	0.384	0.156	2542	0.009816
77.5	38.3	0.58	30	0.019	0.484	0.230	3205	0.009133
81.2	35.0	0.64	30	0.021	0.534	0.271	3536	0.008840
84.5	31.5	0.69	30	0.023	0.575	0.311	3813	0.008725

Table B.6 Observation for 0.01% PAM Solution with *r/R*: 0.024 (Hg)

R (cm)		Weight, *w* (kg)	Time, *t* (s)	Mass flow rate, $\dot{m}$ (kg/s)	Velocity, *v* (m/s)	Head loss, ΔH (m of water)	Reynolds Number, Re	Friction factor, f
50.2	41.6	0.92	20	0.046	1.151	1.080	7626	0.007571
54.2	37.6	1.34	20	0.067	1.676	2.084	11107	0.006889
58.5	33.2	1.72	20	0.086	2.152	3.176	14256	0.006372
61.5	30.2	1.94	20	0.097	2.427	3.929	16080	0.006197
64.9	26.7	2.18	20	0.109	2.727	4.795	18069	0.005990
68.3	23.2	2.40	20	0.120	3.002	5.662	19893	0.005834

Table B.7 Observation for 0.03% PAM Solution with *r/R*: 0.012 (CCl_4)

R (cm)		Weight, *w* (kg)	Time, *t* (s)	Mass flow rate, $\dot{m}$ (kg/s)	Velocity, *v* (m/s)	Head loss, ΔH (m of water)	Reynolds Number, Re	Friction factor, f
50.5	42.5	0.18	30	0.006	0.150	0.047	816	0.019353
54.0	38.6	0.12	10	0.012	0.300	0.090	1633	0.009313
62.0	31.4	0.17	10	0.017	0.413	0.180	2245	0.009788
70.0	23.0	0.23	10	0.023	0.563	0.276	3061	0.008085
78.5	15.0	0.27	10	0.027	0.676	0.373	3673	0.007586
80.0	13.5	0.28	10	0.028	0.701	0.390	3809	0.007387

Table B.8 Observation for 0.03% PAM Solution with *r/R*: 0.012 (Hg)

R (cm)		Weight, *w* (kg)	Time, *t* (s)	Mass flow rate, $\dot{m}$ (kg/s)	Velocity, *v* (m/s)	Head loss, ΔH (m of water)	Reynolds Number, Re	Friction factor, f
50.0	41.8	0.50	10	0.050	1.251	1.029	6803	0.006110
53.8	38.2	0.72	10	0.072	1.801	1.958	9796	0.005606
57.3	34.7	0.92	10	0.092	2.302	2.837	12517	0.004974
60.2	31.6	1.04	10	0.104	2.602	3.590	14149	0.004926
63.5	28.3	1.18	10	0.118	2.952	4.419	16054	0.004709
66.5	25.3	1.28	10	0.128	3.203	5.172	17414	0.004684
86.0	6.0	1.84	10	0.184	4.604	10.043	25033	0.004402

Table B.9 Observation for 0.03% PAM Solution with *r/R*: 0.018 (CCl_4)

R (cm)		Weight, *w* (kg)	Time, *t* (s)	Mass flow rate, $\dot{m}$ (kg/s)	Velocity, *v* (m/s)	Head loss, ΔH (m of water)	Reynolds Number, Re	Friction factor, f
59.0	50.0	0.08	10	0.008	0.200	0.053	1088	0.012247
64.0	45.0	0.14	10	0.014	0.350	0.112	1905	0.008442
69.0	40.0	0.18	10	0.018	0.450	0.170	2449	0.007795
72.0	37.0	0.19	10	0.019	0.463	0.205	2517	0.008906
75.5	33.5	0.21	10	0.021	0.513	0.246	2789	0.008703
80.0	29.0	0.23	10	0.023	0.575	0.299	3129	0.008396
92.0	17.0	0.29	10	0.029	0.713	0.440	3877	0.008041

Table B.10 Observation for 0.03% PAM Solution with *r/R*: 0.018 (Hg)

R (cm)		Weight, *w* (kg)	Time, *t* (s)	Mass flow rate, $\dot{m}$ (kg/s)	Velocity, *v* (m/s)	Head loss, ΔH (m of water)	Reynolds Number, Re	Friction factor, f
48.0	43.8	0.32	10	0.032	0.801	0.527	4354	0.007641
51.1	40.9	0.55	10	0.055	1.376	1.280	7483	0.006281
57.2	34.8	0.86	10	0.086	2.152	2.812	11700	0.005642
60.2	31.8	0.98	10	0.098	2.452	3.565	13333	0.005509
67.6	24.3	1.27	10	0.127	3.178	5.436	17278	0.005001
68.3	23.5	1.30	10	0.130	3.253	5.624	17687	0.004938
89.0	3.0	1.86	10	0.186	4.654	10.796	25305	0.004631

Table B.11 Observation for 0.03% PAM Solution with *r/R*: 0.024 (CCl_4)

R (cm)		Weight, *w* (kg)	Time, *t* (s)	Mass flow rate, $\dot{m}$ (kg/s)	Velocity, *v* (m/s)	Head loss, ΔH (m of water)	Reynolds Number, Re	Friction factor, f
47.3	46.5	0.01	20	0.001	0.013	0.005	68	0.278677
48.5	45.3	0.04	20	0.002	0.050	0.019	272	0.069669
50.5	42.5	0.06	10	0.006	0.150	0.047	816	0.019353
53.8	39.2	0.10	10	0.010	0.250	0.086	1361	0.012715
54.6	38.4	0.11	10	0.011	0.263	0.095	1429	0.012796
60.0	33.0	0.16	10	0.016	0.400	0.158	2177	0.009185
80.1	12.9	0.27	10	0.027	0.663	0.394	3605	0.008334

Table B.12 Observation for 0.03% PAM Solution with *r/R*: 0.024 (Hg)

R (cm)		Weight, *w* (kg)	Time, *t* (s)	Mass flow rate, $\dot{m}$ (kg/s)	Velocity, *v* (m/s)	Head loss, ΔH (m of water)	Reynolds Number, Re	Friction factor, f
48.0	44.0	0.31	10	0.031	0.763	0.502	4150	0.008010
49.2	42.8	0.40	10	0.040	1.001	0.803	5442	0.007451
52.0	40.0	0.56	10	0.056	1.401	1.506	7619	0.007128
58.2	33.8	0.86	10	0.086	2.152	3.063	11700	0.006146
66.3	25.5	1.16	10	0.116	2.902	5.122	15782	0.005648
72.8	19.0	1.35	10	0.135	3.378	6.754	18367	0.005499

Table B.13 Observation for 0.05% PAM Solution with *r/R*: 0.012 (CCl_4)

R (cm)		Weight, w (kg)	Time, t (s)	Mass flow rate, $\dot{m}$ (kg/s)	Velocity, v (m/s)	Head loss, ΔH (m of water)	Reynolds Number, Re	Friction factor, f
60.6	57.5	0.12	30	0.004	0.100	0.018	490	0.016873
61.6	56.5	0.16	30	0.005	0.133	0.030	653	0.015614
62.5	55.5	0.20	30	0.007	0.167	0.041	816	0.013716
72.0	46.0	0.52	30	0.017	0.434	0.153	2122	0.007536
81.6	37.0	0.66	30	0.022	0.550	0.262	2693	0.008025
90.0	28.0	0.27	10	0.027	0.676	0.364	3305	0.007407
100.5	18.5	0.32	10	0.032	0.801	0.481	3917	0.006974

Table B.14 Observation for 0.05% PAM Solution with *r/R*: 0.012 (Hg)

R (cm)		Weight, w (kg)	Time, t (s)	Mass flow rate, $\dot{m}$ (kg/s)	Velocity, v (m/s)	Head loss, ΔH (m of water)	Reynolds Number, Re	Friction factor, f
48.2	43.8	0.35	10	0.035	0.876	0.552	4284	0.006691
48.7	43.0	0.41	10	0.041	1.026	0.716	5018	0.006317
52.5	39.5	0.66	10	0.066	1.651	1.632	8078	0.005560
59.7	32.0	1.06	10	0.106	2.652	3.477	12974	0.004592
67.0	25.0	1.38	10	0.138	3.453	5.272	16891	0.004108
73.0	19.0	1.58	10	0.158	3.953	6.779	19339	0.004030

Table B.15 Observation for 0.05% PAM Solution with *r/R*: 0.018 (CCl_4)

R (cm)		Weight, w (kg)	Time, t (s)	Mass flow rate, $\dot{m}$ (kg/s)	Velocity, v (m/s)	Head loss, ΔH (m of water)	Reynolds Number, Re	Friction factor, f
61.0	56.5	0.12	30	0.004	0.100	0.026	490	0.024493
63.5	54.2	0.14	20	0.007	0.175	0.055	857	0.016529
65.0	52.5	0.18	20	0.009	0.225	0.073	1102	0.013439
71.5	46.5	0.30	20	0.015	0.375	0.147	1836	0.009676
74.5	43.5	0.34	20	0.017	0.425	0.182	2081	0.009341
76.0	41.5	0.36	20	0.018	0.450	0.202	2203	0.009273

Table B.16 Observation for 0.05% PAM Solution with *r/R*: 0.018 (Hg)

R (cm)		Weight, *w* (kg)	Time, *t* (s)	Mass flow rate, $\dot{m}$ (kg/s)	Velocity, *v* (m/s)	Head loss, ΔH (m of water)	Reynolds Number, Re	Friction factor, f
53.0	39.0	0.68	10	0.068	1.701	1.757	8323	0.005640
56.5	35.5	1.72	20	0.086	2.152	2.636	10526	0.005289
61.5	30.5	2.14	20	0.107	2.677	3.892	13097	0.005044
66.9	24.9	2.58	20	0.129	3.228	5.272	15789	0.004702
71.6	20.2	1.44	10	0.144	3.603	6.452	17625	0.004618
77.0	15.0	1.62	10	0.162	4.053	7.783	19828	0.004401

Table B.17 Observation for 0.05% PAM Solution with *r/R*: 0.024 (CCl_4)

R (cm)		Weight, *w* (kg)	Time, *t* (s)	Mass flow rate, $\dot{m}$ (kg/s)	Velocity, *v* (m/s)	Head loss, ΔH (m of water)	Reynolds Number, Re	Friction factor, f
59.3	58.5	0.02	30	0.001	0.017	0.005	82	0.156756
60.3	57.5	0.04	20	0.002	0.050	0.016	245	0.060961
61.3	56.5	0.08	20	0.004	0.100	0.028	490	0.026126
67.1	50.6	0.10	10	0.010	0.250	0.097	1224	0.014369
67.3	50.5	0.08	10	0.008	0.200	0.099	979	0.022860
69.5	48.0	0.10	10	0.010	0.250	0.126	1224	0.018724
77.0	40.4	0.18	10	0.018	0.450	0.215	2203	0.009838

Table B.18 Observation for 0.05% PAM Solution with *r/R*: 0.024 (Hg)

R (cm)		Weight, *w* (kg)	Time, *t* (s)	Mass flow rate, $\dot{m}$ (kg/s)	Velocity, *v* (m/s)	Head loss, ΔH (m of water)	Reynolds Number, Re	Friction factor, f
48.5	43.5	0.35	10	0.035	0.876	0.628	4284	0.007604
48.9	43.0	0.39	10	0.039	0.976	0.741	4774	0.007226
51.5	40.5	0.55	10	0.055	1.376	1.381	6732	0.006774
60.8	30.8	1.00	10	0.100	2.502	3.766	12240	0.005589
63.9	27.6	1.12	10	0.112	2.802	4.557	13709	0.005391
68.3	23.4	1.28	10	0.128	3.203	5.636	15667	0.005105
87.5	4.3	1.80	10	0.180	4.504	10.444	22032	0.004784

Table B.19 Observation for 0.07% PAM Solution with *r/R*: 0.012 (CCl_4)

R (cm)		Weight, *w* (kg)	Time, *t* (s)	Mass flow rate, $\dot{m}$ (kg/s)	Velocity, *v* (m/s)	Head loss, ΔH (m of water)	Reynolds Number, Re	Friction factor, f
47.8	47.0	0.04	25	0.002	0.040	0.005	189	0.027215
59.8	34.8	0.14	10	0.014	0.350	0.147	1657	0.011108
67.7	27.0	0.20	10	0.020	0.500	0.239	2367	0.008861
75.2	19.5	0.26	10	0.026	0.651	0.327	3078	0.007176
81.0	14.0	0.29	10	0.029	0.726	0.393	3433	0.006938
87.0	7.5	0.32	10	0.032	0.801	0.467	3788	0.006761
92.5	2.0	0.36	10	0.036	0.901	0.531	4261	0.006081

Table B.20 Observation for 0.07% PAM Solution with *r/R*: 0.012 (Hg)

R (cm)		Weight, *w* (kg)	Time, *t* (s)	Mass flow rate, $\dot{m}$ (kg/s)	Velocity, *v* (m/s)	Head loss, ΔH (m of water)	Reynolds Number, Re	Friction factor, f
48.8	43.0	0.43	10	0.043	1.076	0.728	5090	0.005843
52.3	39.6	0.68	10	0.068	1.701	1.594	8049	0.005116
56.1	35.7	0.90	10	0.090	2.252	2.561	10653	0.004692
59.0	32.5	1.08	10	0.108	2.702	3.327	12784	0.004232
63.0	28.5	1.28	10	0.128	3.203	4.331	15151	0.003923
67.5	24.0	1.46	10	0.146	3.653	5.461	17282	0.003802
75.0	16.5	1.70	10	0.170	4.253	7.344	20123	0.003771

Table B.21 Observation for 0.07% PAM Solution with *r/R*: 0.018 (CCl_4)

R (cm)		Weight, *w* (kg)	Time, *t* (s)	Mass flow rate, $\dot{m}$ (kg/s)	Velocity, *v* (m/s)	Head loss, ΔH (m of water)	Reynolds Number, Re	Friction factor, f
49.5	44.5	0.06	20	0.003	0.075	0.029	355	0.048381
50.0	44.0	0.04	10	0.004	0.100	0.035	473	0.032657
59.0	34.0	0.12	10	0.012	0.300	0.147	1420	0.015119
62.5	30.9	0.16	10	0.016	0.400	0.185	1894	0.010750
67.5	25.9	0.20	10	0.020	0.500	0.244	2367	0.009057
71.5	22.0	0.22	10	0.022	0.550	0.290	2604	0.008907

Table B.22 Observation for 0.07% PAM Solution with *r/R*: 0.018 (Hg)

R (cm)		Weight, w (kg)	Time, t (s)	Mass flow rate, $\dot{m}$ (kg/s)	Velocity, v (m/s)	Head loss, ΔH (m of water)	Reynolds Number, Re	Friction factor, f
49.5	42.5	0.45	10	0.045	1.126	0.879	5327	0.006440
52.7	39.1	0.70	10	0.070	1.751	1.707	8286	0.005170
56.4	35.4	0.90	10	0.090	2.252	2.636	10653	0.004830
59.5	32.2	1.04	10	0.104	2.602	3.427	12310	0.004702
64.8	26.8	1.26	10	0.126	3.153	4.770	14914	0.004459
69.3	22.3	1.44	10	0.144	3.603	5.900	17045	0.004222
85.8	5.7	1.94	10	0.194	4.854	10.055	22963	0.003965

Table B.23 Observation for 0.07% PAM Solution with *r/R*: 0.024 (CCl_4)

R (cm)		Weight, w (kg)	Time, t (s)	Mass flow rate, $\dot{m}$ (kg/s)	Velocity, v (m/s)	Head loss, ΔH (m of water)	Reynolds Number, Re	Friction factor, f
60.0	57.5	0.04	20	0.002	0.050	0.015	237	0.054429
65.5	51.7	0.06	10	0.006	0.150	0.081	710	0.033383
70.5	41.7	0.12	10	0.012	0.300	0.169	1420	0.017417
78.0	39.5	0.18	10	0.018	0.450	0.226	2131	0.010348
85.0	32.0	0.22	10	0.022	0.550	0.311	2604	0.009536
95.0	22.5	0.28	10	0.028	0.701	0.425	3314	0.008053
100.8	16.8	0.31	10	0.031	0.776	0.493	3669	0.007612

Table B.24 Observation for 0.07% PAM Solution with *r/R*: 0.024 (Hg)

R (cm)		Weight, w (kg)	Time, t (s)	Mass flow rate, $\dot{m}$ (kg/s)	Velocity, v (m/s)	Head loss, ΔH (m of water)	Reynolds Number, Re	Friction factor, f
48.7	43.5	0.37	10	0.037	0.926	0.653	4380	0.007076
51.3	40.7	0.56	10	0.056	1.401	1.331	6629	0.006297
56.8	35.0	0.86	10	0.086	2.152	2.737	10180	0.005491
63.7	28.1	1.14	10	0.114	2.852	4.469	13494	0.005103
68.0	23.6	1.30	10	0.130	3.253	5.574	15388	0.004894
71.1	20.5	1.44	10	0.144	3.603	6.352	17045	0.004546

Table B.25 Observation for 0.10% PAM Solution with *r/R*: 0.012 (CCl_4)

R (cm)		Weight, *w* (kg)	Time, *t* (s)	Mass flow rate, $\dot{m}$ (kg/s)	Velocity, *v* (m/s)	Head loss, ΔH (m of water)	Reynolds Number, Re	Friction factor, f
55.5	54.0	0.04	20	0.002	0.050	0.009	166	0.032657
59.3	50.0	0.08	10	0.008	0.200	0.055	666	0.012655
67.0	42.5	0.16	10	0.016	0.400	0.144	1331	0.008334
70.5	39.0	0.20	10	0.020	0.500	0.185	1664	0.006858
75.0	34.5	0.21	10	0.021	0.525	0.238	1747	0.007998
83.0	26.5	0.26	10	0.026	0.651	0.332	2163	0.007279
105.0	4.5	0.36	10	0.036	0.901	0.590	2995	0.006753

Table B.26 Observation for 0.10% PAM Solution with *r/R*: 0.012 (Hg)

R (cm)		Weight, *w* (kg)	Time, *t* (s)	Mass flow rate, $\dot{m}$ (kg/s)	Velocity, *v* (m/s)	Head loss, ΔH (m of water)	Reynolds Number, Re	Friction factor, f
49.4	42.4	0.46	10	0.046	1.151	0.879	3827	0.006163
55.0	36.7	0.80	10	0.080	2.002	2.297	6655	0.005327
59.0	32.7	1.00	10	0.100	2.502	3.302	8319	0.004899
64.5	27.3	1.28	10	0.128	3.203	4.670	10648	0.004230
70.0	21.8	1.48	10	0.148	3.703	6.051	12312	0.004099
76.9	15.0	1.70	10	0.170	4.253	7.771	14142	0.003990
80.0	12.0	1.82	10	0.182	4.554	8.536	15140	0.003824

Table B.27 Observation for 0.10% PAM Solution with *r/R*: 0.018 (CCl_4)

R (cm)		Weight, *w* (kg)	Time, *t* (s)	Mass flow rate, $\dot{m}$ (kg/s)	Velocity, *v* (m/s)	Head loss, ΔH (m of water)	Reynolds Number, Re	Friction factor, f
56.0	53.5	0.06	20	0.003	0.075	0.015	250	0.024191
61.0	48.5	0.08	10	0.008	0.200	0.073	666	0.017009
63.0	46.5	0.10	10	0.010	0.250	0.097	832	0.014369
66.5	43.0	0.14	10	0.014	0.350	0.138	1165	0.010441
78.5	31.0	0.22	10	0.022	0.550	0.279	1830	0.008547
88.5	21.0	0.28	10	0.028	0.701	0.396	2329	0.007498

Table B.28 Observation for 0.10% PAM Solution with *r/R*: 0.018 (Hg)

R (cm)		Weight, *w* (kg)	Time, *t* (s)	Mass flow rate, $\dot{m}$ (kg/s)	Velocity, *v* (m/s)	Head loss, ΔH (m of water)	Reynolds Number, Re	Friction factor, f
49.0	43.0	0.40	10	0.040	1.001	0.753	3328	0.006986
54.5	37.5	0.74	10	0.074	1.851	2.134	6156	0.005783
57.0	35.0	0.88	10	0.088	2.202	2.762	7321	0.005292
62.5	29.2	1.14	10	0.114	2.852	4.180	9483	0.004773
69.0	22.9	1.38	10	0.138	3.453	5.787	11480	0.004509
74.8	16.9	1.58	10	0.158	3.953	7.268	13144	0.004321
82.8	9.0	1.80	10	0.180	4.504	9.264	14974	0.004243

Table B.29 Observation for 0.10% PAM Solution with *r/R*: 0.024 (CCl_4)

R (cm)		Weight, *w* (kg)	Time, *t* (s)	Mass flow rate, $\dot{m}$ (kg/s)	Velocity, *v* (m/s)	Head loss, ΔH (m of water)	Reynolds Number, Re	Friction factor, f
55.5	54.0	0.02	20	0.001	0.025	0.009	83	0.130630
61.5	48.0	0.08	10	0.008	0.200	0.079	666	0.018370
64.5	45.0	0.10	10	0.010	0.250	0.114	832	0.016982
68.5	40.0	0.12	10	0.012	0.300	0.167	998	0.017236
70.0	39.5	0.14	10	0.014	0.350	0.179	1165	0.013552
81.5	28.0	0.22	10	0.022	0.550	0.314	1830	0.009626
82.0	27.5	0.24	10	0.024	0.600	0.320	1997	0.008240

Table B.30 Observation for 0.10% PAM Solution with *r/R*: 0.024 (Hg)

R (cm)		Weight, *w* (kg)	Time, *t* (s)	Mass flow rate, $\dot{m}$ (kg/s)	Velocity, *v* (m/s)	Head loss, ΔH (m of water)	Reynolds Number, Re	Friction factor, f
49.2	42.5	0.41	10	0.041	1.026	0.841	3411	0.007425
53.2	38.6	0.66	10	0.066	1.651	1.833	5490	0.006244
56.5	35.4	0.82	10	0.082	2.052	2.649	6821	0.005846
59.3	32.5	0.94	10	0.094	2.352	3.364	7820	0.005650
64.0	27.8	1.14	10	0.114	2.852	4.544	9483	0.005189
67.7	24.0	1.28	10	0.128	3.203	5.486	10648	0.004969

Table B.31 Observation for 0.15% PAM Solution with *r/R*: 0.012 (CCl_4)

R (cm)		Weight, *w* (kg)	Time, *t* (s)	Mass flow rate, $\dot{m}$ (kg/s)	Velocity, *v* (m/s)	Head loss, ΔH (m of water)	Reynolds Number, Re	Friction factor, f
54.0	51.0	0.04	10	0.004	0.100	0.018	317	0.016329
60.5	44.5	0.10	10	0.010	0.250	0.094	792	0.013934
70.0	35.0	0.16	10	0.016	0.400	0.205	1268	0.011906
72.0	33.0	0.18	10	0.018	0.450	0.229	1426	0.010483
75.0	30.0	0.22	10	0.022	0.550	0.264	1743	0.008097
85.5	19.3	0.26	10	0.026	0.651	0.388	2060	0.008528
91.0	14.0	0.24	10	0.024	0.600	0.452	1902	0.011642

Table B.32 Observation for 0.15% PAM Solution with *r/R*: 0.012 (Hg)

R (cm)		Weight, *w* (kg)	Time, *t* (s)	Mass flow rate, $\dot{m}$ (kg/s)	Velocity, *v* (m/s)	Head loss, ΔH (m of water)	Reynolds Number, Re	Friction factor, f
47.5	44.4	0.26	10	0.026	0.651	0.389	2060	0.008543
51.5	40.3	0.54	10	0.054	1.351	1.406	4279	0.007155
55.0	36.8	0.70	10	0.070	1.751	2.285	5546	0.006919
60.0	31.8	0.92	10	0.092	2.302	3.540	7289	0.006207
61.5	30.4	0.98	10	0.098	2.452	3.904	7765	0.006032
67.5	24.4	1.18	10	0.118	2.952	5.411	9349	0.005766
76.0	15.8	1.44	10	0.144	3.603	7.557	11410	0.005408

Table B.33 Observation for 0.15% PAM Solution with *r/R*: 0.018 (CCl_4)

R (cm)		Weight, *w* (kg)	Time, *t* (s)	Mass flow rate, $\dot{m}$ (kg/s)	Velocity, *v* (m/s)	Head loss, ΔH (m of water)	Reynolds Number, Re	Friction factor, f
57.0	52.0	0.08	20	0.004	0.100	0.029	317	0.027215
61.5	47.5	0.08	10	0.008	0.200	0.082	634	0.019050
62.8	46.0	0.09	10	0.009	0.225	0.099	713	0.018062
67.0	42.0	0.12	10	0.012	0.300	0.147	951	0.015119
80.5	28.5	0.22	10	0.022	0.550	0.305	1743	0.009356
90.0	19.0	0.26	10	0.026	0.651	0.417	2060	0.009147

Table B.34 Observation for 0.15% PAM Solution with *r/R*: 0.018 (Hg)

R (cm)		Weight, *w* (kg)	Time, *t* (s)	Mass flow rate, $\dot{m}$ (kg/s)	Velocity, *v* (m/s)	Head loss, ΔH (m of water)	Reynolds Number, Re	Friction factor, f
50.8	41.0	0.48	10	0.048	1.201	1.230	3803	0.007924
54.8	37.0	0.67	10	0.067	1.676	2.235	5309	0.007387
58.8	33.0	0.84	10	0.084	2.102	3.239	6656	0.006811
66.0	25.8	1.09	10	0.109	2.727	5.046	8636	0.006303
68.0	23.8	1.16	10	0.116	2.902	5.549	9191	0.006119
73.0	18.8	1.30	10	0.130	3.253	6.804	10300	0.005974
80.0	11.8	1.50	10	0.150	3.753	8.561	11885	0.005647

Table B.35 Observation for 0.15% PAM Solution with *r/R*: 0.024 (CCl_4)

R (cm)		Weight, *w* (kg)	Time, *t* (s)	Mass flow rate, $\dot{m}$ (kg/s)	Velocity, *v* (m/s)	Head loss, ΔH (m of water)	Reynolds Number, Re	Friction factor, f
57.5	51.5	0.08	20	0.004	0.100	0.035	317	0.032657
62.3	46.7	0.08	10	0.008	0.200	0.092	634	0.021227
70.2	38.4	0.12	10	0.012	0.300	0.187	951	0.019232
76.0	32.0	0.18	10	0.018	0.450	0.258	1426	0.011827
84.3	24.5	0.22	10	0.022	0.550	0.351	1743	0.010760
94.0	14.8	0.28	10	0.028	0.701	0.465	2219	0.008798
99.5	9.5	0.32	10	0.032	0.801	0.528	2535	0.007654

Table B.36 Observation for 0.15% PAM Solution with *r/R*: 0.024 (Hg)

R (cm)		Weight, *w* (kg)	Time, *t* (s)	Mass flow rate, $\dot{m}$ (kg/s)	Velocity, *v* (m/s)	Head loss, ΔH (m of water)	Reynolds Number, Re	Friction factor, f
48.0	43.8	0.30	10	0.030	0.751	0.527	2377	0.008693
51.0	40.8	0.47	10	0.047	1.176	1.280	3724	0.008602
56.0	35.9	0.69	10	0.069	1.726	2.523	5467	0.007865
60.0	31.8	0.84	10	0.084	2.102	3.540	6656	0.007445
65.5	26.3	1.02	10	0.102	2.552	4.921	8082	0.007019
71.0	20.8	1.19	10	0.119	2.977	6.302	9429	0.006604

Table B.37 Observation for 0.01% PVA Solution with *r/R*: 0.012 (CCl_4)

R (cm)		Weight, *w* (kg)	Time, *t* (s)	Mass flow rate, $\dot{m}$ (kg/s)	Velocity, *v* (m/s)	Head loss, ΔH (m of water)	Reynolds Number, Re	Friction factor, f
57.7	50.2	0.14	20	0.007	0.175	0.044	1210	0.013330
62.8	45.1	0.12	10	0.012	0.300	0.104	2075	0.010704
70.5	37.0	0.19	10	0.019	0.463	0.197	3199	0.008524
78.5	29.4	0.23	10	0.023	0.575	0.288	3977	0.008083
81.0	26.9	0.25	10	0.025	0.613	0.317	4236	0.007849
95.0	12.9	0.31	10	0.031	0.776	0.482	5360	0.007440

Table B.38 Observation for 0.01% PVA Solution with *r/R*: 0.012 (Hg)

R (cm)		Weight, *w* (kg)	Time, *t* (s)	Mass flow rate, $\dot{m}$ (kg/s)	Velocity, *v* (m/s)	Head loss, ΔH (m of water)	Reynolds Number, Re	Friction factor, f
50.5	41.3	0.52	10	0.052	1.301	1.155	8991	0.006338
53.0	38.8	0.66	10	0.066	1.651	1.783	11412	0.006073
58.8	33.0	0.93	10	0.093	2.327	3.239	16081	0.005557
63.0	28.8	1.11	10	0.111	2.777	4.293	19193	0.005171
66.8	25.0	1.24	10	0.124	3.102	5.247	21441	0.005064
76.5	15.3	1.52	10	0.152	3.803	7.683	26282	0.004935
81.5	10.3	1.64	10	0.164	4.103	8.938	28357	0.004931

Table B.39 Observation for 0.01% PVA Solution with *r/R*: 0.018 (CCl_4)

R(cm)		Weight (kg)	Time (sec)	Mass flow rate (kg/sec)	Velocity (m/s)	Head loss (m of water)	Reynolds Number	Friction factor
54.8	53.2	0.06	20	0.003	0.075	0.009	519	0.015482
58.2	49.8	0.06	10	0.006	0.150	0.049	1037	0.020320
61.8	46.2	0.10	10	0.010	0.250	0.092	1729	0.013585
65.7	42.3	0.13	10	0.013	0.325	0.137	2248	0.012058
69.5	38.5	0.17	10	0.017	0.425	0.182	2939	0.009341
83.0	25.0	0.25	10	0.025	0.626	0.340	4323	0.008082
91.5	16.5	0.29	10	0.029	0.726	0.440	5014	0.007766

Table B.40 Observation for 0.01% PVA Solution with *r/R*: 0.018 (Hg)

R (cm)		Weight, *w* (kg)	Time, *t* (s)	Mass flow rate, $\dot{m}$ (kg/s)	Velocity, *v* (m/s)	Head loss, ΔH (m of water)	Reynolds Number, Re	Friction factor, f
49.0	42.8	0.41	10	0.041	1.026	0.778	7089	0.006871
53.5	38.3	0.66	10	0.066	1.651	1.908	11412	0.006500
58.6	33.2	0.88	10	0.088	2.202	3.189	15216	0.006110
63.4	28.4	1.06	10	0.106	2.652	4.394	18328	0.005803
67.1	24.7	1.21	10	0.121	3.027	5.323	20922	0.005395
73.6	18.2	1.39	10	0.139	3.478	6.955	24034	0.005341
80.5	11.3	1.56	10	0.156	3.903	8.687	26974	0.005297

Table B.41 Observation for 0.01% PVA Solution with *r/R*: 0.024 (CCl_4)

R (cm)		Weight, *w* (kg)	Time, *t* (s)	Mass flow rate, $\dot{m}$ (kg/s)	Velocity, *v* (m/s)	Head loss, ΔH (m of water)	Reynolds Number, Re	Friction factor, f
56.0	51.5	0.08	20	0.004	0.100	0.026	692	0.024493
58.5	49.0	0.08	10	0.008	0.200	0.056	1383	0.012927
61.5	46.0	0.11	10	0.011	0.263	0.091	1816	0.012243
67.2	40.3	0.15	10	0.015	0.375	0.158	2594	0.010412
73.5	34.0	0.20	10	0.020	0.488	0.232	3372	0.009046
81.0	26.5	0.24	10	0.024	0.588	0.320	4063	0.008594
88.0	19.5	0.27	10	0.027	0.676	0.402	4669	0.008183

Table B.42 Observation for 0.01% PVA Solution with *r/R*: 0.024 (Hg)

R (cm)		Weight, *w* (kg)	Time, *t* (s)	Mass flow rate, $\dot{m}$ (kg/s)	Velocity, *v* (m/s)	Head loss, ΔH (m of water)	Reynolds Number, Re	Friction factor, f
48.8	43	0.38	10	0.038	0.951	0.728	6571	0.007482
53.5	38.3	0.65	10	0.065	1.626	1.908	11239	0.006702
59.3	32.6	0.88	10	0.088	2.202	3.352	15216	0.006423
63.5	28.3	1.03	10	0.103	2.577	4.419	17810	0.006181
66.4	25.4	1.14	10	0.114	2.852	5.147	19712	0.005877
71.1	20.7	1.28	10	0.128	3.203	6.327	22132	0.005730

Table B.43 Observation for 0.03% PVA Solution with *r/R*: 0.012 (CCl_4)

R (cm)		Weight, *w* (kg)	Time, *t* (s)	Mass flow rate, $\dot{m}$ (kg/s)	Velocity, *v* (m/s)	Head loss, ΔH (m of water)	Reynolds Number, Re	Friction factor, f
54.6	52.9	0.04	20	0.002	0.050	0.010	341	0.037012
59.8	47.7	0.10	10	0.010	0.250	0.071	1707	0.010537
65.6	41.9	0.19	10	0.019	0.475	0.139	3244	0.005717
71.3	36.2	0.24	10	0.024	0.600	0.206	4098	0.005307
79.0	28.5	0.30	10	0.030	0.751	0.296	5122	0.004887
85.0	22.5	0.34	10	0.034	0.851	0.367	5805	0.004708
99.0	8.5	0.42	10	0.042	1.051	0.531	7171	0.004468

Table B.44 Observation for 0.03% PVA Solution with *r/R*: 0.012 (Hg)

R (cm)		Weight, *w* (kg)	Time, *t* (s)	Mass flow rate, $\dot{m}$ (kg/s)	Velocity, *v* (m/s)	Head loss, ΔH (m of water)	Reynolds Number, Re	Friction factor, f
49.8	42.0	0.59	10	0.059	1.476	0.979	10074	0.004174
54.0	37.8	0.88	10	0.088	2.202	2.034	15025	0.003897
59.5	32.3	1.16	10	0.116	2.902	3.415	19806	0.003766
62.3	29.5	1.30	10	0.130	3.253	4.118	22196	0.003615
69.5	22.3	1.58	10	0.158	3.953	5.925	26977	0.003522
74.8	17.0	1.78	10	0.178	4.454	7.256	30392	0.003398
80.6	11.2	1.96	10	0.196	4.904	8.712	33465	0.003365

Table B.45 Observation for 0.03% PVA Solution with *r/R*: 0.018 (CCl_4)

R (cm)		Weight, *w* (kg)	Time, *t* (s)	Mass flow rate, $\dot{m}$ (kg/s)	Velocity, *v* (m/s)	Head loss, ΔH (m of water)	Reynolds Number, Re	Friction factor, f
54.5	53.0	0.04	20	0.002	0.050	0.009	341	0.032657
56.5	51.0	0.06	10	0.006	0.150	0.032	1024	0.013305
59.5	48.0	0.10	10	0.010	0.250	0.067	1707	0.010015
61.5	46.0	0.12	10	0.012	0.300	0.091	2049	0.009374
71.0	36.5	0.19	10	0.019	0.475	0.202	3244	0.008323
80.0	27.5	0.24	10	0.024	0.600	0.308	4098	0.007938

Table B.46 Observation for 0.03% PVA Solution with *r/R*: 0.018 (Hg)

R (cm)		Weight, *w* (kg)	Time, *t* (s)	Mass flow rate, $\dot{m}$ (kg/s)	Velocity, *v* (m/s)	Head loss, ΔH (m of water)	Reynolds Number, Re	Friction factor, f
48.9	42.9	0.42	10	0.042	1.051	0.753	7171	0.006336
53.3	38.6	0.68	10	0.068	1.701	1.845	11610	0.005922
60.0	31.8	0.98	10	0.098	2.452	3.540	16733	0.005470
66.3	25.5	1.26	10	0.126	3.153	5.122	21513	0.004787
69.7	22.1	1.37	10	0.137	3.428	5.975	23391	0.004724
72.7	19.1	1.46	10	0.146	3.653	6.729	24928	0.004684
81.2	10.6	1.70	10	0.170	4.253	8.863	29026	0.004551

Table B.47 Observation for 0.03% PVA Solution with *r/R*: 0.024 (CCl_4)

R (cm)		Weight, *w* (kg)	Time, *t* (s)	Mass flow rate, $\dot{m}$ (kg/s)	Velocity, *v* (m/s)	Head loss, ΔH (m of water)	Reynolds Number, Re	Friction factor, f
55.0	52.5	0.06	20	0.003	0.075	0.015	512	0.024191
58.2	49.3	0.08	10	0.008	0.200	0.052	1366	0.012110
66.0	41.5	0.15	10	0.015	0.375	0.144	2561	0.009483
72.5	35.0	0.20	10	0.020	0.488	0.220	3329	0.008588
81.5	26.0	0.24	10	0.024	0.600	0.326	4098	0.008391
87.5	20.0	0.27	10	0.027	0.676	0.396	4610	0.008064
100.5	7.0	0.33	10	0.033	0.826	0.549	5634	0.007477

Table B.48 Observation for 0.03% PVA Solution with *r/R*: 0.024 (Hg)

R (cm)		Weight, *w* (kg)	Time, *t* (s)	Mass flow rate, $\dot{m}$ (kg/s)	Velocity, *v* (m/s)	Head loss, ΔH (m of water)	Reynolds Number, Re	Friction factor, f
52.5	39.3	0.62	10	0.062	1.551	1.657	10586	0.006397
58.3	33.5	0.88	10	0.088	2.202	3.113	15025	0.005966
63.7	28.1	1.10	10	0.110	2.752	4.469	18781	0.005481
68.0	23.8	1.25	10	0.125	3.128	5.549	21343	0.005270
72.0	19.8	1.38	10	0.138	3.453	6.553	23562	0.005106
80.5	11.3	1.62	10	0.162	4.053	8.687	27660	0.004912

Table B.49 Observation for 0.05% PVA Solution with *r/R*: 0.012 (CCl_4)

R (cm)		Weight, *w* (kg)	Time, *t* (s)	Mass flow rate, $\dot{m}$ (kg/s)	Velocity, *v* (m/s)	Head loss, ΔH (m of water)	Reynolds Number, Re	Friction factor, f
56.0	51.5	0.12	20	0.006	0.150	0.026	1012	0.010886
61.0	46.5	0.12	10	0.012	0.300	0.085	2024	0.008769
67.5	40.0	0.20	10	0.020	0.500	0.161	3373	0.005987
76.0	31.5	0.27	10	0.027	0.676	0.261	4553	0.005316
86.5	21.0	0.34	10	0.034	0.851	0.384	5734	0.004934
97.5	10.0	0.40	10	0.040	1.001	0.513	6746	0.004763
106.0	1.5	0.44	10	0.044	1.101	0.613	7420	0.004701

Table B.50 Observation for 0.05% PVA Solution with *r/R*: 0.012 (Hg)

R (cm)		Weight, *w* (kg)	Time, *t* (s)	Mass flow rate, $\dot{m}$ (kg/s)	Velocity, *v* (m/s)	Head loss, ΔH (m of water)	Reynolds Number, Re	Friction factor, f
48.5	43.3	0.46	10	0.046	1.151	0.653	7758	0.004578
52.8	39.0	0.78	10	0.078	1.952	1.732	13154	0.004225
56.5	35.3	0.98	10	0.098	2.452	2.661	16527	0.004112
60.9	30.9	1.18	10	0.118	2.952	3.766	19900	0.004014
67.3	24.5	1.44	10	0.144	3.603	5.373	24284	0.003845
71.1	20.7	1.58	10	0.158	3.953	6.327	26645	0.003761
81.0	10.8	1.88	10	0.188	4.704	8.812	31705	0.003700

Table B.51 Observation for 0.05% PAM Solution with *r/R*: 0.018 (CCl_4)

R (cm)		Weight, *w* (kg)	Time, *t* (s)	Mass flow rate, $\dot{m}$ (kg/s)	Velocity, *v* (m/s)	Head loss, ΔH (m of water)	Reynolds Number, Re	Friction factor, f
56.0	51.5	0.10	20	0.005	0.125	0.026	843	0.015676
63.0	44.5	0.12	10	0.012	0.300	0.109	2024	0.011188
69.3	38.2	0.17	10	0.017	0.425	0.183	2867	0.009372
71.5	36.0	0.19	10	0.019	0.475	0.208	3204	0.008564
84.5	23.0	0.26	10	0.026	0.651	0.361	4385	0.007923
93.0	14.5	0.31	10	0.031	0.776	0.461	5228	0.007114

Table B.52 Observation for 0.05% PVA Solution with *r/R*: 0.018 (Hg)

R (cm)		Weight, *w* (kg)	Time, *t* (s)	Mass flow rate, $\dot{m}$ (kg/s)	Velocity, *v* (m/s)	Head loss, ΔH (m of water)	Reynolds Number, Re	Friction factor, f
50.2	41.6	0.50	10	0.050	1.251	1.080	8432	0.006408
54.5	37.3	0.73	10	0.073	1.826	2.159	12311	0.006013
60.5	31.3	0.98	10	0.098	2.452	3.666	16527	0.005664
67.1	24.7	1.24	10	0.124	3.102	5.323	20912	0.005137
72.1	19.7	1.40	10	0.140	3.503	6.578	23610	0.004980
77.2	14.6	1.54	10	0.154	3.853	7.858	25971	0.004917
80.7	11.1	1.64	10	0.164	4.103	8.737	27657	0.004821

Table B.53 Observation for 0.05% PVA Solution with *r/R*: 0.024 (CCl_4)

R (cm)		Weight, *w* (kg)	Time, *t* (s)	Mass flow rate, $\dot{m}$ (kg/s)	Velocity, *v* (m/s)	Head loss, ΔH (m of water)	Reynolds Number, Re	Friction factor, f
55.0	52.5	0.06	20	0.003	0.075	0.015	506	0.024191
60.0	47.5	0.10	10	0.010	0.250	0.073	1686	0.010886
67.0	40.5	0.15	10	0.015	0.375	0.156	2530	0.010257
79.0	28.5	0.23	10	0.023	0.563	0.296	3794	0.008687
89.5	18.0	0.28	10	0.028	0.701	0.420	4722	0.007942
96.5	11.0	0.31	10	0.031	0.776	0.502	5228	0.007748
104.5	3.0	0.34	10	0.034	0.851	0.596	5734	0.007646

Table B.54 Observation for 0.05% PVA Solution with *r/R*: 0.024 (Hg)

R (cm)		Weight, *w* (kg)	Time, *t* (s)	Mass flow rate, $\dot{m}$ (kg/s)	Velocity, *v* (m/s)	Head loss, ΔH (m of water)	Reynolds Number, Re	Friction factor, f
48.8	43	0.38	10	0.038	0.951	0.728	6408	0.007482
54.8	37	0.72	10	0.072	1.801	2.235	12142	0.006396
59.7	32.2	0.92	10	0.092	2.302	3.452	15515	0.006053
64.6	27.2	1.09	10	0.109	2.727	4.695	18382	0.005864
68	23.9	1.23	10	0.123	3.077	5.536	20743	0.005430
75.1	16.7	1.42	10	0.142	3.553	7.331	23947	0.005395

Table B.55 Observation for 0.07% PVA Solution with *r/R*: 0.012 (CCl_4)

R (cm)		Weight, *w* (kg)	Time, *t* (s)	Mass flow rate, $\dot{m}$ (kg/s)	Velocity, *v* (m/s)	Head loss, ΔH (m of water)	Reynolds Number, Re	Friction factor, f
54.7	52.8	0.06	20	0.003	0.075	0.011	493	0.018385
60.9	46.6	0.10	10	0.010	0.250	0.084	1642	0.012453
65.5	42.0	0.15	10	0.015	0.375	0.138	2463	0.009096
77.3	30.2	0.22	10	0.022	0.550	0.276	3612	0.008475
80.4	27.1	0.24	10	0.024	0.600	0.313	3940	0.008059
94.0	13.5	0.30	10	0.030	0.751	0.472	4925	0.007789
97.8	9.7	0.32	10	0.032	0.801	0.517	5253	0.007493

Table B.56 Observation for 0.07% PVA Solution with *r/R*: 0.012 (Hg)

R (cm)		Weight, *w* (kg)	Time, *t* (s)	Mass flow rate, $\dot{m}$ (kg/s)	Velocity, *v* (m/s)	Head loss, ΔH (m of water)	Reynolds Number, Re	Friction factor, f
49.0	42.8	0.40	10	0.040	1.001	0.778	6567	0.007219
51.6	40.2	0.58	10	0.058	1.451	1.431	9522	0.006313
55.8	36.0	0.79	10	0.079	1.977	2.486	12969	0.005910
60.3	31.5	0.98	10	0.098	2.452	3.615	16089	0.005586
65.8	26.0	1.18	10	0.118	2.952	4.996	19372	0.005325
69.8	22.0	1.30	10	0.130	3.253	6.001	21342	0.005269
80.5	11.3	1.60	10	0.160	4.003	8.687	26267	0.005036

Table B.57 Observation for 0.07% PVA Solution with *r/R*: 0.018 (CCl_4)

R (cm)		Weight, *w* (kg)	Time, *t* (s)	Mass flow rate, $\dot{m}$ (kg/s)	Velocity, *v* (m/s)	Head loss, ΔH (m of water)	Reynolds Number, Re	Friction factor, f
54.5	53.0	0.04	20	0.002	0.050	0.009	328	0.032657
59.4	48.0	0.08	10	0.008	0.200	0.067	1313	0.015512
62.8	44.6	0.12	10	0.012	0.300	0.107	1970	0.011007
69.5	37.9	0.17	10	0.017	0.425	0.185	2791	0.009522
75.0	32.5	0.20	10	0.020	0.500	0.249	3283	0.009253
79.5	28.0	0.23	10	0.023	0.575	0.302	3776	0.008478

Table B.58 Observation for 0.07% PVA Solution with *r/R*: 0.018 (Hg)

R (cm)		Weight, *w* (kg)	Time, *t* (s)	Mass flow rate, $\dot{m}$ (kg/s)	Velocity, *v* (m/s)	Head loss, ΔH (m of water)	Reynolds Number, Re	Friction factor, f
48.1	43.7	0.32	10	0.032	0.801	0.552	5253	0.008004
52.6	39.2	0.60	10	0.060	1.501	1.682	9850	0.006934
56.8	35.0	0.79	10	0.079	1.977	2.737	12969	0.006507
59.9	31.9	0.91	10	0.091	2.277	3.515	14939	0.006299
64.8	27.0	1.10	10	0.110	2.752	4.745	18059	0.005820
70.4	21.4	1.28	10	0.128	3.203	6.151	21014	0.005571
80.7	11.1	1.54	10	0.154	3.853	8.737	25282	0.005467

Table B.59 Observation for 0.07% PVA Solution with *r/R*: 0.024 (CCl_4)

R (cm)		Weight, *w* (kg)	Time, *t* (s)	Mass flow rate, $\dot{m}$ (kg/s)	Velocity, *v* (m/s)	Head loss, ΔH (m of water)	Reynolds Number, Re	Friction factor, f
54.7	52.8	0.06	20	0.003	0.075	0.011	493	0.018385
60.5	47.0	0.09	10	0.009	0.225	0.079	1478	0.014514
65.0	42.4	0.12	10	0.012	0.300	0.133	1970	0.013668
67.0	40.4	0.14	10	0.014	0.350	0.156	2298	0.011819
70.0	37.5	0.16	10	0.016	0.400	0.191	2627	0.011056
79.5	28.0	0.22	10	0.022	0.550	0.302	3612	0.009266
95.0	12.5	0.30	10	0.030	0.738	0.484	4843	0.008256

Table B.60 Observation for 0.07% PVA Solution with *r/R*: 0.024 (Hg)

R (cm)		Weight, *w* (kg)	Time, *t* (s)	Mass flow rate, $\dot{m}$ (kg/s)	Velocity, *v* (m/s)	Head loss, ΔH (m of water)	Reynolds Number, Re	Friction factor, f
49.3	42.5	0.40	10	0.040	1.001	0.854	6567	0.007917
53.6	38.2	0.64	10	0.064	1.601	1.933	10507	0.007004
57.8	34.0	0.81	10	0.081	2.027	2.988	13298	0.006758
65.0	26.8	1.06	10	0.106	2.652	4.795	17402	0.006333
70.0	21.8	1.20	10	0.120	3.002	6.051	19700	0.006235
74.0	17.8	1.31	10	0.131	3.278	7.055	21506	0.006101

Table B.61 Observation for 0.10% PVA Solution with *r/R*: 0.012 (CCl_4)

R (cm)		Weight, *w* (kg)	Time, *t* (s)	Mass flow rate, $\dot{m}$ (kg/s)	Velocity, *v* (m/s)	Head loss, ΔH (m of water)	Reynolds Number, Re	Friction factor, f
56.5	50.5	0.01	20	0.001	0.019	0.035	122	0.928923
64.8	42.2	0.10	20	0.005	0.125	0.133	815	0.078726
71.0	36.0	0.19	10	0.019	0.463	0.205	3015	0.008906
82.3	24.7	0.25	10	0.025	0.626	0.338	4075	0.008026
93.5	13.5	0.30	10	0.030	0.751	0.469	4890	0.007741
100.0	7.0	0.32	10	0.032	0.801	0.546	5216	0.007909
106.2	0.8	0.35	10	0.035	0.876	0.619	5705	0.007493

Table B.62 Observation for 0.10% PVA Solution with *r/R*: 0.012 (Hg)

R (cm)		Weight, *w* (kg)	Time, *t* (s)	Mass flow rate, $\dot{m}$ (kg/s)	Velocity, *v* (m/s)	Head loss, ΔH (m of water)	Reynolds Number, Re	Friction factor, f
48.6	43.2	0.37	10	0.037	0.926	0.678	6031	0.007348
53.0	38.8	0.65	10	0.065	1.626	1.783	10595	0.006261
57.0	34.8	0.82	10	0.082	2.052	2.787	13366	0.006150
63.5	28.3	1.08	10	0.108	2.702	4.419	17604	0.005622
69.2	22.6	1.26	10	0.126	3.153	5.850	20538	0.005468
75.0	16.8	1.44	10	0.144	3.603	7.306	23472	0.005229
80.5	11.3	1.58	10	0.158	3.953	8.687	25754	0.005164

Table B.63 Observation for 0.10% PVA Solution with *r/R*: 0.018 (CCl_4)

R (cm)		Weight, *w* (kg)	Time, *t* (s)	Mass flow rate, $\dot{m}$ (kg/s)	Velocity, *v* (m/s)	Head loss, ΔH (m of water)	Reynolds Number, Re	Friction factor, f
54.0	53.0	0.02	20	0.001	0.025	0.006	163	0.087087
58.0	49.0	0.08	10	0.008	0.200	0.053	1304	0.012247
64.8	42.2	0.13	10	0.013	0.325	0.133	2119	0.011646
69.5	37.5	0.16	10	0.016	0.400	0.188	2608	0.010886
76.6	30.4	0.21	10	0.021	0.525	0.271	3423	0.009123
89.0	18.0	0.27	10	0.027	0.676	0.417	4401	0.008482

Table B.64 Observation for 0.10% PVA Solution with *r/R*: 0.018 (Hg)

R (cm)		Weight, *w* (kg)	Time, *t* (s)	Mass flow rate, $\dot{m}$ (kg/s)	Velocity, *v* (m/s)	Head loss, ΔH (m of water)	Reynolds Number, Re	Friction factor, f
49.9	41.9	0.45	10	0.045	1.126	1.004	7335	0.007359
53.5	38.3	0.63	10	0.063	1.576	1.908	10269	0.007134
57.5	34.3	0.81	10	0.081	2.027	2.912	13203	0.006587
61.0	30.8	0.94	10	0.094	2.352	3.791	15322	0.006367
65.0	26.8	1.07	10	0.107	2.677	4.795	17441	0.006216
74.5	17.3	1.34	10	0.134	3.353	7.181	21842	0.005934
80.5	11.3	1.50	10	0.150	3.753	8.687	24450	0.005729

Table B.65 Observation for 0.10% PVA Solution with *r/R*: 0.024 (CCl_4)

R (cm)		Weight, *w* (kg)	Time, *t* (s)	Mass flow rate, $\dot{m}$ (kg/s)	Velocity, *v* (m/s)	Head loss, ΔH (m of water)	Reynolds Number, Re	Friction factor, f
54.0	53.0	0.02	20	0.001	0.025	0.006	163	0.087087
59.0	48.0	0.08	10	0.008	0.200	0.065	1304	0.014968
67.5	39.5	0.14	10	0.014	0.350	0.164	2282	0.012441
73.0	34.0	0.19	10	0.019	0.463	0.229	3015	0.009924
78.5	28.5	0.22	10	0.022	0.538	0.293	3504	0.009420
87.9	19.1	0.26	10	0.026	0.651	0.404	4238	0.008863
98.0	9.0	0.30	10	0.030	0.751	0.522	4890	0.008612

Table B.66 Observation for 0.10% PVA Solution with *r/R*: 0.024 (Hg)

R (cm)		Weight, *w* (kg)	Time, *t* (s)	Mass flow rate, $\dot{m}$ (kg/s)	Velocity, *v* (m/s)	Head loss, ΔH (m of water)	Reynolds Number, Re	Friction factor, f
49.2	42.6	0.39	10	0.039	0.976	0.829	6357	0.008083
52.0	39.8	0.55	10	0.055	1.376	1.532	8965	0.007513
58.2	33.6	0.81	10	0.081	2.027	3.088	13203	0.006985
61.5	30.3	0.93	10	0.093	2.327	3.917	15159	0.006720
68.7	23.1	1.15	10	0.115	2.877	5.724	18745	0.006423
73.7	18.1	1.28	10	0.128	3.203	6.980	20864	0.006322

Table B.67 Observation for 0.15% PVA Solution with *r/R*: 0.012 (CCl_4)

R (cm)		Weight, *w* (kg)	Time, *t* (s)	Mass flow rate, $\dot{m}$ (kg/s)	Velocity, *v* (m/s)	Head loss, ΔH (m of water)	Reynolds Number, Re	Friction factor, f
54.0	51.5	0.02	20	0.001	0.025	0.015	141	0.217716
56.0	49.5	0.04	10	0.004	0.100	0.038	562	0.035379
64.5	41.0	0.12	10	0.012	0.300	0.138	1686	0.014212
71.5	34.0	0.16	10	0.016	0.400	0.220	2249	0.012757
77.2	28.3	0.22	10	0.022	0.550	0.287	3092	0.008799
85.0	20.5	0.26	10	0.026	0.651	0.379	3654	0.008309
99.0	6.5	0.32	10	0.032	0.801	0.543	4497	0.007867

Table B.68 Observation for 0.15% PVA Solution with *r/R*: 0.012 (Hg)

R (cm)		Weight, *w* (kg)	Time, *t* (s)	Mass flow rate, $\dot{m}$ (kg/s)	Velocity, *v* (m/s)	Head loss, ΔH (m of water)	Reynolds Number, Re	Friction factor, f
49.0	42.8	0.39	10	0.039	0.976	0.778	5481	0.007594
52.8	39.0	0.61	10	0.061	1.526	1.732	8572	0.006909
56.9	34.9	0.80	10	0.080	2.002	2.762	11243	0.006404
62.0	29.8	0.98	10	0.098	2.452	4.042	13772	0.006246
69.5	22.3	1.23	10	0.123	3.077	5.925	17285	0.005812
73.0	18.8	1.34	10	0.134	3.353	6.804	18831	0.005623
78.7	13.1	1.48	10	0.148	3.703	8.235	20799	0.005579

Table B.69 Observation for 0.15% PVA Solution with *r/R*: 0.018 (CCl_4)

R (cm)		Weight, *w* (kg)	Time, *t* (s)	Mass flow rate, $\dot{m}$ (kg/s)	Velocity, *v* (m/s)	Head loss, ΔH (m of water)	Reynolds Number, Re	Friction factor, f
55.0	50.5	0.02	20	0.001	0.025	0.026	141	0.391889
57.0	48.5	0.04	10	0.004	0.100	0.050	562	0.046265
65.5	40.0	0.12	10	0.012	0.300	0.150	1686	0.015422
72.5	33.0	0.18	10	0.018	0.450	0.232	2530	0.010617
78.2	27.3	0.22	10	0.022	0.538	0.299	3021	0.009589
86.0	19.5	0.25	10	0.025	0.626	0.390	3513	0.009266

Table B.70 Observation for 0.15% PAM Solution with *r/R*: 0.018 (Hg)

R (cm)		Weight, *w* (kg)	Time, *t* (s)	Mass flow rate, $\dot{m}$ (kg/s)	Velocity, *v* (m/s)	Head loss, ΔH (m of water)	Reynolds Number, Re	Friction factor, f
48.7	43.1	0.35	10	0.035	0.876	0.703	4919	0.008516
53.0	38.8	0.60	10	0.060	1.501	1.783	8432	0.007348
57.7	34.1	0.79	10	0.079	1.977	2.963	11102	0.007044
62.0	29.8	0.95	10	0.095	2.377	4.042	13351	0.006646
69.5	22.3	1.18	10	0.118	2.952	5.925	16583	0.006315
74.0	17.8	1.29	10	0.129	3.228	7.055	18129	0.006291
83.0	8.8	1.50	10	0.150	3.753	9.315	21080	0.006143

Table B.71 Observation for 0.15% PVA Solution with *r/R*: 0.024 (CCl_4)

R (cm)		Weight, *w* (kg)	Time, *t* (s)	Mass flow rate, $\dot{m}$ (kg/s)	Velocity, *v* (m/s)	Head loss, ΔH (m of water)	Reynolds Number, Re	Friction factor, f
56.0	49.5	0.02	20	0.001	0.025	0.038	141	0.566062
58.0	47.5	0.04	10	0.004	0.100	0.062	562	0.057151
66.5	39.0	0.12	10	0.012	0.300	0.161	1686	0.016631
73.5	32.0	0.16	10	0.016	0.400	0.244	2249	0.014118
79.2	26.3	0.21	10	0.021	0.525	0.310	2951	0.010446
87.0	18.5	0.25	10	0.025	0.626	0.402	3513	0.009545
103.0	2.5	0.31	10	0.031	0.776	0.590	4357	0.009107

Table B.72 Observation for 0.15% PVA Solution with *r/R*: 0.024 (Hg)

R (cm)		Weight, *w* (kg)	Time, *t* (s)	Mass flow rate, $\dot{m}$ (kg/s)	Velocity, *v* (m/s)	Head loss, ΔH (m of water)	Reynolds Number, Re	Friction factor, f
48.3	43.5	0.32	10	0.032	0.788	0.603	4427	0.009012
51.7	40.1	0.52	10	0.052	1.301	1.456	7308	0.007992
57.5	34.3	0.76	10	0.076	1.902	2.912	10680	0.007482
61.5	30.3	0.90	10	0.090	2.252	3.917	12648	0.007175
68.7	23.1	1.11	10	0.111	2.777	5.724	15599	0.006894
73.5	18.3	1.24	10	0.124	3.102	6.929	17426	0.006688

Table B.73 Observation for 0.01% Anionic PAM Solution with *r/R*: 0.012 (CCl_4)

R (cm)		Weight, w (kg)	Time, t (s)	Mass flow rate, $\dot{m}$ (kg/s)	Velocity, v (m/s)	Head loss, ΔH (m of water)	Reynolds Number, Re	Friction factor, f
60.3	45.2	0.12	10	0.012	0.300	0.089	1813	0.009132
68.5	37.0	0.18	10	0.018	0.450	0.185	2720	0.008467
83.0	22.4	0.26	10	0.026	0.638	0.356	3853	0.008116
87.5	18.0	0.35	10	0.035	0.876	0.408	5288	0.004941
95.2	10.2	0.40	10	0.040	1.001	0.499	6044	0.004626
103.0	2.5	0.44	10	0.044	1.101	0.590	6648	0.004521

Table B.74 Observation for 0.01% Anionic PAM Solution with *r/R*: 0.012 (Hg)

R (cm)		Weight, w (kg)	Time, t (s)	Mass flow rate, $\dot{m}$ (kg/s)	Velocity, v (m/s)	Head loss, ΔH (m of water)	Reynolds Number, Re	Friction factor, f
49.5	42.5	0.58	10	0.058	1.451	0.879	8763	0.003876
53.7	38.3	0.94	10	0.094	2.352	1.933	14203	0.003247
58.7	33.3	1.30	10	0.130	3.253	3.189	19642	0.002800
62.3	29.7	1.56	10	0.156	3.903	4.092	23571	0.002495
66.7	25.3	1.78	10	0.178	4.454	5.197	26895	0.002434
72.7	19.3	2.14	10	0.214	5.354	6.704	32334	0.002172

Table B.75 Observation for 0.01% Anionic PAM Solution with *r/R*: 0.018 (CCl_4)

R (cm)		Weight, w (kg)	Time, t (s)	Mass flow rate, $\dot{m}$ (kg/s)	Velocity, v (m/s)	Head loss, ΔH (m of water)	Reynolds Number, Re	Friction factor, f
56.9	48.3	0.06	10	0.006	0.150	0.050	907	0.020804
61.5	43.7	0.12	10	0.012	0.300	0.104	1813	0.010765
67.3	37.9	0.18	10	0.018	0.450	0.173	2720	0.007902
78.9	26.3	0.28	10	0.028	0.701	0.309	4231	0.005843
89.0	16.2	0.34	10	0.034	0.851	0.427	5137	0.005484
100.4	4.8	0.40	10	0.040	1.001	0.561	6044	0.005203

Table B.76 Observation for 0.01% Anionic PAM Solution with *r/R*: 0.018 (Hg)

R (cm)		Weight, *w* (kg)	Time, *t* (s)	Mass flow rate, $\dot{m}$ (kg/s)	Velocity, *v* (m/s)	Head loss, ΔH (m of water)	Reynolds Number, Re	Friction factor, f
49.5	42.5	0.54	10	0.054	1.351	0.879	8159	0.004472
53.3	38.7	0.86	10	0.086	2.152	1.833	12994	0.003677
57.7	34.3	1.16	10	0.116	2.902	2.937	17527	0.003240
61.7	30.3	1.38	10	0.138	3.453	3.942	20851	0.003072
67.3	24.7	1.68	10	0.168	4.203	5.348	25384	0.002812
72.9	19.1	1.96	10	0.196	4.904	6.754	29615	0.002609

Table B.77 Observation for 0.01% Anionic PAM Solution with *r/R*: 0.024 (CCl_4)

R (cm)		Weight, *w* (kg)	Time, *t* (s)	Mass flow rate, $\dot{m}$ (kg/s)	Velocity, *v* (m/s)	Head loss, ΔH (m of water)	Reynolds Number, Re	Friction factor, f
58.5	46.7	0.06	10	0.006	0.150	0.069	907	0.028545
64.7	40.5	0.14	10	0.014	0.350	0.142	2115	0.010753
72.0	33.0	0.18	10	0.018	0.450	0.229	2720	0.010483
80.5	24.5	0.28	10	0.028	0.701	0.329	4231	0.006220
87.0	18.0	0.32	10	0.032	0.801	0.405	4835	0.005868
91.2	13.8	0.34	10	0.034	0.851	0.454	5137	0.005831

Table B.78 Observation for 0.01% Anionic PAM Solution with *r/R*: 0.024 (Hg)

R (cm)		Weight, *w* (kg)	Time, *t* (s)	Mass flow rate, $\dot{m}$ (kg/s)	Velocity, *v* (m/s)	Head loss, ΔH (m of water)	Reynolds Number, Re	Friction factor, f
49.4	42.6	0.50	10	0.050	1.251	0.854	7555	0.005067
53.5	38.5	0.80	10	0.080	2.002	1.883	12088	0.004366
57.7	34.3	1.04	10	0.104	2.602	2.937	15714	0.004030
62.8	29.2	1.30	10	0.130	3.253	4.218	19642	0.003704
66.0	26.0	1.46	10	0.146	3.653	5.021	22060	0.003496
72.0	20.0	1.72	10	0.172	4.303	6.528	25988	0.003274

Table B.79 Observation for 0.03% Anionic PAM Solution with *r/R*: 0.012 (CCl_4)

R (cm)		Weight, *w* (kg)	Time, *t* (s)	Mass flow rate, $\dot{m}$ (kg/s)	Velocity, *v* (m/s)	Head loss, ΔH (m of water)	Reynolds Number, Re	Friction factor, f
57.0	48.0	0.06	10	0.006	0.150	0.053	672	0.021772
64.4	40.6	0.12	10	0.012	0.300	0.140	1344	0.014393
73.0	32.0	0.20	10	0.020	0.500	0.241	2239	0.008926
81.5	23.5	0.31	10	0.031	0.776	0.340	3471	0.005256
95.0	10.0	0.40	10	0.040	1.001	0.499	4478	0.004626
101.0	4.0	0.43	10	0.043	1.076	0.569	4814	0.004569

Table B.80 Observation for 0.03% Anionic PAM Solution with *r/R*: 0.012 (Hg)

R (cm)		Weight, *w* (kg)	Time, *t* (s)	Mass flow rate, $\dot{m}$ (kg/s)	Velocity, *v* (m/s)	Head loss, ΔH (m of water)	Reynolds Number, Re	Friction factor, f
49.0	43.0	0.52	10	0.052	1.301	0.753	5822	0.004134
54.5	37.5	1.05	10	0.105	2.627	2.134	11756	0.002872
58.3	33.7	1.30	10	0.130	3.253	3.088	14555	0.002712
62.6	29.4	1.62	10	0.162	4.053	4.168	18138	0.002357
66.7	25.3	1.88	10	0.188	4.704	5.197	21049	0.002182
72.0	20.0	2.14	10	0.214	5.354	6.528	23960	0.002115

Table B.81 Observation for 0.03% Anionic PAM Solution with *r/R*: 0.018 (CCl_4)

R (cm)		Weight, *w* (kg)	Time, *t* (s)	Mass flow rate, $\dot{m}$ (kg/s)	Velocity, *v* (m/s)	Head loss, ΔH (m of water)	Reynolds Number, Re	Friction factor, f
58.6	46.7	0.04	10	0.004	0.100	0.070	448	0.064771
64.6	40.7	0.10	10	0.010	0.250	0.140	1120	0.020814
71.8	33.3	0.18	10	0.018	0.450	0.226	2015	0.010348
78.0	27.0	0.27	10	0.027	0.676	0.299	3023	0.006092
86.5	18.5	0.32	10	0.032	0.801	0.399	3583	0.005783
101.5	3.5	0.40	10	0.040	1.001	0.575	4478	0.005334

Table B.82 Observation for 0.03% Anionic PAM Solution with *r/R*: 0.018 (Hg)

R (cm)		Weight, *w* (kg)	Time, *t* (s)	Mass flow rate, $\dot{m}$ (kg/s)	Velocity, *v* (m/s)	Head loss, ΔH (m of water)	Reynolds Number, Re	Friction factor, f
49.8	42.2	0.56	10	0.056	1.401	0.954	6270	0.004515
54.2	37.8	0.94	10	0.094	2.352	2.059	10524	0.003458
57.6	34.4	1.18	10	0.118	2.952	2.912	13212	0.003104
61.8	30.2	1.42	10	0.142	3.553	3.967	15899	0.002919
66.3	25.7	1.64	10	0.164	4.103	5.097	18362	0.002812
72.0	20.0	1.90	10	0.190	4.754	6.528	21273	0.002683

Table B.83 Observation for 0.03% Anionic PAM Solution with *r/R*: 0.024 (CCl_4)

R (cm)		Weight, *w* (kg)	Time, *t* (s)	Mass flow rate, $\dot{m}$ (kg/s)	Velocity, *v* (m/s)	Head loss, ΔH (m of water)	Reynolds Number, Re	Friction factor, f
58.7	46.3	0.06	10	0.006	0.150	0.073	672	0.029996
63.8	41.2	0.10	10	0.010	0.250	0.133	1120	0.019682
70.5	34.5	0.16	10	0.016	0.400	0.211	1791	0.012247
80.5	24.5	0.22	10	0.022	0.550	0.329	2463	0.010076
89.3	15.7	0.26	10	0.026	0.651	0.432	2911	0.009482
98.5	6.5	0.37	10	0.037	0.926	0.540	4143	0.005852

Table B.84 Observation for 0.03% Anionic PAM Solution with *r/R*: 0.024 (Hg)

R (cm)		Weight, *w* (kg)	Time, *t* (s)	Mass flow rate, $\dot{m}$ (kg/s)	Velocity, *v* (m/s)	Head loss, ΔH (m of water)	Reynolds Number, Re	Friction factor, f
49.4	42.6	0.49	10	0.049	1.226	0.854	5486	0.005276
53.5	38.5	0.82	10	0.082	2.052	1.883	9181	0.004156
58.1	33.9	1.10	10	0.110	2.752	3.038	12316	0.003726
61.7	30.3	1.30	10	0.130	3.253	3.942	14555	0.003461
66.5	25.5	1.52	10	0.152	3.803	5.147	17018	0.003306
72.0	20.0	1.76	10	0.176	4.404	6.528	19705	0.003127

Table B.85 Observation for 0.05% Anionic PAM Solution with *r/R*: 0.012 (CCl_4)

R (cm)		Weight, w (kg)	Time, t (s)	Mass flow rate, $\dot{m}$ (kg/s)	Velocity, v (m/s)	Head loss, ΔH (m of water)	Reynolds Number, Re	Friction factor, f
57.0	48.3	0.02	10	0.002	0.050	0.051	152	0.189413
66.7	38.7	0.10	10	0.010	0.250	0.164	759	0.024384
74.3	31.0	0.18	10	0.018	0.450	0.254	1366	0.011638
80.5	24.7	0.22	10	0.022	0.550	0.327	1670	0.010040
85.4	20.0	0.26	10	0.026	0.651	0.384	1973	0.008425
95.8	9.3	0.32	10	0.032	0.801	0.508	2428	0.007356

Table B.86 Observation for 0.05% Anionic PAM Solution with *r/R*: 0.012 (Hg)

R (cm)		Weight, w (kg)	Time, t (s)	Mass flow rate, $\dot{m}$ (kg/s)	Velocity, v (m/s)	Head loss, ΔH (m of water)	Reynolds Number, Re	Friction factor, f
49.8	42.2	0.56	10	0.056	1.401	0.954	4250	0.004515
53.5	38.5	0.90	10	0.090	2.252	1.883	6830	0.003450
57.5	34.5	1.22	10	0.122	3.052	2.887	9258	0.002879
62.0	30.0	1.50	10	0.150	3.753	4.017	11383	0.002649
66.5	25.5	1.74	10	0.174	4.353	5.147	13205	0.002523
72.3	19.7	2.08	10	0.208	5.204	6.603	15785	0.002265

Table B.87 Observation for 0.05% Anionic PAM Solution with *r/R*: 0.018 (CCl_4)

R (cm)		Weight, w (kg)	Time, t (s)	Mass flow rate, $\dot{m}$ (kg/s)	Velocity, v (m/s)	Head loss, ΔH (m of water)	Reynolds Number, Re	Friction factor, f
56.5	48.0	0.04	10	0.004	0.100	0.050	304	0.046265
69.5	35.0	0.12	10	0.012	0.300	0.202	911	0.020864
75.5	29.0	0.18	10	0.018	0.450	0.273	1366	0.012499
87.0	27.5	0.22	10	0.022	0.550	0.349	1670	0.010706
93.0	11.5	0.28	10	0.028	0.701	0.478	2125	0.009053
98.5	6.0	0.30	10	0.030	0.751	0.543	2277	0.008951

Table B.88 Observation for 0.05% Anionic PAM Solution with *r/R*: 0.018 (Hg)

R (cm)		Weight, *w* (kg)	Time, *t* (s)	Mass flow rate, $\dot{m}$ (kg/s)	Velocity, *v* (m/s)	Head loss, ΔH (m of water)	Reynolds Number, Re	Friction factor, f
49.7	42.3	0.50	10	0.050	1.251	0.929	3794	0.005514
53.5	38.5	0.80	10	0.080	2.002	1.883	6071	0.004366
57.5	34.5	1.04	10	0.104	2.602	2.887	7892	0.003961
61.1	30.9	1.26	10	0.126	3.153	3.791	9562	0.003544
65.9	26.1	1.52	10	0.152	3.803	4.996	11535	0.003209
72.5	19.5	1.84	10	0.184	4.604	6.653	13963	0.002916

Table B.89 Observation for 0.05% Anionic PAM Solution with *r/R*: 0.024 (CCl_4)

R (cm)		Weight, *w* (kg)	Time, *t* (s)	Mass flow rate, $\dot{m}$ (kg/s)	Velocity, *v* (m/s)	Head loss, ΔH (m of water)	Reynolds Number, Re	Friction factor, f
59.0	45.5	0.04	10	0.004	0.100	0.079	304	0.073479
66.5	38.0	0.10	10	0.010	0.250	0.167	759	0.024820
71.0	33.5	0.12	10	0.012	0.300	0.220	911	0.022679
77.0	27.5	0.16	10	0.016	0.400	0.290	1214	0.016839
83.2	21.3	0.18	10	0.018	0.450	0.363	1366	0.016638
95.0	9.5	0.26	10	0.026	0.651	0.502	1973	0.011015

Table B.90 Observation for 0.05% Anionic PAM Solution with *r/R*: 0.024 (Hg)

R (cm)		Weight, *w* (kg)	Time, *t* (s)	Mass flow rate, $\dot{m}$ (kg/s)	Velocity, *v* (m/s)	Head loss, ΔH (m of water)	Reynolds Number, Re	Friction factor, f
49.0	43.0	0.34	10	0.034	0.851	0.753	2580	0.009669
52.7	39.3	0.70	10	0.070	1.751	1.682	5312	0.005094
56.2	35.8	0.92	10	0.092	2.302	2.561	6982	0.004490
61.0	31.0	1.18	10	0.118	2.952	3.766	8955	0.004014
65.0	27.0	1.36	10	0.136	3.403	4.770	10321	0.003827
72.6	19.4	1.70	10	0.170	4.253	6.678	12901	0.003429

Table B.91 Observation for 0.07% Anionic PAM Solution with r/R: 0.012 (CCl_4)

R (cm)		Weight, w (kg)	Time, t (s)	Mass flow rate, $\dot{m}$ (kg/s)	Velocity, v (m/s)	Head loss, ΔH (m of water)	Reynolds Number, Re	Friction factor, f
60.1	44.5	0.02	10	0.002	0.050	0.092	112	0.339637
69.7	35.1	0.10	10	0.010	0.250	0.203	562	0.030132
76.5	28.2	0.14	10	0.014	0.350	0.283	786	0.021461
84.7	20.1	0.20	10	0.020	0.500	0.379	1123	0.014064
91.3	13.4	0.24	10	0.024	0.600	0.457	1348	0.011778
99.0	5.7	0.28	10	0.028	0.701	0.548	1573	0.010364

Table B.92 Observation for 0.07% Anionic PAM Solution with r/R: 0.012 (Hg)

R (cm)		Weight, w (kg)	Time, t (s)	Mass flow rate, $\dot{m}$ (kg/s)	Velocity, v (m/s)	Head loss, ΔH (m of water)	Reynolds Number, Re	Friction factor, f
49.5	42.5	0.52	10	0.052	1.301	0.879	2921	0.004822
53.3	35.7	0.92	10	0.092	2.302	2.209	5167	0.003874
58.1	33.9	1.14	10	0.114	2.852	3.038	6403	0.003469
62.8	29.2	1.46	10	0.146	3.653	4.218	8200	0.002936
67.7	24.3	1.70	10	0.170	4.253	5.448	9548	0.002798
72.1	19.9	1.92	10	0.192	4.804	6.553	10784	0.002638

Table B.93 Observation for 0.07% Anionic PAM Solution with r/R: 0.018 (CCl_4)

R (cm)		Weight, w (kg)	Time, t (s)	Mass flow rate, $\dot{m}$ (kg/s)	Velocity, v (m/s)	Head loss, ΔH (m of water)	Reynolds Number, Re	Friction factor, f
59.9	44.0	0.04	10	0.004	0.100	0.093	225	0.086542
70.0	33.8	0.10	10	0.010	0.250	0.212	562	0.031525
79.5	24.3	0.16	10	0.016	0.400	0.324	899	0.018778
88.6	25.2	0.20	10	0.020	0.500	0.372	1123	0.013803
96.6	7.2	0.24	10	0.024	0.600	0.525	1348	0.013517
102.8	1.0	0.26	10	0.026	0.651	0.597	1460	0.013115

Table B.94 Observation for 0.07% Anionic PAM Solution with *r/R*: 0.018 (Hg)

R (cm)		Weight, *w* (kg)	Time, *t* (s)	Mass flow rate, $\dot{m}$ (kg/s)	Velocity, *v* (m/s)	Head loss, ΔH (m of water)	Reynolds Number, Re	Friction factor, f
49.3	42.7	0.38	10	0.038	0.951	0.829	2134	0.008514
52.3	39.7	0.68	10	0.068	1.701	1.582	3819	0.005076
55.2	36.8	0.86	10	0.086	2.152	2.310	4830	0.004634
61.3	30.7	1.22	10	0.122	3.052	3.841	6852	0.003830
66.2	25.8	1.46	10	0.146	3.653	5.072	8200	0.003531
73.0	19.0	1.74	10	0.174	4.353	6.779	9773	0.003323

Table B.95 Observation for 0.07% Anionic PAM Solution with *r/R*: 0.024 (CCl_4)

R (cm)		Weight, *w* (kg)	Time, *t* (s)	Mass flow rate, $\dot{m}$ (kg/s)	Velocity, *v* (m/s)	Head loss, ΔH (m of water)	Reynolds Number, Re	Friction factor, f
61.0	44.3	0.04	10	0.004	0.100	0.098	225	0.090897
70.2	35.0	0.10	10	0.010	0.250	0.207	562	0.030654
78.5	26.7	0.14	10	0.014	0.350	0.304	786	0.023016
83.3	21.7	0.16	10	0.016	0.400	0.362	899	0.020955
97.1	7.9	0.22	10	0.022	0.550	0.523	1236	0.016050
101.5	3.6	0.24	10	0.024	0.600	0.575	1348	0.014802

Table B.96 Observation for 0.07% Anionic PAM Solution with *r/R*: 0.024 (Hg)

R (cm)		Weight, *w* (kg)	Time, *t* (s)	Mass flow rate, $\dot{m}$ (kg/s)	Velocity, *v* (m/s)	Head loss, ΔH (m of water)	Reynolds Number, Re	Friction factor, f
49.1	42.9	0.34	10	0.034	0.851	0.778	1910	0.009991
53.8	38.2	0.74	10	0.074	1.851	1.958	4156	0.005307
58.7	33.3	1.00	10	0.100	2.502	3.189	5617	0.004732
62.1	29.9	1.20	10	0.120	3.002	4.042	6740	0.004166
67.5	24.5	1.44	10	0.144	3.603	5.398	8088	0.003863
72.3	19.7	1.64	10	0.164	4.103	6.603	9211	0.003643

Table B.97 Observation for 0.10% Anionic PAM Solution with *r/R*:0.012 (CCl_4)

R (cm)		Weight, *w* (kg)	Time, *t* (s)	Mass flow rate, $\dot{m}$ (kg/s)	Velocity, *v* (m/s)	Head loss, ΔH (m of water)	Reynolds Number, Re	Friction factor, f
61.0	43.0	0.04	10	0.004	0.100	0.106	169	0.097972
80.0	24.0	0.14	10	0.014	0.350	0.329	590	0.024882
86.5	17.5	0.20	10	0.020	0.500	0.405	843	0.015022
93.5	10.5	0.26	10	0.026	0.651	0.487	1096	0.010693

Table B.98 Observation for 0.10% Anionic PAM Solution with *r/R*: 0.012 (Hg)

R (cm)		Weight, *w* (kg)	Time, *t* (s)	Mass flow rate, $\dot{m}$ (kg/s)	Velocity, *v* (m/s)	Head loss, ΔH (m of water)	Reynolds Number, Re	Friction factor, f
50.0	42.0	0.42	10	0.042	1.051	1.004	1771	0.008448
54.7	37.3	0.78	10	0.078	1.952	2.184	3288	0.005328
59.5	32.5	1.08	10	0.108	2.702	3.389	4553	0.004312
63.7	28.3	1.30	10	0.130	3.253	4.444	5481	0.003902
67.8	24.2	1.48	10	0.148	3.703	5.473	6240	0.003708

Table B.99 Observation for 0.10% Anionic PAM Solution with *r/R*: 0.018 (CCl_4)

R (cm)		Weight, *w* (kg)	Time, *t* (s)	Mass flow rate, $\dot{m}$ (kg/s)	Velocity, *v* (m/s)	Head loss, ΔH (m of water)	Reynolds Number, Re	Friction factor, f
57.5	47.0	0.02	10	0.002	0.050	0.062	84	0.228602
68.5	36.0	0.06	10	0.006	0.150	0.191	253	0.078620
80.5	24.0	0.14	10	0.014	0.350	0.332	590	0.025104
88.5	16.0	0.16	10	0.016	0.400	0.425	675	0.024663
100.5	4.0	0.22	10	0.022	0.550	0.566	928	0.017363

Table B.100 Observation for 0.10% Anionic PAM Solution with *r/R*: 0.018 (Hg)

R (cm)		Weight, *w* (kg)	Time, *t* (s)	Mass flow rate, $\dot{m}$ (kg/s)	Velocity, *v* (m/s)	Head loss, ΔH (m of water)	Reynolds Number, Re	Friction factor, f
50.0	42.0	0.36	10	0.036	0.901	1.004	1518	0.011499
54.5	37.5	0.74	10	0.074	1.851	2.134	3120	0.005783
58.9	33.1	0.96	10	0.096	2.402	3.239	4047	0.005215
64.0	28.0	1.18	10	0.118	2.952	4.519	4975	0.004816
67.5	24.5	1.34	10	0.134	3.353	5.398	5649	0.004461
72.0	20.0	1.50	10	0.150	3.753	6.528	6324	0.004305

Table B.101 Observation for 0.10% Anionic PAM Solution with *r/R*: 0.024 (CCl_4)

R (cm)		Weight, *w* (kg)	Time, *t* (s)	Mass flow rate, $\dot{m}$ (kg/s)	Velocity, *v* (m/s)	Head loss, ΔH (m of water)	Reynolds Number, Re	Friction factor, f
60.0	44.7	0.02	10	0.002	0.050	0.090	84	0.333106
71.5	33.2	0.06	10	0.006	0.150	0.225	253	0.092650
82.0	22.7	0.12	10	0.012	0.300	0.348	506	0.035863
91.3	13.4	0.14	10	0.014	0.350	0.457	590	0.034612
102.2	2.5	0.20	10	0.020	0.500	0.585	843	0.021706

Table B.102 Observation for 0.10% Anionic PAM Solution with *r/R*: 0.024 (Hg)

R (cm)		Weight, *w* (kg)	Time, *t* (s)	Mass flow rate, $\dot{m}$ (kg/s)	Velocity, *v* (m/s)	Head loss, ΔH (m of water)	Reynolds Number, Re	Friction factor, f
49.8	42.2	0.32	10	0.032	0.801	0.954	1349	0.013826
54.0	38.0	0.64	10	0.064	1.601	2.009	2698	0.007277
58.7	33.3	0.90	10	0.090	2.252	3.189	3794	0.005842
62.8	29.2	1.08	10	0.108	2.702	4.218	4553	0.005366
66.7	25.3	1.22	10	0.122	3.052	5.197	5143	0.005182
72.5	19.5	1.42	10	0.142	3.553	6.653	5987	0.004896

Table B.103 Observation for 0.01%Cationic PAM Solution with *R/R*: 0.012 (CCl_4)

R (cm)		Weight, *w* (kg)	Time, *t* (s)	Mass flow rate, $\dot{m}$ (kg/s)	Velocity, *v* (m/s)	Head loss, ΔH (m of water)	Reynolds Number, Re	Friction factor, f
55.0	40.0	0.12	10	0.012	0.300	0.088	2024	0.009072
61.5	33.5	0.20	10	0.020	0.500	0.164	3373	0.006096
70.0	25.0	0.26	10	0.026	0.651	0.264	4385	0.005797
76.0	19.0	0.30	10	0.030	0.751	0.335	5059	0.005515
85.0	10.0	0.36	10	0.036	0.901	0.440	6071	0.005040
93.5	1.5	0.40	10	0.040	1.001	0.540	6746	0.005007

Table B.104 Observation for 0.01% Cationic PAM Solution with *r/R*: 0.012 (Hg)

R (cm)		Weight, *w* (kg)	Time, *t* (s)	Mass flow rate, $\dot{m}$ (kg/s)	Velocity, *v* (m/s)	Head loss, ΔH (m of water)	Reynolds Number, Re	Friction factor, f
49.8	42.2	0.56	10	0.056	1.401	0.954	9444	0.004515
53.3	38.7	0.82	10	0.082	2.052	1.833	13829	0.004045
59.8	32.2	1.22	10	0.122	3.052	3.465	20574	0.003454
63.8	28.2	1.44	10	0.144	3.603	4.469	24284	0.003198
71.8	20.2	1.80	10	0.180	4.504	6.478	30355	0.002967

Table B.105 Observation for 0.01% Cationic PAM Solution with *r/R*: 0.018 (CCl_4)

R (cm)		Weight, *w* (kg)	Time, *t* (s)	Mass flow rate, $\dot{m}$ (kg/s)	Velocity, *v* (m/s)	Head loss, ΔH (m of water)	Reynolds Number, Re	Friction factor, f
56.0	50.5	0.08	20	0.004	0.100	0.032	675	0.029936
65.8	40.6	0.14	10	0.014	0.350	0.148	2361	0.011197
73.0	33.4	0.23	10	0.023	0.575	0.232	3879	0.006519
81.0	25.4	0.28	10	0.028	0.701	0.326	4722	0.006176
91.2	15.2	0.34	10	0.034	0.851	0.446	5734	0.005725
102.0	4.5	0.40	10	0.040	1.001	0.572	6746	0.005307

Table B.106 Observation for 0.01% Cationic PAM Solution with *r/R*: 0.018 (Hg)

R (cm)		Weight, *w* (kg)	Time, *t* (s)	Mass flow rate, $\dot{m}$ (kg/s)	Velocity, *v* (m/s)	Head loss, ΔH (m of water)	Reynolds Number, Re	Friction factor, f
50.0	42.0	0.55	10	0.055	1.376	1.004	9275	0.004927
53.8	38.2	0.80	10	0.080	2.002	1.958	13491	0.004541
56.8	35.2	0.96	10	0.096	2.402	2.712	16190	0.004366
60.5	31.5	1.14	10	0.114	2.852	3.640	19225	0.004157
65.9	26.1	1.35	10	0.135	3.378	4.996	22767	0.004068
72.0	20.0	1.58	10	0.158	3.953	6.528	26645	0.003880

Table B.107 Observation for 0.01% Cationic PAM Solution with *r/R*: 0.024 (CCl_4)

R (cm)		Weight, *w* (kg)	Time, *t* (s)	Mass flow rate, $\dot{m}$ (kg/s)	Velocity, *v* (m/s)	Head loss, ΔH (m of water)	Reynolds Number, Re	Friction factor, f
56.1	50.5	0.04	10	0.004	0.100	0.033	675	0.030480
64.0	42.5	0.12	10	0.012	0.300	0.126	2024	0.013003
74.0	32.5	0.23	10	0.023	0.575	0.244	3879	0.006832
84.5	21.9	0.29	10	0.029	0.726	0.367	4891	0.006482
92.5	13.9	0.33	10	0.033	0.826	0.461	5565	0.006286

Table B.108 Observation for 0.01% Cationic PAM Solution with *r/R*: 0.024 (Hg)

R (cm)		Weight, *w* (kg)	Time, *t* (s)	Mass flow rate, $\dot{m}$ (kg/s)	Velocity, *v* (m/s)	Head loss, ΔH (m of water)	Reynolds Number, Re	Friction factor, f
50.6	41.4	0.56	10	0.056	1.401	1.155	9444	0.005465
53.8	38.2	0.75	10	0.075	1.877	1.958	12648	0.005166
58.2	33.8	0.95	10	0.095	2.377	3.063	16021	0.005036
62.6	29.4	1.13	10	0.113	2.827	4.168	19057	0.004844

Table B.109 Observation for 0.03% Cationic PAM Solution with *r/R*: 0.012 (CCl_4)

R (cm)		Weight, *w* (kg)	Time, *t* (s)	Mass flow rate, $\dot{m}$ (kg/s)	Velocity, *v* (m/s)	Head loss, ΔH (m of water)	Reynolds Number, Re	Friction factor, f
51.7	43.3	0.04	10	0.004	0.100	0.049	619	0.045720
60.2	34.8	0.12	10	0.012	0.300	0.149	1858	0.015361
71.0	24.0	0.27	10	0.027	0.676	0.276	4182	0.005615
78.0	17.0	0.32	10	0.032	0.801	0.358	4956	0.005188
85.5	9.5	0.36	10	0.036	0.901	0.446	5575	0.005107
91.3	3.7	0.40	10	0.040	1.001	0.514	6195	0.004768

Table B.110 Observation for 0.03% Cationic PAM Solution with *r/R*: 0.012 (Hg)

R (cm)		Weight, *w* (kg)	Time, *t* (s)	Mass flow rate, $\dot{m}$ (kg/s)	Velocity, *v* (m/s)	Head loss, ΔH (m of water)	Reynolds Number, Re	Friction factor, f
49.5	42.5	0.56	10	0.056	1.401	0.879	8673	0.004158
54.2	37.8	0.93	10	0.093	2.327	2.059	14403	0.003532
58.3	33.7	1.18	10	0.118	2.952	3.088	18275	0.003291
61.5	30.5	1.35	10	0.135	3.378	3.892	20908	0.003169
65.5	26.5	1.58	10	0.158	3.953	4.896	24470	0.002910
71.5	20.5	1.84	10	0.184	4.604	6.402	28497	0.002806

Table B.111 Observation for 0.03% Cationic PAM Solution with *r/R*: 0.018 (CCl_4)

R (cm)		Weight, *w* (kg)	Time, *t* (s)	Mass flow rate, $\dot{m}$ (kg/s)	Velocity, *v* (m/s)	Head loss, ΔH (m of water)	Reynolds Number, Re	Friction factor, f
50.0	45.0	0.04	10	0.004	0.100	0.029	619	0.027215
55.3	39.7	0.10	10	0.010	0.250	0.092	1549	0.013585
63.0	32.0	0.18	10	0.018	0.450	0.182	2788	0.008332
74.3	20.7	0.28	10	0.028	0.701	0.315	4336	0.005954
81.0	14.0	0.32	10	0.032	0.801	0.393	4956	0.005698
91.0	4.0	0.38	10	0.038	0.951	0.511	5885	0.005247

Table B.112 Observation for 0.03% Cationic PAM Solution with *r/R*: 0.018 (Hg)

R (cm)		Weight, *w* (kg)	Time, *t* (s)	Mass flow rate, $\dot{m}$ (kg/s)	Velocity, *v* (m/s)	Head loss, ΔH (m of water)	Reynolds Number, Re	Friction factor, f
49.0	43.0	0.48	10	0.048	1.201	0.753	7434	0.004851
52.5	39.5	0.76	10	0.076	1.902	1.632	11770	0.004193
55.2	36.8	0.94	10	0.094	2.352	2.310	14558	0.003879
60.2	31.8	1.22	10	0.122	3.052	3.565	18895	0.003555
65.0	27.0	1.46	10	0.146	3.653	4.770	22612	0.003321
71.0	21.0	1.76	10	0.176	4.404	6.277	27258	0.003007

Table B.113 Observation for 0.03% Cationic PAM Solution with *r/R*: 0.024(CCl_4)

R (cm)		Weight, *w* (kg)	Time, *t* (s)	Mass flow rate, $\dot{m}$ (kg/s)	Velocity, *v* (m/s)	Head loss, ΔH (m of water)	Reynolds Number, Re	Friction factor, f
53.5	41.5	0.06	10	0.006	0.150	0.070	929	0.029029
60.0	35.0	0.12	10	0.012	0.300	0.147	1858	0.015119
69.3	25.7	0.24	10	0.024	0.600	0.256	3717	0.006592
78.0	17.0	0.29	10	0.029	0.726	0.358	4491	0.006317
82.0	13.0	0.31	10	0.031	0.776	0.405	4801	0.006253
91.8	3.2	0.36	10	0.036	0.901	0.520	5575	0.005954

Table B.114 Observation for 0.03% Cationic PAM Solution with *r/R*: 0.024 (Hg)

R (cm)		Weight, *w* (kg)	Time, *t* (s)	Mass flow rate, $\dot{m}$ (kg/s)	Velocity, *v* (m/s)	Head loss, ΔH (m of water)	Reynolds Number, Re	Friction factor, f
49.5	42.5	0.50	10	0.050	1.251	0.879	7744	0.005216
53.3	38.7	0.77	10	0.077	1.927	1.833	11925	0.004587
57.3	34.7	1.00	10	0.100	2.502	2.837	15487	0.004210
61.1	30.9	1.18	10	0.118	2.952	3.791	18275	0.004040
65.5	26.5	1.38	10	0.138	3.453	4.896	21373	0.003815

Table B.115 Observation for 0.05% Cationic PAM Solution with *r/R*: 0.012 (CCl_4)

R (cm)		Weight, *w* (kg)	Time, *t* (s)	Mass flow rate, $\dot{m}$ (kg/s)	Velocity, *v* (m/s)	Head loss, ΔH (m of water)	Reynolds Number, Re	Friction factor, f
52.6	42.4	0.06	10	0.006	0.150	0.060	868	0.024675
59.7	35.3	0.14	10	0.014	0.350	0.143	2026	0.010841
69.5	25.5	0.26	10	0.026	0.651	0.258	3762	0.005668
77.0	18.0	0.32	10	0.032	0.801	0.346	4630	0.005018
89.0	6.0	0.40	10	0.040	1.001	0.487	5788	0.004518
94.8	0.2	0.44	10	0.044	1.101	0.555	6367	0.004255

Table B.116 Observation for 0.05% Cationic PAM Solution with *r/R*: 0.012 (Hg)

R (cm)		Weight, *w* (kg)	Time, *t* (s)	Mass flow rate, $\dot{m}$ (kg/s)	Velocity, *v* (m/s)	Head loss, ΔH (m of water)	Reynolds Number, Re	Friction factor, f
49.5	42.5	0.59	10	0.059	1.476	0.879	8537	0.003746
52.7	39.3	0.88	10	0.088	2.202	1.682	12733	0.003223
57.4	34.6	1.24	10	0.124	3.102	2.862	17942	0.002762
61.0	31.0	1.50	10	0.150	3.753	3.766	21704	0.002484
66.0	26.0	1.80	10	0.180	4.504	5.021	26045	0.002300
72.0	20.0	2.18	10	0.218	5.454	6.528	31543	0.002038

Table B.117 Observation for 0.05% Cationic PAM Solution with *r/R*: 0.018(CCl_4)

R (cm)		Weight, *w* (kg)	Time, *t* (s)	Mass flow rate, $\dot{m}$ (kg/s)	Velocity, *v* (m/s)	Head loss, ΔH (m of water)	Reynolds Number, Re	Friction factor, f
52.5	42.5	0.04	10	0.004	0.100	0.059	579	0.054429
62.0	33.0	0.12	10	0.012	0.300	0.170	1736	0.017538
72.0	23.0	0.20	10	0.020	0.500	0.288	2894	0.010668
82.0	13.0	0.34	10	0.034	0.851	0.405	4920	0.005198
88.8	6.2	0.38	10	0.038	0.951	0.485	5498	0.004982
92.5	2.5	0.40	10	0.040	1.001	0.528	5788	0.004899

Table B.118 Observation for 0.05% Cationic PAM Solution with *r/R*: 0.018 (Hg)

R (cm)		Weight, *w* (kg)	Time, *t* (s)	Mass flow rate, $\dot{m}$ (kg/s)	Velocity, *v* (m/s)	Head loss, ΔH (m of water)	Reynolds Number, Re	Friction factor, f
49.5	42.5	0.54	10	0.054	1.351	0.879	7814	0.004472
54.0	38.0	0.92	10	0.092	2.302	2.009	13312	0.003521
59.5	32.5	1.30	10	0.130	3.253	3.389	18810	0.002976
63.3	28.7	1.54	10	0.154	3.853	4.343	22283	0.002718
67.0	25.0	1.74	10	0.174	4.353	5.272	25177	0.002584
72.3	19.7	2.00	10	0.200	5.004	6.603	28939	0.002450

Table B.119 Observation for 0.05% Cationic PAM Solution with *r/R*: 0.024 (CCl_4)

R (cm)		Weight, *w* (kg)	Time, *t* (s)	Mass flow rate, $\dot{m}$ (kg/s)	Velocity, *v* (m/s)	Head loss, ΔH (m of water)	Reynolds Number, Re	Friction factor, f
53.0	45.0	0.06	10	0.006	0.150	0.047	868	0.019353
58.5	39.5	0.12	10	0.012	0.300	0.112	1736	0.011491
69.5	28.5	0.20	10	0.020	0.500	0.241	2894	0.008926
78.9	19.1	0.29	10	0.029	0.726	0.351	4196	0.006192
85.5	12.5	0.33	10	0.033	0.826	0.428	4775	0.005838
90.0	8.0	0.36	10	0.036	0.901	0.481	5209	0.005510

Table B.120 Observation for 0.05% Cationic PAM Solution with *r/R*: 0.024 (Hg)

R (cm)		Weight, *w* (kg)	Time, *t* (s)	Mass flow rate, $\dot{m}$ (kg/s)	Velocity, *v* (m/s)	Head loss, ΔH (m of water)	Reynolds Number, Re	Friction factor, f
48.7	43.3	0.44	10	0.044	1.101	0.678	6367	0.005196
53.0	39.0	0.77	10	0.077	1.927	1.757	11141	0.004399
58.2	33.8	1.08	10	0.108	2.702	3.063	15627	0.003897
61.6	30.4	1.26	10	0.126	3.153	3.917	18232	0.003661
65.7	26.3	1.46	10	0.146	3.653	4.946	21125	0.003443
72.0	20.0	1.74	10	0.174	4.353	6.528	25177	0.003200

Table B.121 Observation for 0.07% Cationic PAM Solution with *r/R*: 0.012 (CCl_4)

R (cm)		Weight, w (kg)	Time, t (s)	Mass flow rate, $\dot{m}$ (kg/s)	Velocity, v (m/s)	Head loss, ΔH (m of water)	Reynolds Number, Re	Friction factor, f
59.5	46.0	0.10	10	0.010	0.250	0.079	1422	0.011757
66.0	39.5	0.18	10	0.018	0.450	0.156	2560	0.007123
72.2	33.3	0.23	10	0.023	0.575	0.228	3272	0.006404
81.8	23.7	0.29	10	0.029	0.726	0.341	4125	0.006016
91.7	13.8	0.35	10	0.035	0.876	0.457	4979	0.005538
98.0	7.5	0.38	10	0.038	0.951	0.531	5405	0.005458

Table B.122 Observation for 0.07% Cationic PAM Solution with *r/R*: 0.012 (Hg)

R (cm)		Weight, w (kg)	Time, t (s)	Mass flow rate, $\dot{m}$ (kg/s)	Velocity, v (m/s)	Head loss, ΔH (m of water)	Reynolds Number, Re	Friction factor, f
49.8	42.2	0.53	10	0.053	1.326	0.954	7539	0.005040
52.8	39.2	0.73	10	0.073	1.826	1.707	10384	0.004754
57.0	35.0	0.96	10	0.096	2.402	2.762	13656	0.004447
61.8	30.2	1.16	10	0.116	2.902	3.967	16501	0.004375
66.0	26.0	1.32	10	0.132	3.303	5.021	18777	0.004277
72.5	19.5	1.54	10	0.154	3.853	6.653	21906	0.004163

Table B.123 Observation for 0.07% Cationic PAM Solution with *r/R*:0.018 (CCl_4)

R (cm)		Weight, w (kg)	Time, t (s)	Mass flow rate, $\dot{m}$ (kg/s)	Velocity, v (m/s)	Head loss, ΔH (m of water)	Reynolds Number, Re	Friction factor, f
60.0	45.5	0.08	10	0.008	0.200	0.085	1138	0.019731
70.0	35.5	0.16	10	0.016	0.400	0.202	2276	0.011736
81.2	24.3	0.27	10	0.027	0.676	0.334	3841	0.006797
89.4	16.1	0.32	10	0.032	0.801	0.430	4552	0.006234
95.1	10.4	0.35	10	0.035	0.876	0.497	4979	0.006021

Table B.124 Observation for 0.07% Cationic PAM Solution with *r/R*: 0.018 (Hg)

R (cm)		Weight, *w* (kg)	Time, *t* (s)	Mass flow rate, $\dot{m}$ (kg/s)	Velocity, *v* (m/s)	Head loss, ΔH (m of water)	Reynolds Number, Re	Friction factor, f
49.3	42.7	0.47	10	0.047	1.176	0.829	6686	0.005566
54.6	37.4	0.80	10	0.080	2.002	2.159	11380	0.005006
57.8	34.2	0.95	10	0.095	2.377	2.963	13514	0.004871
61.8	30.2	1.12	10	0.112	2.802	3.967	15932	0.004693
66.0	26.0	1.28	10	0.128	3.203	5.021	18208	0.004548
72.0	20.0	1.47	10	0.147	3.678	6.528	20910	0.004483

Table B.125 Observation for 0.07% Cationic PAM Solution with *r/R*:0.024 (CCl_4)

R (cm)		Weight, *w* (kg)	Time, *t* (s)	Mass flow rate, $\dot{m}$ (kg/s)	Velocity, *v* (m/s)	Head loss, ΔH (m of water)	Reynolds Number, Re	Friction factor, f
55.5	50.0	0.04	10	0.004	0.100	0.032	569	0.029936
60.5	45.0	0.10	10	0.010	0.250	0.091	1422	0.013498
67.0	38.5	0.16	10	0.016	0.400	0.167	2276	0.009695
74.0	31.5	0.20	10	0.020	0.500	0.249	2845	0.009253
82.5	23.0	0.27	10	0.027	0.676	0.349	3841	0.007108
94.0	11.5	0.33	10	0.033	0.826	0.484	4694	0.006597

Table B.126 Observation for 0.07% Cationic PAM Solution with *r/R* : 0.024 (Hg)

R (cm)		Weight, *w* (kg)	Time, *t* (s)	Mass flow rate, $\dot{m}$ (kg/s)	Velocity, *v* (m/s)	Head loss, ΔH (m of water)	Reynolds Number, Re	Friction factor, f
49.0	43.0	0.42	10	0.042	1.051	0.753	5974	0.006336
53.2	38.8	0.69	10	0.069	1.726	1.808	9815	0.005634
58.5	33.5	0.93	10	0.093	2.327	3.138	13229	0.005385
61.8	30.2	1.06	10	0.106	2.652	3.967	15078	0.005239
65.3	26.7	1.18	10	0.118	2.952	4.846	16785	0.005164
71.5	20.5	1.38	10	0.138	3.453	6.402	19630	0.004989

Table B.127 Observation for 0.10% Cationic PAM Solution with *r/R*: 0.012 (CCl_4)

R (cm)		Weight, w (kg)	Time, t (s)	Mass flow rate, $\dot{m}$ (kg/s)	Velocity, v (m/s)	Head loss, ΔH (m of water)	Reynolds Number, Re	Friction factor, f
56.7	48.8	0.04	10	0.004	0.100	0.046	439	0.042999
64.0	41.5	0.14	10	0.014	0.350	0.132	1537	0.009997
72.8	32.7	0.20	10	0.020	0.500	0.235	2196	0.008730
81.0	24.5	0.26	10	0.026	0.651	0.332	2855	0.007279
88.5	17.0	0.32	10	0.032	0.801	0.420	3514	0.006081
99.3	6.2	0.38	10	0.038	0.951	0.546	4173	0.005615

Table B.128 Observation for 0.10% Cationic PAM Solution with *r/R*: 0.012 (Hg)

R (cm)		Weight, w (kg)	Time, t (s)	Mass flow rate, $\dot{m}$ (kg/s)	Velocity, v (m/s)	Head loss, ΔH (m of water)	Reynolds Number, Re	Friction factor, f
49.5	42.5	0.52	10	0.052	1.301	0.879	5710	0.004822
53.5	38.5	0.86	10	0.086	2.152	1.883	9443	0.003778
58.3	33.7	1.16	10	0.116	2.902	3.088	12737	0.003406
61.3	30.7	1.32	10	0.132	3.303	3.841	14494	0.003272
65.5	26.5	1.54	10	0.154	3.853	4.896	16910	0.003063
72.0	20.0	1.82	10	0.182	4.554	6.528	19984	0.002924

Table B.129 Observation for 0.10% Cationic PAM Solution with *r/R*: 0.018 (CCl_4)

R (cm)		Weight, w (kg)	Time, t (s)	Mass flow rate, $\dot{m}$ (kg/s)	Velocity, v (m/s)	Head loss, ΔH (m of water)	Reynolds Number, Re	Friction factor, f
56.0	49.5	0.02	10	0.002	0.050	0.038	220	0.141516
63.0	42.5	0.10	10	0.010	0.250	0.120	1098	0.017853
68.5	37.0	0.14	10	0.014	0.350	0.185	1537	0.013996
73.4	32.1	0.18	10	0.018	0.450	0.242	1976	0.011101
81.6	23.9	0.24	10	0.024	0.600	0.339	2635	0.008724
92.0	13.5	0.34	10	0.034	0.851	0.461	3733	0.005914

Table B.130 Observation for 0.10% Cationic PAM Solution with *r/R*: 0.018 (Hg)

R (cm)		Weight, *w* (kg)	Time, *t* (s)	Mass flow rate, $\dot{m}$ (kg/s)	Velocity, *v* (m/s)	Head loss, ΔH (m of water)	Reynolds Number, Re	Friction factor, f
49.7	42.3	0.52	10	0.052	1.301	0.929	5710	0.005098
54.5	37.5	0.86	10	0.086	2.152	2.134	9443	0.004282
58.4	33.6	1.08	10	0.108	2.702	3.113	11859	0.003961
64.0	28.0	1.36	10	0.136	3.403	4.519	14933	0.003626
67.5	24.5	1.52	10	0.152	3.803	5.398	16690	0.003467
72.5	19.5	1.74	10	0.174	4.353	6.653	19106	0.003261

Table B.131 Observation for 0.10% Cationic PAM Solution with *r/R:* 0.024 (CCl_4)

R (cm)		Weight, *w* (kg)	Time, *t* (s)	Mass flow rate, $\dot{m}$ (kg/s)	Velocity, *v* (m/s)	Head loss, ΔH (m of water)	Reynolds Number, Re	Friction factor, f
54.5	51.0	0.02	10	0.002	0.050	0.021	220	0.076201
58.0	47.5	0.06	10	0.006	0.150	0.062	659	0.025400
64.5	41.0	0.14	10	0.014	0.350	0.138	1537	0.010441
73.5	32.0	0.20	10	0.020	0.500	0.244	2196	0.009035
83.0	22.5	0.24	10	0.024	0.600	0.355	2635	0.009147
94.5	11.0	0.34	10	0.034	0.851	0.490	3733	0.006290

Table B.132 Observation for 0.10% Cationic PAM Solution with *r/R*: 0.024 (Hg)

R (cm)		Weight, *w* (kg)	Time, *t* (s)	Mass flow rate, $\dot{m}$ (kg/s)	Velocity, *v* (m/s)	Head loss, ΔH (m of water)	Reynolds Number, Re	Friction factor, f
49.4	42.6	0.46	10	0.046	1.151	0.854	5051	0.005987
53.3	38.7	0.74	10	0.074	1.851	1.833	8125	0.004967
58.0	34.0	0.98	10	0.098	2.452	3.013	10761	0.004655
60.2	31.8	1.09	10	0.109	2.727	3.565	11969	0.004453
65.3	26.7	1.30	10	0.130	3.253	4.846	14275	0.004255
71.8	20.2	1.56	10	0.156	3.903	6.478	17129	0.003950

Vita

Mr. Arsanchai Sukkuea was born in Nakhon Si Thammarat, Thailand on 12 July, 1984. He obtained a Bachelor degree in Mechanical Engineer from Kasetsart University in 2006. Thereafter, he started the study for Master Degree in Mechanical Engineering at Chulalongkorn in 2007.